

¹¹B NMR Spectra of Boranes, Main-Group Heteroboranes, and Substituted Derivatives. Factors Influencing Chemical Shifts of Skeletal Atoms

STANISLAV HEŘMÁNEK

Institute of Inorganic Chemistry, Czechoslovak Academy of Sciences, 250 68 Řež near Prague, Czechoslovakia

Received January 29, 1992 (Revised Manuscript Received February 25, 1992)

Contents

I. Introduction	325
II. Architecture and Electron Structure of Boranes and Their Derivatives	327
III. NMR Techniques for Structural Analysis of Boron Clusters	330
IV. Chemical Shift	332
A. Hybridization	333
1. Tri- and Tetracoordinated Compounds	333
2. B-Cluster Compounds	333
B. Electron Density on Skeletal Atoms	335
C. Distribution of Bonds around the Observed Nucleus and within the Whole Open B Skeleton	336
1. μ H Rule	336
2. Edge Rule	337
3. NMR Isospectrality	338
4. Calculations of ¹¹ B Chemical Shifts	338
D. Effect of Substituent X on the ¹¹ B NMR Chemical Shifts of Individual B Vertices in Borane Clusters	341
1. Rigid Compounds	344
2. B Skeletons with H Tautomerism	349
3. Effect of Uncharged Ligands on Chemical Shifts in B Skeletons	353
E. Effect of Heteroatom Vertex on Chemical Shifts	353
1. Rigid <i>closo</i> -Heteroboranes Derived from <i>closo</i> -Boranes B _n H _n ²⁻ for n = 5, 6, 7, 10, 12	353
2. Fluxional <i>closo</i> -Heteroboranes Derived from B _n H _n ²⁻ for n = 8, 9, 11	355
3. Open-Face Boranes without and with H Tautomerism	356
F. Probable Origin of Antipodal and Trans Effects of Substituents and Heteroatoms	356
V. Conclusions	358
VI. Acknowledgments	359
VII. References	359

I. Introduction

Boron is second only to carbon in its ability to bond to itself to form polyboron units. The results of intensive investigation of boron compounds over the last four decades allows us to anticipate the theoretical existence of tens of basic boron skeletons, hundreds of their combinations, many thousands of heteroboranes, and hundreds of thousands of their derivatives. In this immense field of chemistry, ¹¹B NMR spectroscopy has been found to be the most economical, fastest, and most reliable method for the determination of structures of compounds with boron skeletons.¹⁻¹³



Stanislav Heřmánek was born in 1929 in Prague. He completed his studies at the Institute of Chemical Technology in Prague and was appointed assistant professor in the Department of Organic Chemistry at this University. Between 1958 and 1960 he was employed in the Research Institute of Natural Drugs in Prague. In 1961 he started the Department of Boron Chemistry at the Institute of Inorganic Chemistry, Řež near Prague. In 1966 he received his Ph.D. for his work on this subject. Prize of Czechoslovak Academy of Sciences (1969). He has won awards from the CSAS (1963, 1971, 1977). He has been a visiting professor under the NA USA program 1969-1970 (Harvard, UCLA). He is the author, co-author, or editor of 11 books and more than 170 papers on boron chemistry, hydrides, chromatography, and organic compounds. He was also the author of the idea to break the secrecy in the field of boranes and to hold International Meetings in Boron Chemistry (IMEBORON). In 1991-1992 he is also teaching at the Charles University Prague.

The informative value of ¹¹B chemical shifts is very high for two reasons: (i) it helps significantly to analyze not only structures but also the center of equilibrium in fluxional molecules, and (ii) it can provide additional and significant insight into the distribution of valence-bond electrons in some fragments of a given molecule or/and in individual atomic orbitals, which is important for understanding both physical and chemical behavior. In several cases, analyses of individual ¹¹B spectra from this point of view have indicated unexpected deviations that called for explanation. In this way, some new principles dominating the behavior of B-cluster compounds have been revealed.

Both naturally occurring isotopes, ¹⁰B and ¹¹B, are NMR active but the latter one is more advantageous for NMR investigations. The success of ¹¹B NMR spectroscopy stems from several favorable factors:

1. Strong signal of the ¹¹B nucleus (0.133, i.e. 16% of the relative receptivity to ¹H, or 754 relative to ¹³C) and 80.4% natural abundance.
2. Resonance at relatively high frequency (32.1 MHz at 2.3 T, i.e. 100 MHz for ¹H).

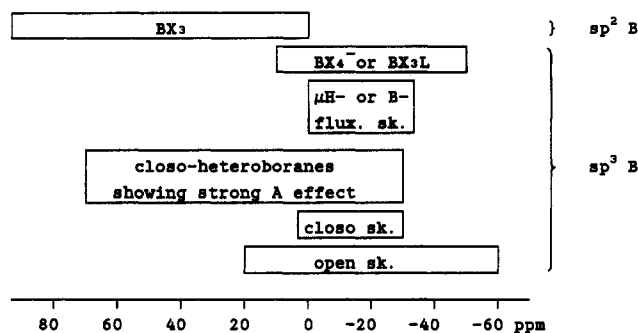


Figure 1. Approximate span and location of lowest and highest signals in ^{11}B NMR spectra of individual borane classes.

TABLE 1. Nuclear Characteristics of B Nuclei

nucleus:	^{10}B	^{11}B
resonance at 2.301 T (100.00 MHz for ^1H)	10.743657 ¹⁰	32.083971 ¹⁰
signal of B (ppm)		
in $\text{BF}_3\cdot\text{OEt}_2$ in CDCl_3 15% v/v	0	0
in $\text{B}(\text{OMe})_3$ neat	18.1	18.1
spin, I	3	3/2
natural abundance	19.58	80.42
relative receptivity		
to ^1H	0.0039	0.133
to ^{13}C	22.1	754
electric quadrupole moment, $Q \times 10^{-28}$	0.074	0.0355

3. Relative sensitivity of the ^{11}B nucleus to different perturbations (bonding strains, substituents, heteroatoms, etc.).

4. In most cases a sufficient spectrum span in compounds with borane skeletons (Figure 1).

5. Optimum B-H coupling (BH, 120–190 Hz; BH_2 , 110–130 Hz; BH_3 , 90–110 Hz; BH_4 , 70–80 Hz; μH , 5–60 Hz).

6. An acceptable width at half height of peaks (2–100 Hz, usually 30–60 Hz). Of the peak width, only a small part must be attributed to the influence of electric quadrupole moment (1–20 Hz),¹⁴ while further widening is due to the interactions of ^{11}B with bridge hydrogens, the B-H long-range coupling (ca. 0–5 Hz), the ^{11}B - ^{11}B (intramolecular, 5–40 Hz; exo-two-electron B-B bonds, 50–150 Hz¹⁵), and ^{11}B - ^{10}B couplings (ca. 3 times lower than the former one).

7. Short relaxation times of ^{11}B nuclei (1–100 ms, commonly 10–50 ms,^{16–18} exceptionally a few seconds, e.g. see ref 19).

The ^{10}B nucleus, in contrast, is present in low natural abundance (19.58%), exhibits a low receptivity (22.1 relative to ^{13}C), and has a quadrupole moment that is 3 times higher, which broadens its NMR signals. Last but not least, ^{10}B is found at a lower resonance frequency on a given instrument (10.75 MHz in comparison with 32.08 MHz for ^{11}B). This results in 2.99 times lower resolution and coupling constants (in Hz). (For more exact values see Table 1.) Despite these disadvantages, the measurement of ^{10}B NMR spectra is exceptionally helpful in selected mechanistic studies including rearrangements^{20,21} and other reactions.²²

The intensive development of NMR spectroscopy has made it into an extremely important tool for the elucidation of structures of boron compounds and for studying their behavior in solutions. The introduction of higher magnetic fields and, especially, the progress in computational and programming techniques make

it possible to obtain the following kinds of information:

1. The number of different types of boron atoms, their mutual ratios within a molecule, and the chemical shift of each signal (from ^{11}B proton decoupled spectra);³ $\delta(^{11}\text{B})$ relative to $\text{BF}_3\cdot\text{OEt}_2 = 0$ ppm with the “+” sign for signals at lower magnetic field, i.e. at higher frequencies; $\delta(^{11}\text{B})$ $\text{B}(\text{OMe})_3 = 18.1$ ppm. [This convention was adopted at IMEBORON III, in Munich-Ettal 1976, but it took several years to be generally accepted. Before this date, the signs were reversed, and sometimes $\text{B}(\text{OMe})_3$ was used as the standard (0 ppm, see e.g. ref 23).]

2. The number of terminal hydrogens on each boron atom, the position of each substituent, and the splitting or broadening of relevant signals by hydrogen bridges if present (via the comparison of undecoupled spectra with proton decoupled ^{11}B spectra of equivalent intensity).

3. The number of terminal H(B) and H(C) and bridge hydrogens (from ^1H or $^1\text{H}\{^{11}\text{B}\}$ spectra).

4. The number of different C atoms in the molecule, their mutual ratios, and the number of hydrogen atoms they bear (from ^{13}C NMR spectra).

5. The structure of boron networks and the assignments of individual signals (from ^{11}B - $^{11}\text{B}\{^1\text{H}\}$ 2D COSY spectra^{24–27}).

6. The assignments of all H signals (from selective $^1\text{H}\{^{11}\text{B}\}$ spectra^{28,29} or from ^1H - $^{11}\text{B}\{^1\text{H}\}$ 2D spectra).¹⁷

7. The presence of B-C links (from ^{13}C NMR spectra decoupled by frequencies of individual B atoms).³⁰

8. The presence of fragments with H-B-C-H links (from ^{11}B -decoupled ^1H - ^1H 2D spectra).³¹

9. A relatively high $J(^{11}\text{B}$ - $^1\text{H})$ of a B* signal³² indicates a connection of the observed B* atom with an adjacent heteroatom such as S.

10. The magnitude of electric field gradients around various B atoms (from high and low T_1 of appropriate signals).^{16–19,33}

At present, practically all of this information can be obtained on commercially available FT spectrometers; the information under items 3, 6, 7, and 8 is obtained when using an inverse probe.

An excellent tool for the elucidation of the skeletal connectivity is ^{11}B - ^{11}B and ^1H - ^1H 2D NMR spectroscopy. This method is not a panacea in all cases. It fails to determine reliable structures in the cases of the following:²⁴

(a) Symmetrical compounds in which the symmetry causes an insufficient number of cross-peaks to be observed.

(b) Missing cross-peak(s).

(c) A reduced number of cross-peaks due to overlapping signals.

(d) Heteroboranes, since these spectra do not provide information on the links of boron to the heteroatom(s).³³

When 2D studies fail to determine specific unique structures, other additional information is required. We have reduced to practice techniques for extracting such additional structural and bonding information from the ^{11}B chemical shift values of individual boron atoms. In practice, we compare all of the $\delta^{11}\text{B}$ values within a given molecule to each other. The ^{11}B chemical shift values found at high frequency (compared to the entire range of ^{11}B δ values) are found to be associated with a certain set of architectural and bonding features while

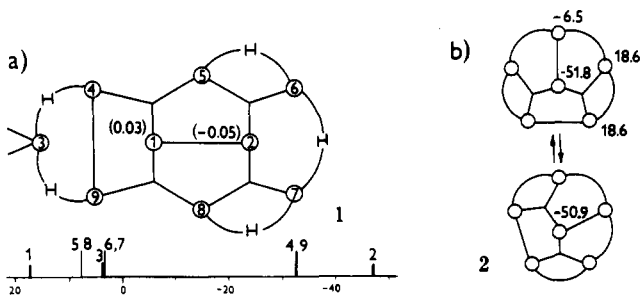


Figure 2. ^{11}B chemical shifts (in ppm): (a) in $n\text{-B}_9\text{H}_{15}$ (1) depicted by the *styx* notation 5421 (see section II) and the PRDDO-SCF derived atomic charges²⁶ (in electrons) on the B(1) and B(2) atoms in 1, and (b) of the apex boron in the H-tautomerizing from (-50.9) and in the static form (-51.8).

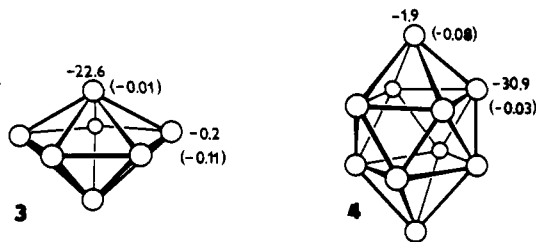


Figure 3. ^{11}B chemical shifts^{27,28} and skeletal atom charges (in electrons) from the PRDDO-SCF calculations²⁹ on the polyhedral anions $\text{B}_7\text{H}_7^{2-}$ (3) and $\text{B}_{10}\text{H}_{10}^{2-}$ (4), respectively.

δ values found at low frequency are associated with a different (mutually exclusive) set of architectural and bonding arrangements.¹¹ Unique structures may frequently be deduced by incorporating such additional information.

By extrapolation from other heavily NMR-active nuclei, such as ^{13}C , ^{14}N , ^{31}P , etc., it would have been expected that the chemical shielding of the ^{11}B atom in question would have depended on: (a) electron density, (b) coordination number, (c) hybridization, and (d) on any ring current which is present between it and its skeletal neighbor atoms. In contrast, in many ^{11}B NMR spectra it has been found that ^{11}B chemical shift values are not always dependent upon such factors.

For instance, when we address the ^{11}B NMR spectrum of $n\text{-B}_9\text{H}_{15}$ (1) whose structure is illustrated by a *styx* formula (Figure 2), (for *styx* formulae see section 2) we see that B(1) and B(2) atoms have identical connectivities, hybridizations, and bonding environments. Despite these similarities, the B(2) atom resonates at highest field and the B(1) atom at lowest field in the spectrum. These resonances differ by 64.7 ppm, which is a larger value than the average span observed in the ^{11}B NMR spectra of open cluster compounds (see Figure 1).

It is improbable that the dominant factor is solely the electron density (ed) at particular skeletal atoms. This may be demonstrated by the relative simple ^{11}B NMR spectra of the anions $\text{B}_7\text{H}_7^{2-}$ (3) and $\text{B}_{10}\text{H}_{10}^{2-}$ (4) (Figure 3) in which the B atoms of higher ed, i.e. B(2-6) of 3 and B(1,10) of 4 are less shielded than those of lower ed, i.e. B(1,7) and B(2-9), respectively.

The possibility that such a great difference in shielding results from enhanced ring current shielding⁴¹ around the B(2) atom and of low shielding around B(1) is not probable, as is illustrated by the comparison of chemical shifts of the apex boron in B_6H_{10} (2) at room temperature and at lower temperatures. In both cases,

the apex ^{11}B chemical shifts are identical, in spite of the fluxional dynamic H tautomerism at room temperature in contrast to the static structure observed at low temperature where the individual basal borons reveal three different δ ^{11}B values (Figure 2).

These examples indicate that the chemical shifts of the vertices in B-polyhedral compounds are dominated by the geometry of the boron atom and by the existence and location of B_B^{B} and B_B^{H} multicenter bonds. For understanding these "other" factors which influence ^{11}B chemical shift values, a short survey on borane architecture and bonding peculiarities are presented (see section II).

The number of published NMR ^{11}B chemical shift values is enormous. Almost any new boron-containing compound has been subjected to ^{11}B NMR spectroscopic analysis in order to help to determine its structure. This has resulted in thousands of spectra and tens of thousands of individual δ ^{11}B values. Presentation of such values exceeds the space requirements of this article. This review is therefore somewhat different from those mentioned in refs 1-13. The aim here is to give to the reader a deeper insight into the specificities of ^{11}B spectra, to indicate which factors play the main role in the location of individual signals within the ^{11}B spectrum of a given molecule, and to show how to use the NMR spectral data in predicting preferred distributions of chemical bonds within the observed molecule and the preferred H tautomers in various series of substituted compounds.

The review is focused on (1) the chemical shifts in B skeletons, (2) the relationships between NMR characteristics and structural features with B-cluster compounds, and (3) changes in $\delta(^{11}\text{B})$ resulting from the substitution of a heteroatom for a B(H) vertex or of a substituent for an exo-terminal H atom.

For the presentation of data of main representatives, papers of the whole period 1960-1990 have to be excerpted. Many of the parent skeletons or appropriate derivatives were therefore prepared and remeasured in our laboratory. A part of this survey is based on our studies which have not been published yet. No attention is paid here to metalla(hetero)boranes, spectra of which are still less understandable due to the changeable character of skeletal metal atoms; this arises from a different measure of connectivity to neighbor skeletal atoms, which is indicated by different bond lengths. This outstandingly large class of compounds is still waiting for a systematic study from the viewpoint of NMR characteristics. ^{11}B chemical shifts of many of these compounds were gathered in general surveys.^{6,7,10,13}

II. Architecture and Electron Structure of Boranes and Their Derivatives

The behavior of boron atoms stems from their electron deficiency, i.e. from the presence of only three bonding electrons in four available atomic orbitals. As a consequence, boron forms both the three-coordinated BX_3 (sp^2 hybridization) and four-coordinated BX_4^- or BX_3L (sp^3 , L = ligand) compounds.

The unique property of boron is in particular its ability to form polyhedral skeletons, composed of triangular boron facets (i.e. of deltahedra), which are the main structural features of all boranes, of their deriv-

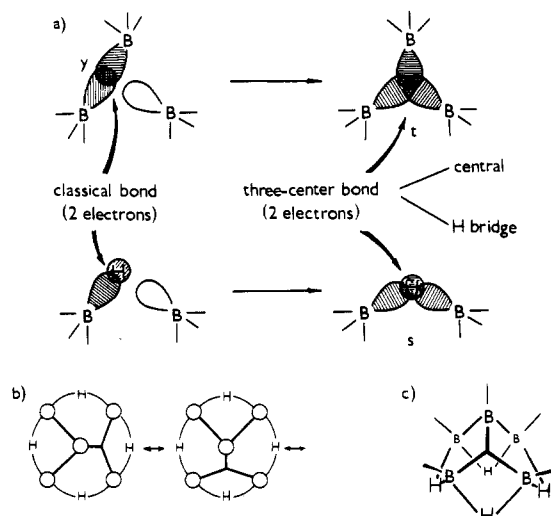


Figure 4. (a) Formation of the three-center two-electron bonds B-H-B (*s*) and B^B_B (*t*) (Lipscomb's topological notation);⁴² (b) canonic 4120 *styx* formulae of B₅H₉; (c) spacial static distribution of bonds in B₅H₉.

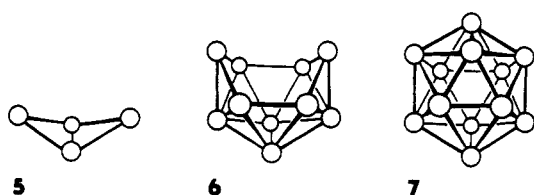


Figure 5. Successive building of borane skeletons.

atives, and by analogy also of the majority of electron-unsatisfied clusters. The reason that such structures exist is because sp³-hybridized boron atoms complete their vacant fourth orbital either by an addition of a Lewis base or by sharing electron pairs with classical B-H or B-B bonds forming the B-H-B hydrogen bridge (*s*) or the B^B_B three-center two-electron bond (*t*) among three B atoms (Figure 4). B triangle formed in this way the formed B triangle is a basic building unit in B skeletons.

Every additional boron atom combines with one or, simultaneously, several edges in a precursor, thus forming one or more triangular faces in a new deltahedral cluster (Figure 5, structures 5-7). This may account for the shortage of synthetic methods which can hardly result from principles used in organic chemistry.

Because of the approximate sp³ hybridization of the individual B atoms, triangles joined at an edge contain an obtuse angle (see 5). An increase in the number of triangles in the boron skeleton causes it to acquire the shape of a nest (6) and ultimately to produce a closed deltahedral skeleton (7). Further examples can be found in the general skeletal system (cf. Figure 6).

According to Lipscomb's topological concept,⁴² neutral boron hydrides B_nH_{n+m} consist thus of *n* BH vertices (in topological formulae symbol O) and *m* extra hydrogens (H) and can be described by one or more valence structures, composed of *s* H bridges (⌒), *t* three-center bonds (—<), *y* classical bonds (—), and *x* endo-terminal hydrogens (⊙). Accordingly, each borane can be described by one or several *styx* formulae. Mutual ratio of the number of individual bonds in each *styx* formula follows from three equations, expressing the balances of vacancies filled by the formation of *s*, *t*

class	closo	$\frac{+2e}{-2E}$	nido	$\frac{+2e}{-2E}$	arachno
general formula	B _n H _n ²⁻		B _n H _n ²⁻		B _n H _n ²⁻
number of edges	3 <i>n</i> - 6		3 <i>n</i> - 8		3 <i>n</i> - 9
open faces	no		pentagon or two squares		hexagon

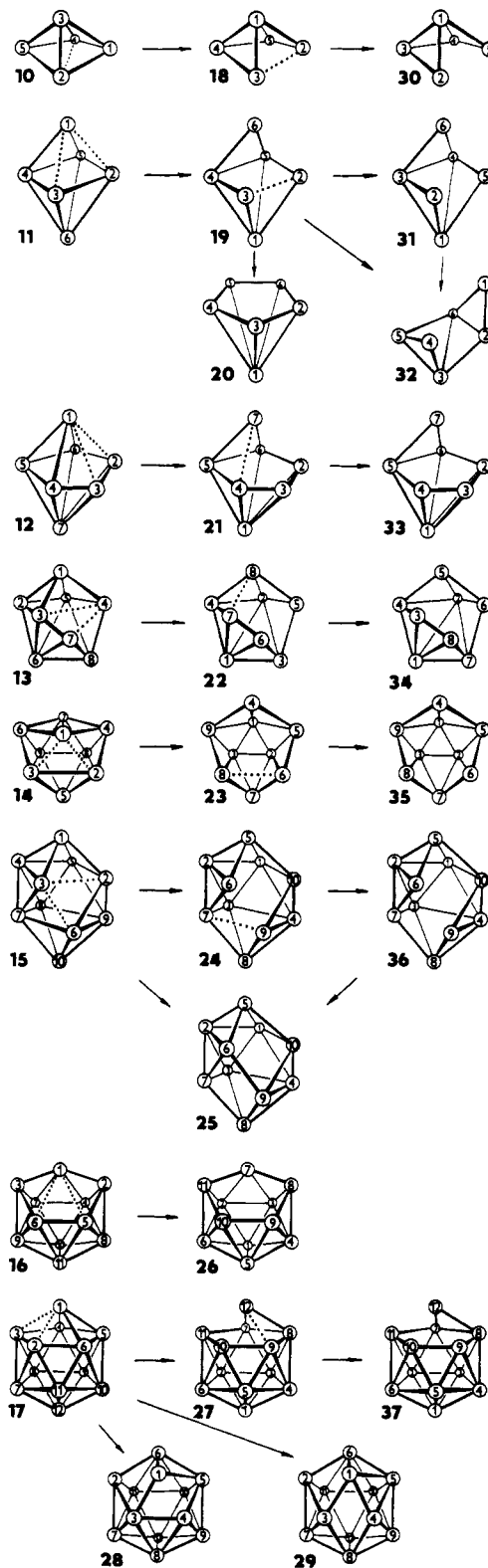


Figure 6. "Seco principle". Systematization of prototypes of boron clusters according to the stepwise addition of electrons pairs as reflected in the elimination of skeletal edges (E); - - - edge to be taken off.

bonds (eq 1), of surplus hydrogen atoms accommodated in *s,x* bonds (eq 2), and of skeletal electrons in *t,y* bonds (eq 3).⁴²

$$s + t = n \quad (1)$$

$$s + x = m \quad (2)$$

$$t + y = n - m/2 \quad (3)$$

A brief explanation of the deduction of eq 3 is deserved: the number of electrons in *t + y* bonds with two electrons in each of them (i.e. 2(*t + y*) electrons) equals the total of bonding electrons brought by *n* boron atoms (3*n* electrons), diminished by electrons which the boron atoms use for binding all H atoms (*n + m*), namely:

$$2(t + y) = 3n - (n + m)$$

which after adaptation reduces to eq 3.

As an illustration, borane B₅H₉ (8) must incorporate five three center bonds (*n* = 5) with a maximum of four hydrogen bridges (*s* ≤ *m* = 4). The allowable *styx* formulae are therefore 4120, 3211, and 2302. The proton NMR spectra reveal the presence of four hydrogen bridges in B₅H₉, which prefers the 4120 formula. On the planar projection of this topological formula (Figure 4b), we can see the possibility of the existence of several canonical formulae and we can understand a delocalization of skeletal electrons on the surface of the tetragonal pyramid (Figure 4c).

A consequence of the delocalization of electrons is a pseudoaromatic character of borane compounds. This "aromaticity" is based on the *delocalization of the formally insufficient number of skeletal electrons*, and it is therefore dramatically different from the "classical aromaticity" originating in the *delocalization of surplus π-electrons*. With an increasing number of skeletal boron atoms, the number of possible valence-bond structures grows rapidly and reflects an increasing delocalization of skeletal electrons. This delocalization is greatest with closo compounds which can be advantageously described in terms of MO theory.^{42,43} These compounds can be therefore treated as molecules composed of (i) sp³-hybridized B atoms (when speaking on a deviation of sp³ bonding orbitals from 109° in tetrahedron) and/or (ii) atoms with p_x, p_y, and p_z atomic orbitals (when speaking on the transfer of electrons between the atomic orbitals evoked by +M substituents or by heteroatoms).

An important characteristic of boron compounds of the general formula B_{*n*}H_{*n+m*}^{*x-*}, is the number of skeletal electrons 2*n* + (*m + x*). This permits a systematization of polyboranes into the closo (2*n* + 2 electrons), nido (2*n* + 4), arachno (2*n* + 6), and hypho (2*n* + 8) classes.⁴⁴⁻⁴⁶ The stepwise acquisition of electron pairs to the closo species may be envisaged either as a successive elimination of vertices (the "debor principle")⁴⁴⁻⁴⁶ or, more recently, as a successive elimination of deltahedral edges (the "seco principle")⁴⁷ (Figure 6), resulting in the formation of the prototypes B_{*n*}H_{*n*}⁴⁻, B_{*n*}H_{*n*}⁶⁻, and B_{*n*}H_{*n*}⁸⁻ with increasingly opened skeletons.

The "seco" systematization is closer to the chemist's thinking style, showing structural changes arising from redox interconversions. According to this scheme, the successive opening of closo to nido, arachno, and hypho structures caused by the addition of two, four, and six

electrons requires a stepwise elimination of two, three, and four edges, respectively (cf. Figure 6, dashed lines represent edges to be removed). Due to the fact that this known principle has not been published as a concept,⁴⁷ some advantages of it will be mentioned.

The "seco" principle allows one:⁴⁷

1. To reject an ungrounded identity of nido and arachno ten-vertex skeletons which both are visualized as 36;⁴⁵ instead, new nido structures as 24 (considered as an intermediate in alkaline conversion of 6-ClB₁₀H₁₃ to B₁₀H₁₀²⁻),⁴⁸ and 25 can be now proposed.

2. To deduce at least three twelve-vertex nido skeletons namely 37,⁴⁹ 29,⁵⁰ and 28.

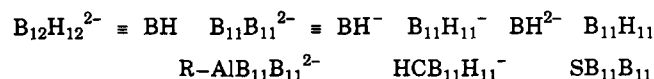
3. To propose the existence of further nido skeletons not accessible by the "debor" route, e.g. 19 and 33.

4. To consider an edge tautomerism, e.g. an interconversion of 28 to 29, and further -2E twelve-vertex analogues (i.e. analogues which all originated by an elimination of two edges from the closo precursor), which can cause an averaging of some NMR signals and, consequently, an apparent increase in symmetry of some skeletons.

5. To describe appropriate molecules analogously as it is performed with organic compounds, namely by indicating the positions and the number of eliminated edges, e.g. (1,2;3,4-diseco)dodecahydrododecaborate(2-) (29). This nomenclature concept can replace the less suitable "debor" nomenclature descriptions with which the number of locants is sometimes higher than the number of actual vertices and desorientates the reader. In this paper, the "seco" principle is systematically used.

If geometric relations among the redox classes shown in Figure 6 are valid then *nido prototypes exhibit one pentagonal or two square open faces while arachno prototypes show the hexagonal one*. These considerations are not an end in itself for they indicate the connectivity (i.e. the number of adjacent skeletal atoms) of each vertex, which significantly influences their NMR chemical shifts (vide infra).

The multicharged prototypes B_{*n*}H_{*n*}^{*x-*} with *x* ≥ 4 in Figure 6 represent rather hypothetical anions, but their derivatives with one or several electron-rich heteroatoms (C, N, S, etc.) in individual vertices, i.e. their less-charged or uncharged heteroanalogues, may theoretically exist, and many of these species are known. Basic molecules of boranes and their derivatives may be, namely, envisaged as composed of three types of sp³-hybridized BH units, each of them providing the skeleton with three bonding skeletal orbitals (lobes) and with two (HB:), three (HB:-) and four (HB::²⁻) skeletal bonding electrons. Besides, vertices H₂B:- with two bonding lobes and two skeletal electrons are also common. These vertices can be substituted by *isoelectronic* and *isolobal* heteroatoms directing the same number of skeletal electrons and lobes to the skeletal sphere and to the exo position(s). The examples of the permutable vertices⁴⁴ are shown in Table 2. Any polyhedral skeleton can be formally split to several moieties, e.g.



the individual BH^{*n-*} vertices of which can then be substituted by various heteroververtices as indicated in the lower line. Molecules with two-, three, etc. heteroververtices can be deduced similarly.

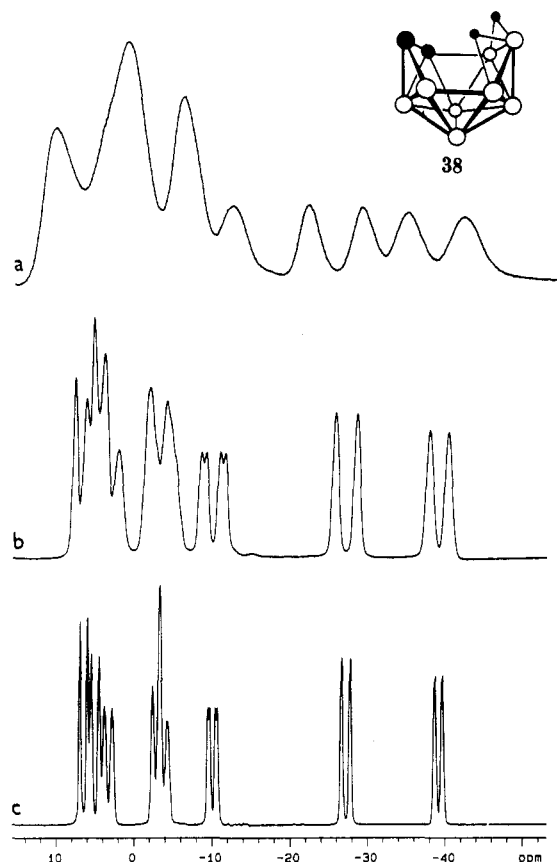


Figure 7. Proton-coupled ^{11}B NMR spectra of the $5,6\text{-C}_2\text{B}_8\text{H}_{12}$ carborane in CDCl_3 measured at (a) 25.7, (b) 64.2, and (c) 160.4 MHz.

TABLE 2. Mutually Interchangeable sp^3 Vertices (■ = free electron pair)

:BH	:BH ⁻	:BH ²⁻	:B<sup>-H
CH ⁺	CH	CH ⁻	C<sup>-H
AlH	SiH	N ■	N<sup>-H
GaH	GeH	P ■	P<sup>-H
(InH)	SnH	As ■	S<sup>-H
	PbH	Sb ■	Se<sup>-H

Due to the outstanding ability of boron frameworks to accommodate the majority of elements in the place of one or several BH vertices in the parent molecule, we can suggest the existence of an enormous number of hetero analogues. Also with them, in the case they should be prepared, the NMR chemical shifts of individual skeletal atoms will be important information on the electronic changes which emerged.

III. NMR Techniques for Structural Analysis of Boron Clusters

With the advent of new NMR techniques, the "legibility" of ^{11}B NMR spectra has improved greatly. For the majority of one or two cluster boron com-

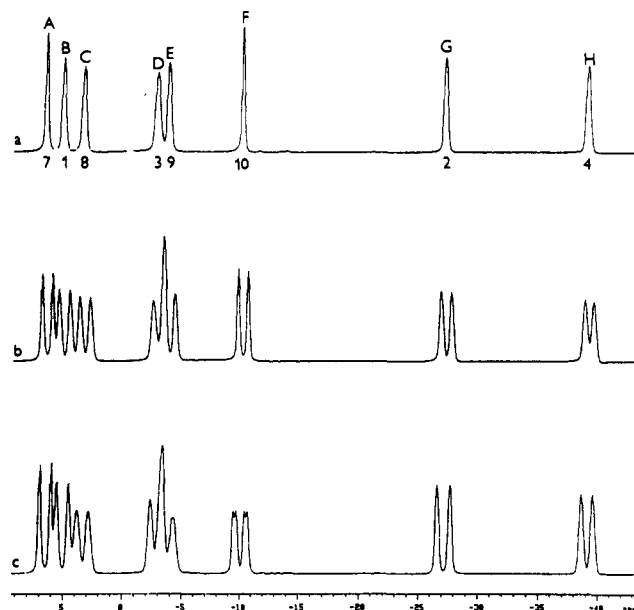


Figure 8. ^{11}B NMR spectra of $5,6\text{-C}_2\text{B}_8\text{H}_{12}$ in CDCl_3 : (a) ^1H decoupled; (b) selectively decoupled by the μH frequency; (c) undecoupled.

TABLE 3. NMR Characteristics and Assignments of Individual Atoms at $5,6\text{-C}_2\text{B}_8\text{H}_{12}$ (38); in CDCl_3 , at 160.5 MHz

signal	vertex	$\delta(^{11}\text{B})$	$J(^{11}\text{B}^1\text{H})$	$\delta(^1\text{H})$
A	B(7)	6.49	146 ^d	3.53
B	1	5.01	159 ^d	3.53
C	8	3.31	159 ^d , μH	3.13
D	3	-2.83	159 ^d	2.95
E	9	-3.79	165 ^d , 30^{tr}	3.13
F	10	-10.11	155 ^d , 50^{d}	2.63
G	2	-27.20	183 ^d	1.04
H	4	-39.15	153	0.78
	CH(6)			6.48
	CH(5)			4.98
	μH			-2.22
	μH			-2.48

pounds, the magnetic field of 11.5 T (500 MHz for ^1H , 160.5 MHz for ^{11}B) is strong enough to get well-separated signals, affording necessary information. For illustration, the informative quality of ^{11}B undecoupled spectra of the unsymmetrical carborane $5,6\text{-C}_2\text{B}_8\text{H}_{12}$ (38) at 25.7, 64.2, and 160.4 MHz are shown in Figure 7.

With compound 38, a general approach to the elucidation of boron cluster structures on the basis of ^{11}B , ^1H , and two-dimensional spectra, obtained by means of commercially available NMR techniques, will be demonstrated. The proposal of the structure and the assignment of individual signals stems successively from the following:

- The ^{11}B spectra (Figure 8), namely of
 - ^1H broad-band decoupled spectrum
 - ^{11}B spectrum, decoupled selectively by the frequency of μH signal at -2.4 ppm
 - undecoupled spectrum

These spectra show that the measured B compound is composed of eight different BH vertices (from the coupling $J(^{11}\text{B}\text{-}^1\text{H}) > 120$ Hz) of equal intensity (i.e. the molecule has no element of symmetry), the characteristics of which are given in Table 3.

μH broadenings of signals C (a higher intensity in spectrum b when compared with spectrum c in Figure 8), E (by two μH bridges, as indicates the quartet-like

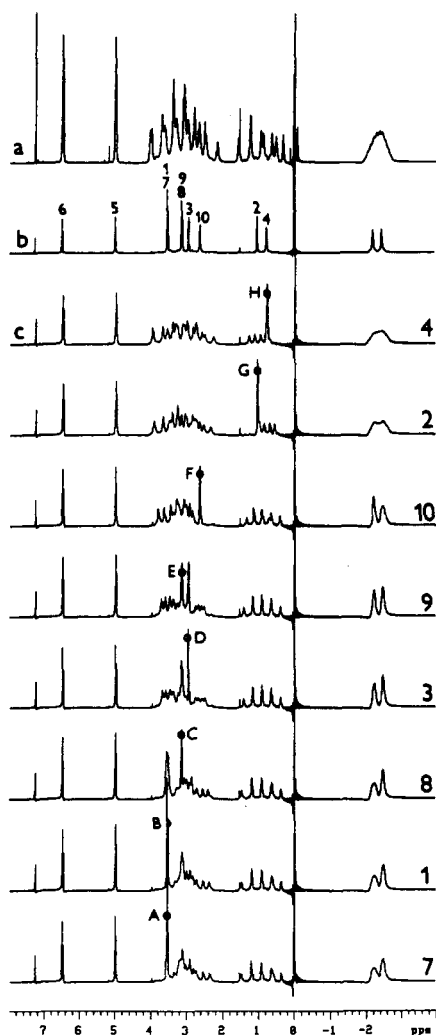


Figure 9. ^1H NMR spectra of $5,6\text{-C}_2\text{B}_8\text{H}_{12}$ in CDCl_3 : (a) undecoupled; (b) ^{11}B broad-band decoupled; (c) successive ^{11}B selectively decoupled by the frequencies of the A-H signals (A on the bottom).

character frequent at $\mu\text{H-B-}\mu\text{H}$ B atoms), and F (significant μH splitting characteristic of B atoms adjacent to a skeletal C atom)⁵¹ confirm the presence of, at the minimum, two H bridges and locate the C, E, and F boron atoms in the open face of the molecule. An open-cluster character follows also from the spectrum span (see Figure 1).

2. The ^1H NMR spectra (Figure 9) of

(a) undecoupled

(b) $\{^{11}\text{B}\}$ broad-band decoupled

(c) selectively $\{^{11}\text{B}\}$ decoupled using precise frequencies of eight individual A-H ^{11}B nuclei.

According to these spectra, the observed molecule contains two (C)H carborane signals unperturbed by ^{11}B decoupling at 6.479 and 4.983 ppm and two slightly different H bridges, each of the intensity one, and eight (B)H signals (see Table 3) bound to appropriate A-H boron atoms. No other H signals (with the exception of CHCl_3 and TMS [7.2, 0.0 ppm, respectively]) are present. Provided that no other atoms are present, the formula of the B compound is $\text{C}_2\text{B}_8\text{H}_{12}$ with two μH bonds and no BH_2 group, i.e. of topology 2640.

3. The 2D NMR spectra, namely of

(a) $^{11}\text{B-}^{11}\text{B}\{^1\text{H}\}$ spectrum (Figure 10a) which shows a set of cross-peaks (i.e. bonding interactions) among

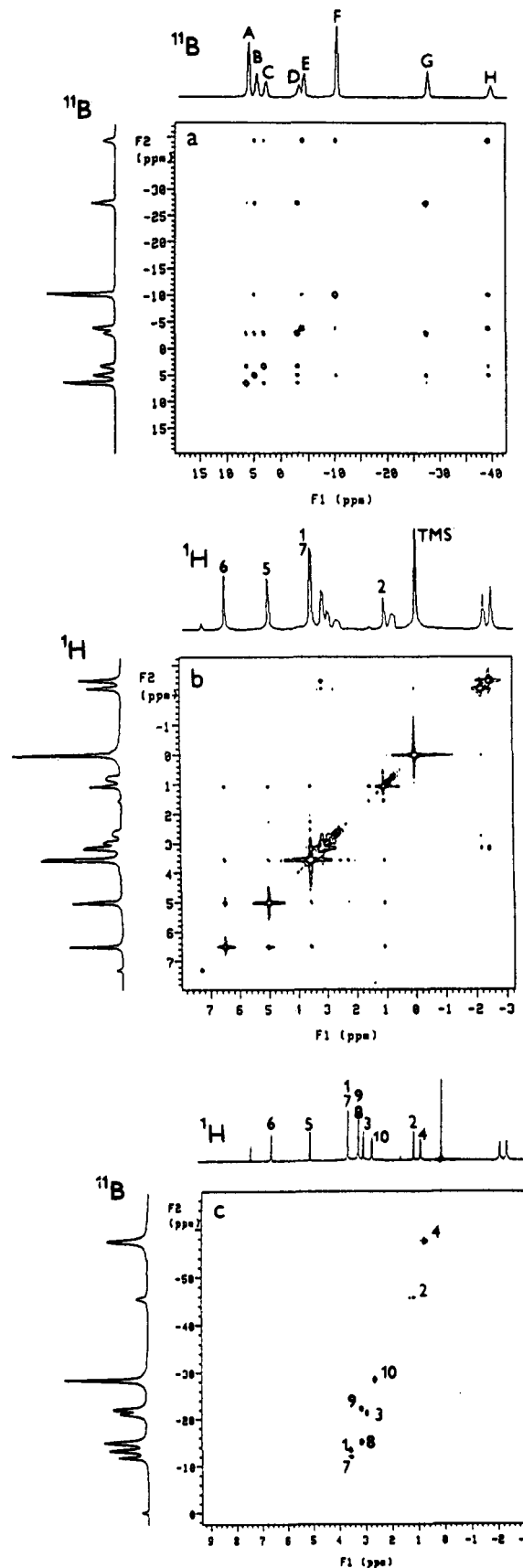


Figure 10. Two-dimensional $^{11}\text{B-}^{11}\text{B}$ NMR spectra of $5,6\text{-C}_2\text{B}_8\text{H}_{12}$ in CDCl_3 : (a) $^{11}\text{B-}^{11}\text{B}\{^1\text{H}\}$; (b) $^1\text{H-}^1\text{H}\{^{11}\text{B}\}$; (c) $^1\text{H}\{^{11}\text{B}\}\text{-}^{11}\text{B}\{^1\text{H}\}$.

individual boron atoms A-H (Figure 11a), of which a B-B network can be drawn (Figure 11b). The missing cross-peak D-H follows unambiguously from other connections. As stated on the basis of the μH decoupled

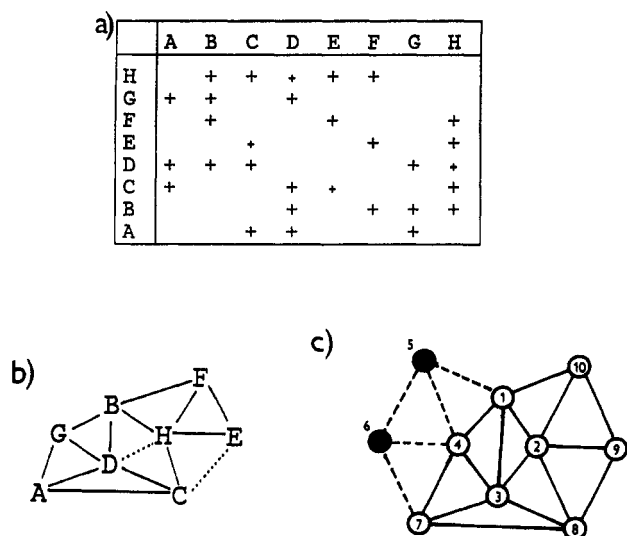


Figure 11. (a) Scheme showing cross-peaks between individual B-atoms: +, strong interaction; +, weak interaction. (b) Boron network constructed from the found interactions. (c) Connections found in the B-B (—) and H-H (---) 2D NMR spectra.

^{11}B spectrum (Figure 8b), atoms C, E, and F bear μH and must be located in the open face, with E between two H bridges.

(b) The $^1\text{H}\text{-}^1\text{H}\{^{11}\text{B}\}$ spectrum (Figure 10b) which indicates connections between C-C vertices in which both are bound to boron G, and one of them to A, the other one to B (Figure 11c). From these conclusions, the structure of **38** and assignments of individual signals presented in Table 3 confirm both the structure and assignments published earlier.^{52,53}

(c) The $^1\text{H}\{^{11}\text{B}\}\text{-}^{11}\text{B}\{^1\text{H}\}$ 2D spectrum which fully confirms the pertinence of appropriate H atoms to their B partners deduced from spectra in Figure 9c.

In this way, a majority of structures of new compounds and the assignments of their individual NMR signals can be performed. This method enabled us to confirm the reliability of all ^{11}B NMR rules or regularities which will be discussed in the next paragraphs.

IV. Chemical Shift

The most informative characteristic of an NMR-active nucleus is its chemical shift which reflects^{54,55}

(1) Its bonding surroundings, i.e. coordination, hybridization, bond angles, π bonding, etc.

(2) The charges on individual atoms originating from their positions in the skeleton, inductive, and mesomeric effects of terminal substituents, electronegativity of skeletal heteroatoms, etc.

(3) The magnetic anisotropy of neighboring groups, i.e. the effect of heavy nuclei, "ring current", etc.

The NMR behavior of atoms forming deltahedral cages (B, H, C) is, however, so unusual that experiences extrapolated from organic compounds with classical structures are of limited use. In particular, present knowledge does not allow us to state reliably which of the nuclei present in the borane molecule will resonate at low frequency and which at high frequency in a given ^{11}B , ^1H and ^{13}C spectrum. (Due to a definitive change in NMR technique, using now largely a constant magnetic field and changing frequency, the specification "high" and "low" frequency for "low" and "high" shielded nuclei, respectively, are used.) Due to these

and other peculiarities, boron was labeled as the enfant terrible of the periodic table.⁵

Basic theory of chemical shifts of NMR active nuclei was developed by Ramsay^{54a} and later modified by Pople,^{54b} using an independent electron model where two-electron terms vanished. According to this, the nuclear screening is expressed as the sum of five terms in eq 4:

$$\sigma = \sigma_d^L + \sigma_p^L + \sigma_p^N + \sigma_d^N + \sigma_s \quad (4)$$

which are the local diamagnetic and paramagnetic, neighboring paramagnetic and interatomic diamagnetic, and solvent shielding contributions, respectively.

Both boron isotopes belong to the heavier nuclei whose chemical shifts are primarily governed by the paramagnetic "deshielding" σ^p term, for the calculation of which a number of equations have been proposed.^{54,55}

The whole concept of the ^{11}B chemical shifts of skeletal atoms in B clusters is consistent through this review and is based on four factors which have clear chemical meaning and are generally acceptable: (a) hybridization of each atom in question; (b) the magnitude of bond strains around each skeleton atom; (c) electron density on each vertex; and (d) distribution of bond electrons around the observed nucleus. All these factors are involved in an Average Excitation Energy (AEE) method,⁵⁴ whose expression for an individual atom A is given by eq 5:

$$\sigma_{p(A)}^L = -\frac{\mu_0 e^2 h^2}{6\pi m^2 \Delta E} \langle r^{-3} \rangle_{2p} P_u \quad (5)$$

In eq 5, three variables are present: ΔE which is the average excitation energy, $\langle r^{-3} \rangle_{2p}$ which expresses the size (proportional to the electron density) of 2p orbital and is called occasionally "the orbital expansion term", and P_u which describes the elements of the bond-order charge-density matrix, i.e. populations of the 2p orbitals and a p-electron "imbalance" about the nucleus in question.

The minus sign in eq 5 indicates that an increase in the paramagnetic shielding $\sigma_{p(A)}^L$ causes, in reality, deshielding of the observed nucleus and, consequently, a shift of the signal to higher frequencies (i.e. to "lower magnetic field"). This equation is oversimplified but allows with sufficient reliability one to estimate for each nucleus in the observed molecule the trends and extent of deshielding which is evoked by the discussed three main terms and increases with (1) decreasing average excitation energy ΔE of the whole molecule; (2) decreasing electron density in the 2p orbitals ($\langle r^{-3} \rangle_{2p}$) of individual atoms in a given molecule [factor c]; and (3) increasing p-electron "imbalance" P_u , i.e. the asymmetry of the distribution of bonding electrons around the ^{11}B nucleus [factors a, b, and d].

With individual B-cluster compounds, the ΔE term can be considered constant for all skeletal atoms within the observed molecule. A very low influence of ΔE can therefore be expected for closo compounds absorbing in UV under 220 nm (high ΔE) on which transmissions of electrons were studied. Heteroatoms with lone-pair electrons tend to have ΔE dominated by relatively low energy $n \rightarrow \pi^*$ transitions.⁵⁴ The same holds for a series of structurally related molecules.⁵⁴

In order to find which of the two remaining variables ($\langle r^{-3} \rangle_{2p}$ and P_u) plays a dominating role, we have com-

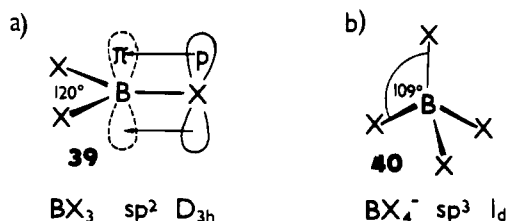


Figure 12. Measure of bonding electrons anisotropy ("imbalance"): (a) very high anisotropy for BX_3 without $p-\pi$ interaction (B, H, R) due to very different angles between filled orbitals (120° in plane, 180° over plane), a decrease in anisotropy with successive filling of the vacant π orbital; (b) a very low or zero anisotropy for BX_4^- of I_d symmetry.

pared hundreds of ^{11}B NMR spectra of basic skeletons and their derivatives that differ by one perturbation element (heterovertex or substituent). The aim was to find common denominators for signals located at the highest or lowest frequencies. Successively, hybridization, bond angles, electron density on individual skeletal atoms, structural features, distribution of bonds within the skeleton, and effect of substituents, ligands, and heteroatoms were analyzed from this point of view, and their importance was stated.

In the course of this long-term investigation, several empirical rules were defined and their reliability was systematically checked.¹¹ These rules are now a basis for the evaluation of individual factors and, consequently, for the explanation of principles governing the chemical shifts of skeletal ^{11}B nuclei and, analogously, the chemical shifts of further skeletal nuclei, such as ^{13}C , ^{29}Si , ^{32}P , etc.

A. Hybridization

1. Tri- and Tetracoordinated Compounds

Hybridization is one of the most important factors influencing the chemical shift. This is well documented in compounds of carbon (^{13}C NMR), with which a change from sp^3 to sp^2 hybridization causes a shift of ca. 100 ppm to lower frequencies. A similar shift dependence can also be observed for the ^{11}B nucleus.

In contrast to carbon, boron can form stable tri-coordinated compounds BX_3 , showing the sp^2 arrangement of substituents (39, Figure 12). In the case that substituents X do not bear a free electron pair (e.g. X = H, R), the fourth orbital can remain unoccupied (vacant), which results in a great "imbalance" (term P_u) of bonding electrons around the observed ^{11}B nucleus and, consequently, a large shift to high frequency (80–120 ppm). In contrast, the same substituents in the tetracoordinated anions BX_4^- (40) exhibit a very symmetrical I_d arrangement, i.e. the paramagnetic contribution P_u vanishes, which results in minimum deshielding originating from this very important factor. The ^{11}B chemical shifts of BX_4^- anions depend therefore primarily on the shielding quality of substituents R lacking a free electron pair (cf. Table 4).

On the other hand, substituents possessing a free electron pair can interact with the unoccupied boron orbital, decreasing the "imbalance", i.e. lowering the "deshielding" (Figure 12). The stronger the $p-\pi$ interaction, the more the orbital electrons approximate the D_{3h} symmetry, and the signal of BX_3 species in the spectrum approaches the signal of the related anions BX_4^- . With the first- and second-row elements as

TABLE 4. ^{11}B Chemical Shifts of sp^2 (BX_3) and sp^3 (BX_4^-) Hybridized Boron Atoms [$\delta(^{11}\text{B})$ in ppm, $\Delta = \delta(sp^2) - \delta(sp^3)$]^a

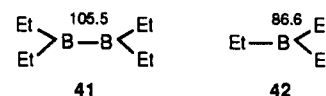
X	$sp^2(BX_3)$	ref	$sp^3(BX_4^-)$		Δ	
				ref		
CH_3	86.2 ^a	56	-20.2 ^a	Li^+	56	106.4
C_2H_5	86.6 ^a	56	-17.5 ^a	Li^+	56	104.1
<i>n</i> - C_3H_7	86.6 ^a	56	-17.5 ^a	Li^+	56	104.1
<i>n</i> - C_4H_9	86.5 ^a	56	-17.6 ^a	Li^+	56	104.1
C_6H_5	68.0 ^c	5	-6.7 ^b	K^+	57	74.7
$\text{CH}=\text{CH}_2$	56.4	58	-16.1 ^e	Li^+	56	72.5
I	-7.9 ^a	59	-127.5 ^c	NBu_4^+	56	119.6
Br	38.7 ^a	59	-23.8 ^c	NEt_4^+	56	62.5
Cl	46.5 ^a	59	6.7 ^c	CPh_3^+	56	39.8
F	10.0 ^a	59	-1.6 ^c	CPh_3^+	56	11.6
NHMe	24.6 ^f	60	0.2 ^f		60	24.4
OH	18.8 ^g	5	1.1 ^h	Na^+	60	17.7
OCH ₃	18.3 ^m	60	2.7 ^m	Li^+	60	15.6
SPh	61.6 ^r	62	6.3 ^r	NHET_3^+	62	55.3

^a Today current commercial pulse-FT spectrometers provide us with the frequencies of resonance signals which can be readily converted to δ values. Most data obtained with these spectrometers are of this origin. All compounds measured by the author were recorded using an external capillary with $\text{B}(\text{OMe})_3$ ($\delta = 18.1$ ppm) in order to circumvent the influence of temperature, solvent and concentration on the values of the ^{11}B chemical shifts. Abbreviations for solvents (superscripts to δ values): ^a pentane, hexane, methylhexane (hydrocarbons); ^b benzene; ^c dichloromethane; ^d chloroform; ^e diethyl ether; ^f tetrahydrofuran; ^g glyme; ^h acetone; ⁱ acetonitrile; ^j carbon disulfide; ^k H-halogen; ^l deuterium oxide, water; ^m methanol; ⁿ neat; ^p dimethylformamide; ^r not stated; ^s Me_2O .

substituents, the differences $\Delta = \delta(sp^2) - \delta(sp^3)$ (Table 4) very nicely reflect the measure of $p-\pi$ interactions, due to the fact that other factors are here greatly eliminated.¹²

High Δ values for bromine and, especially, for iodine are primarily caused by the additive character of their B-X bond magnetic anisotropy contribution. From the differences in chemical shifts accompanying the introduction of heavier halogens in the $BX_{4-n}Y_n$ series (X, Y = F, Cl, Br, I),⁶³ the increase in shielding evoked by the magnetic anisotropy of the fourth halogen atom introduced can be estimated: Cl, 0 ppm; Br, ca. -10; and I, > -45 ppm. By the subtraction of these values, more real increments Δ of ca. 50 and 75 ppm can be considered for bromine and iodine, respectively.

In contrast, the lowest $p-\pi$ interaction can be found with R_2B substituent (41) which shows minimum hyperconjugation, if any, when comparing with the alkyl group (42).⁶⁴



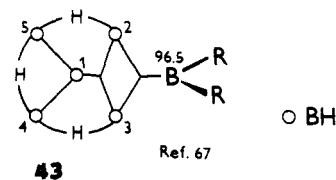
In this way, the following order of increasing $p-\pi$ interactions results: $\text{B} < \text{R} < \text{C}=\text{C} \leq \text{Ph} < \text{I} < \text{Br} < \text{Cl} < \text{NR}_2 < \text{OR} < \text{F}$. This order is somewhat different from that indicating the C-X interactions and used in organic chemistry, but corresponds well with stabilization energies calculated for H_2BX species (X = $\text{BH}_2 < \text{CH}_3 < \text{NH}_2 < \text{OH} < \text{F}$)⁶⁵ as well as with observations, based on the $p-\pi$ back-bonding (e.g. the measure of the antipodal effect of these substituents, cf. section IV. D.1).

2. B-Cluster Compounds

In boron skeletons, the boron atoms are rarely sp^2 hybridized, except when a BX_2 group is attached to two basal atoms by a three-center two-electron bond, as in

TABLE 5. *closo*-Hydroborate Anions $B_nH_n^{2-}$ ^{11}B NMR Characteristics (those from the first reference are presented)^a

<i>closo</i> - $B_nH_n^{2-}$ <i>styx</i>	structure	B	$\delta(^{11}B)$	J_{BH}	atom charge ⁴⁰	ref
$B_6H_6^{2-}$ 0430	11	1-6	-13.6	122	-0.11	38; 3, 70
$B_7H_7^{2-}$ 0530	12	2-6 1, 7	-0.2 -22.6	119 120	-0.11 -0.01	71; 3, 73
$B_8H_8^{2-}$ 0630	13	2, 8 1, 3, 4, 7	9.5 -3.6			72; 3, 38, 73
C_{2v} D_{4d}	-32 °C 25 °C	5, 6 1-8	-22.2 -6.8			72; 3
$B_9H_9^{2-}$ 0730	14	4, 5, 6 1-3, 7-9	-2.9 -20.5	135 120	-0.10 -0.01	74; 3, 71 75
$B_{10}H_{10}^{2-}$ 0830	15	1, 10 2-9	0.89 ^{1D} -30.86	141 124	-0.08 -0.03	32; 3, 76 77
$B_{11}H_{11}^{2-}$ 0930	16	1-11	-16.95 ^m	130		78; 3, 71 79
$B_{12}H_{12}^{2-}$	17	1-12	-15.63 ^b	124	-0.02	32; 80 81

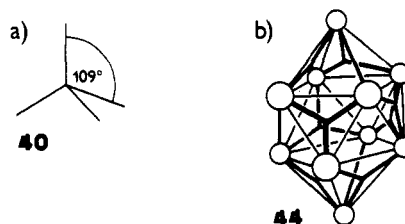
^a See Table 4 for solvent abbreviations.Figure 13. Topological formula and NMR characteristics of μ - $BR_2B_5H_8$ (43) and δ of parent B_5H_5 (60).

B	43 δ	J_{BH}	60 δ
1	-33.3	175	-51.8
4, 5	-4.4	162	-12.5
2, 3	-10.4	162	-12.5
μ - BMe_2	+96.5	-	

μ - $BR_2B_5H_8$ (43) (Figure 13). Although tetracoordinate, the bridging boron is sp^2 hybridized and therefore resonates at extremely high frequency (96.5 ppm).^{66,67} The replacement of μ - R_2B for a μ H bridge shows an interesting feature: a significant shift of the apex B(1) atom downfield by 18.5 ppm,⁶⁷ which indicates a dramatic change in the symmetry of electron distribution around this atom (Figure 13).

On the other hand, the majority of boron vertices in B-cluster compounds are formally sp^3 hybridized, irrespective of their tetra- to heptacoordination. In this respect, it is instructive to present here the $B_nH_n^{2-}$ class of anions 10-17 which are representative of the fundamental *closo* skeletons. All of these cages can be constructed from n sp^3 -hybridized B atoms, $n - 2$ three-center B^B_B , and 3 classical B-B bonds.^{40,68,69} Comparison of these compounds illustrates the difficulties encountered in searching for regularities. The first member $B_5H_5^{2-}$ has not been reported and the B_8 and B_{11} analogues are highly fluxional and thus average to single signals (see section IV.E). Thus, of eight candidates, only B_6 , B_7 , B_9 , B_{10} , and B_{12} homologues afford ^{11}B NMR spectra which correspond to static structures (Table 5).

Quantum chemical calculations⁴⁰ as well as rough estimates based upon *styx* formulae⁴² indicate that the atom charges in $B_nH_n^{2-}$ drop from a tetracoordinated (-0.23 electrons) to a penta- (-0.08 to -0.11) and to a hexa- (-0.01 to -0.03) coordinated B atom. A look at Table 5, however shows that, contrary to expectation, the B atoms of higher electron density resonate at higher (!) frequency in given *closo* anions. This indi-

Figure 14. (a) sp^3 arrangement and bonding angles, and (b) one of the canonical formulae composed of the *t,y* bonds in the *closo*- $B_{10}H_{10}^{2-}$ molecule.

cates that a more important factor which overrides electron density must be involved in the $B_nH_n^{2-}$ class.

Such a factor has been found¹¹ in the measure of the deviation of an " sp^3 -hybridized" skeletal atom from T_d symmetry (40) with a bonding angle of $109^\circ 29'$. The *closo* cages 10-17 are composed of trigonal, tetragonal, pentagonal, and hexagonal pyramids with one orbital pointing radially out of molecule. The three remaining orbitals of the apex atom form a skeletal bonding cone composed of *t* and *y* bonds. For example in $B_{10}H_{10}^{2-}$ (44) it can be demonstrated that the classical bonds can only be located in the edges while three-center bonds point to the centers of triangles (Figure 14).

Angles α and β , formed by the B-H bond and by the edge or plane orbital (45) and calculated for ideal pyramids composed of equilateral triangles, are shown in Table 6. Deviations from 109° show also angles γ between endo orbitals pointing out to the bases of the idealized tri- to pentagonal pyramids (Table 6). The γ angles were calculated provided that the combination of all three classical and three-center bonds bonding three to five basal B atoms together is a result of many canonical formulae, the result of which is an equidistant distribution of three endo orbitals in the "umbrella-like" arrangement. When taking into account all deviations in individual molecules within the *closo* series 10-17, we see that the deviation from the ideal angle of ca. 109° increases in the order: pentagonal < tetragonal < trigonal pyramid. The same trend can be expected in the increase of the paramagnetic component, i.e. in the "imbalance" of bonding electrons and, consequently, in the "deshielding" of individual skeletal atoms. The chemical shifts of B vertices in Table 5 are in agreement with this idea.

These conclusions are in agreement not only with the chemical shifts exhibited in the *closo* anions mentioned

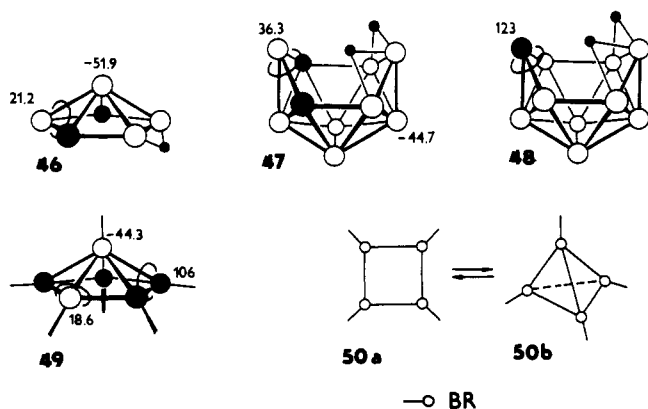


Figure 15. Narrowed bonding cones (noted by ellipses) resulting in high-frequency resonances of the ¹¹B and ¹³C atoms of connectivity 4 in carboranes 46,⁸² 47,⁸⁴ 48,⁸⁵ and 49.⁸⁸

TABLE 6. Bond Angles between Exo-Orbital and the Orbital in the Edge (α) and in the Plane (β) at Individual n -Gonal Equilateral Pyramids in 45a and Averaged "Umbrella" Angles γ between Endo-Orbitals of Symmetry C_{3v} in n -Gonal Equilateral Pyramids 45b

n	45a		45b
	α	β	
3	144	160	60
4	135	144	66
5	121	127	80

above but also with some "unexpected" shifts to high frequencies of skeletal B and C atoms in the open faces, cf. compounds 46–49 (Figure 15).

The greatest ¹¹B chemical shift of skeletal B atoms to high frequency in nonmetallic B clusters known to the author was observed with the *t*-Bu₄B₄ species (50, δ = 135.7 ppm)⁸⁶ which can be considered either as substituted cyclotetaborane (50a) or tetraheder (50b) (Figure 15). In both structures, a high deviation of bonding angles combines with further factors which all act in the same sense, namely: (a) presence of only $2n$ skeletal electrons in contrast with $2n + 2$ electron count customary for *closo*-hydroborates B_{*n*}H_{*n*}²⁻; (b) strong effect of alkyl group shifting the substituted (α) boron to high frequency by ca. +20 ppm; (c) additive vicinal effect of three neighboring alkyls (cf. section IV.D.1.f).

When comparing the difference of only 32 ppm caused by bonding angle deviations in sterically strained and nonstrained cyclohydrocarbons [δ (¹³C) C₃H₆ -3.5 ppm, C₄H₈ 22.4, C₆H₁₂ 26.9, C₇H₁₄ 28.5]⁸⁷ we see that both boron and carbon vertices in deltahedral cluster compounds are substantially more sensitive to these deviations. This follows from the differences of almost 90 ppm between ¹¹B signals in trigonal arrangement (36.3 ppm in 47) and in pentagonal arrangement (-51.9 ppm in 46) and from the ca. 68-ppm difference between the δ (¹³C) values of C vertices in the asymmetric trigonal fragment (123 ppm at 48) and in the pentagonal arrangement (55.4 ppm in 1,7-C₂B₁₀H₁₂).⁸⁸

The principle of deviate bonding angles affords a plausible explanation for the long known empirical rule of Williams⁸⁹ which relates the chemical shifts and coordination numbers of boron atoms. This rule was

extended to the ¹³C chemical shifts of skeletal carbon atoms by Todd⁹⁰ and recently exploited by Teixidor et al.⁹¹ (see section IV.E).

B. Electron Density on Skeletal Atoms

With the exception of a few highly symmetrical species such as B₆H₆²⁻, B₂H₆, B₁₂H₁₂²⁻, and B₄Cl₄, exhibiting one type of B atom in the molecule, boron compounds tend to have uneven electron distributions throughout their molecules. This was mentioned above in the discussion of the *closo* anions, B_{*n*}H_{*n*}²⁻, wherein the negative charge drops with rising connectivity of the boron atoms $3 > 4 > 5 > 6$.⁴⁰ On the other hand, the open-skeleton nonionic boranes B_{*n*}H_{*n+4*} and B_{*n*}H_{*n+6*} incorporate both negatively and positively charged B atoms,⁹² the latter are generally in the open face of the molecule.

These partial charges and, especially, the π -electron density,⁹³ influence two main shielding parameters, i.e. the diamagnetic σ^d and paramagnetic σ^p shielding components.⁵⁴ The influence of electron density on the ¹¹B chemical shift is significant, but as indicated above, it is not the primarily factor.

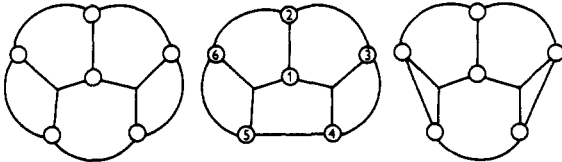
Very recently, a new idea appeared dealing with the relation between δ (¹¹B) and B-vertex electron density. We have found with the *closo*-1-EB₉H₉ and -EB₁₁H₁₁ series (E = BH²⁻, CH⁻, NH, S, etc.) that not all p orbitals⁹³ but mainly the tangential p_x and p_y orbitals are NMR active,^{94,95} and an excellent correlation was obtained between δ (¹¹B) and p_x + p_y electron densities of B-skeletal atoms located in the plane of symmetry. From the slopes in both series it is now possible to deduce that a change in ed of 0.1 e evokes a shift of 30.8 ppm at B(10) in the EB₉H₉ series and 42.9 ppm at B(12) in the EB₁₁H₁₁ series (from CNDO/2 calculations). Similarly, a value of 380 ppm/e was obtained from the correlation of δ (¹¹B) of the B(10) atoms with total atomic (natural) charges [from 3-21 G(*)]⁹⁵ in the former series.

The above results indicate that the sensitivity of the ¹¹B shielding to the changes in ed is high. Such a great charge effect as with the class EB₉H₉ is, however, exceptional and occurs with compounds which amalgamate both a strong perturbation and a high symmetry relation to the couple of vertices in question. In reality, the majority of compounds do not fulfill this condition, and changes brought by a perturbation (e.g. E, X) influence more distinctly the exo direction than the NMR-active tangential p_{xy} orbitals which take part in the delocalization of electrons within the molecule. This is, in our opinion, the reason why ed customarily evokes only relatively small changes in chemical shift (to 15 pp) in B clusters.

These consideration can be documented on the influence of the charge on δ (¹¹B) in the B₆H₁₁⁺ (51), B₆H₁₀ (52), and B₆H₉⁻ (53) series⁹⁶ (Table 7), an analogy of the more extensive ¹³C NMR series, C₃H₃⁺, C₇H₇⁺, C₆H₆, C₉H₉⁻, C₅H₅⁻ and C₈H₈²⁻, with which a change of about 160 ppm/e (for ¹³C) was deduced.⁹⁷

As the δ (¹¹B) values in Table 7 indicate, the differences in charge are evident primarily on the basal atoms. A formal change of two electrons distributed about five basal atoms (i.e. 0.4 e per B) causes a shift of about 11 ppm on each basal boron i.e. 28 ppm per electron. The effect of charge is in reality much greater

TABLE 7. Influence of Electron Density on the ^{11}B and ^1H Chemical Shifts $\delta(^{11}\text{B})$ and Coupling Constants $J(\text{BH})$ with B_6 Series 51–53⁹⁶



	$\text{B}_6\text{H}_{11}^+$ (51)	B_6H_{10} (52)	B_6H_9^- (53)
B(2-6)	20.9 [179]	16.5	10.1
B(1)	-48.7 [173]	-50.9 [155]	-49.3 [137]
H(2-6)	4.9	4.2	3.1
H(1)	0.1	-1.2	-2.4
μH	2.1	-1.1	-4.2

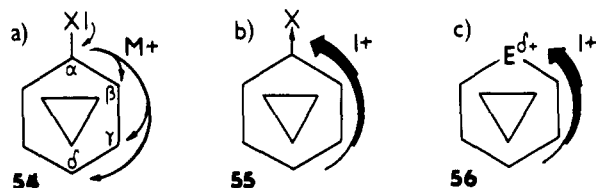


Figure 16. Transmissions of electrons evoked by (a) +M effect of the substituent X; (b) +I effect of the substituent X; (c) +I effect of a positively charged heteroatom E.

since a part of this charge is transferred to the neighboring hydrogen atoms. This is evident from the ^1H signals of B_6 species 51–53 which show a significant decrease in δ on H atoms at 51 and an increase at 53. This, together with the $J(\text{BH})$ values, reflects the ability of both exo and endo B–H bonds to be polarized toward hydrogen which can function as an acceptor or a donor of that portion of electrons which cannot be accommodated at skeletal boron atoms. Chemical shifts of the apex B(1) atoms with all three species 51–53 exhibit minimum changes without any reasonable trend (Table 7) and confirm the idea that of the total increase or decrease in electron density evoked by a perturbing element, only a fraction of this δ takes part in NMR-active orbitals and produces a change in the chemical shift of the skeletal atom considered.

Calculations^{40,92} and other methods⁹⁸ have shown that in most B compounds, the differences in charge on B atoms amount up to 0.15 e. units. Due to this and additional facts discussed above, the charge contribution to the NMR shift of individual skeletal atoms is relatively low, amounting generally to 10 ppm and, exceptionally, to 15 ppm when compared with the parent molecule. This contribution is relatively low when one considers the ^{11}B signals range from 20 to -60 ppm, i.e. 80 ppm in unperturbed boron skeletons.

The effects of charge are relatively small but can be well understood. They reflect among others (Figure 16):

(a) A decrease or an increase in electron density on the edge atoms in open skeleton molecules, caused by the formation or abstraction of a μH bridge (see 51, 53, Table 7).

(b) An enrichment of the whole skeleton in electrons owing to p- π back-donation (54, see sections IV.D.1.b and e):



(c) A transmission of electrons from p_z to p_{xy} orbitals due to the influence of the X substituent bearing

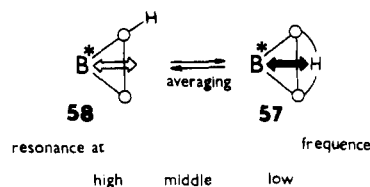


Figure 17. Shielding interactions between the B^* atom and the arrangements: μH bridge (57)—missing μH bridge (58)—fast tautomerizing system on the NMR scale.

free-electron pair(s) (see trans and antipodal effect, section IV.F).

(d) Successive decreases in the electron density from δ to α positions due to the +I effect of the substituent X (55) or of the heteroatom $\text{E}^{\delta+}$ (56).

(e) A transmission of electrons from the p_{xy} to the p_z orbital evoked by the presence of $\delta+$ or $\delta-$ charge on the skeletal atom (trans and antipodal effect, section IV.D.1, Figure 32).

C. Distribution of Bonds around the Observed Nucleus and within the Whole Open B Skeleton

1. μH Rule

When comparing the ^{11}B NMR chemical shift values of closo and open-skeleton boranes one sees an appreciable difference in their respective spans which is significantly greater in the latter (cf. Figure 1). It follows from the previous discussion that this fact cannot be the result of hybridization, valence angles, or charge effects.

In the early 1970s while studying the available ^{11}B spectra of open-cage boron compounds, we noted some regularities which were expressed in the form of three empirical rules.⁹⁹

In a given ^{11}B NMR spectrum the B^* atom in the arrangement (Figure 17):

1. 57 resonates at the low(est) frequency.

2. 58 resonates at high(est) frequency.

3. Alternatively 57 and 58 shows—due to an H tautomerism—an averaged signal. Such molecules, consequently, exhibit narrower spans than the spectra of open molecules in which H tautomerism does not occur or is slow on an NMR time scale (Figure 18c, cf. also Figure 1).

These regularities can be called the “ μH rules”, being related to the presence or absence of μH bridge behind the edge of the open-face opposite to the observed B^* atom. Several examples in Figure 18 document their validity.

Although based on practical experience only, they were successfully used by Heřmánek in correctly predicting the assignment of resonances to borons in many dozens of open-cage boranes, heteroboranes, and metallaboranes.

In some cases, an apparent disagreement with the μH rule identified an incorrect structure. After a reinvestigation, the earlier proposed structure was found incorrect and the revised one obeyed the rule. In this way, the proposed *nido*- $\text{C}_2\text{B}_7\text{H}_{11}$ carborane¹⁰⁰ has proved to be *arachno*-4,5- $\text{C}_2\text{B}_7\text{H}_{13}$ carborane,³³ and the proposed *nido*-4- SB_8H_{10} ¹⁰¹ was revealed to be *arachno*-4- SB_8H_{12} thiaborane.¹⁰² In the case of 6- Me_3N -6- CB_9H_{11} , the ^{11}B signal of intensity 1 found at lowest frequencies indicated that two the μH bridges present must be in op-

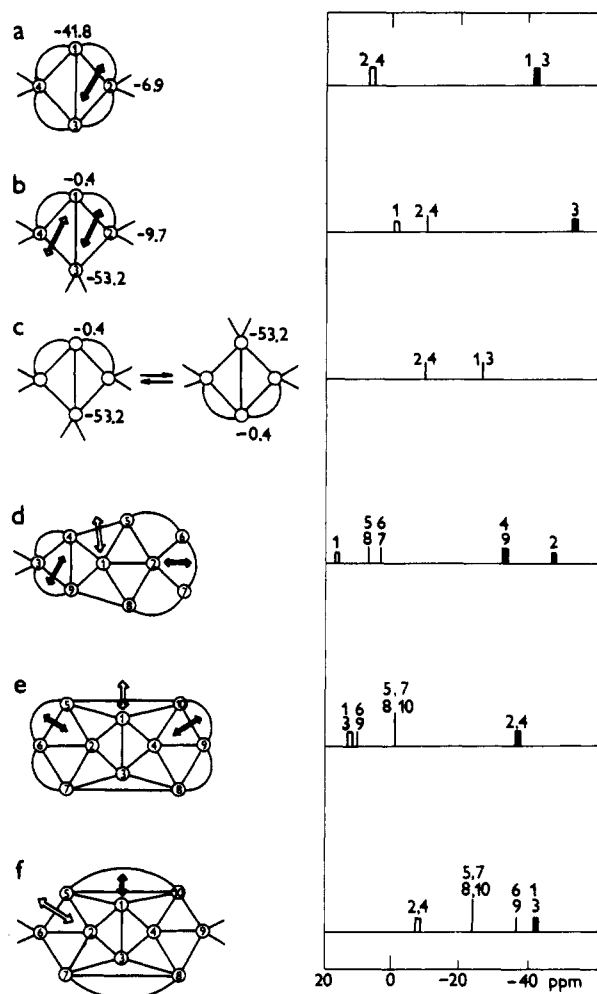


Figure 18. μ H rule: ¹¹B NMR signals at the highest frequency (↔, ||) and at the lowest frequency (↔, ⊥) with boranes (a) B₄H₁₀; (b,c) B₄H₉⁺, (d) n-B₃H₁₅, (e) B₁₀H₁₄, (f) B₁₀H₁₄²⁻. For exact values of boranes d, e, and f, see Tables 8 and 9.

position to one B atom only, i.e. to B(4) and, consequently, to be located between vertices 5–6–7,¹⁰³ and not between 5–10 and 7–8 as was proposed earlier,¹⁰⁴ in which two B atoms, e.g. B(1,3) are opposite. Recently, this correction was confirmed by a 2D NMR study.³⁹

The μ H rule has also proved its value in selecting one of two or more possible candidates in the analysis of a given ¹¹B NMR spectrum. For example, the dehydrogenation of 4-CB₈H₁₄ afforded a sole isomer of CB₈H₁₂ which showed the relative signal areas 1:2:2:2:1 and a great difference between the two low-frequency signals centered at -31.2 (2) and -57.1 (1) in the ¹¹B spectrum. This favors the seemingly less probable 7-CB₈H₁₂ isomer for which only one signal of intensity 1 is expected at the low frequency, while with the 4-isomer a signal of intensity 2, namely B(2,3) is to be expected at the lowest frequency¹⁰⁵ (Figure 19). These conclusions were confirmed by a two-dimensional ¹¹B NMR experiment.²⁷

It is not surprising, that the μ H rule works also in the case when μ H is opposite to a carbon atom as in 7-CB₈H₁₂ with a tautomerizing H bridge between B(6) and B(8)²⁷ and, especially, with nonmigrating H bridges in C₂B₈H₁₂ [$\delta(^{13}\text{C})$ -10.4 ppm!].¹⁰⁶

Up to the present, only a few compounds have been found (e.g. *arachno*-4,5-C₂B₆H₁₁⁻,¹⁰⁷ *hypho*-7,8-Me₂-

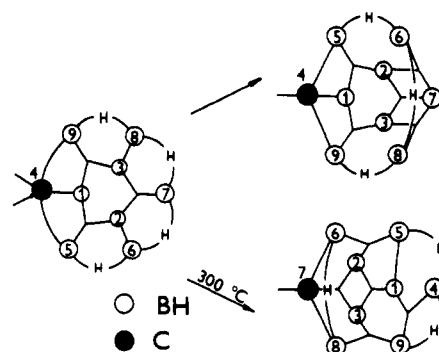


Figure 19. Dehydrogenation of 4-CB₈H₁₄ to one of two possible CB₈H₁₂ isomers; the μ H rule prefers the 7-CB₈H₁₂ isomer.

7,8-SB₆H₈¹⁰⁸) with which the B atom opposite to the μ H bridge is not at the lowest frequency. But even in these cases, its nucleus behaves as strongly shielded.

The general applicability of the μ H rules is summarized in Tables 8–10, which list $\delta(^{11}\text{B})$ chemical shifts values of B vertices in nido, arachno, hypho, and composed boranes and their anions, as well as in open heteroboranes (section IV.E.3). Of a considerable importance are the structures and $\delta(^{11}\text{B})$ of the anionic species which can be envisaged as parent compounds for many heteroboranes, formally derivable by substituting isoelectrolobal fragments (see Table 2) for B vertices.

The examples discussed emphasize the importance of the μ H rules in a practical use. As will be shown later, these rules are of a substantial value with open-skeleton compounds in which an H tautomerism is influenced by the presence of a substituent (section IV.D.2). To our disappointment, these useful rules have been used intensively only by the Czech boron group and only rarely by others.

2. Edge Rule

In 1976, the μ H rules were extended to additional bonding arrangements.¹⁴⁷ On three elected compounds with two (98), one (99), and no “extra” hydrogen (100) in the open face of the eleven-vertex B skeleton (Figure 20), we have now by means of 2D ¹¹B–¹¹B measurements confirmed⁸⁵ an earlier assumption^{11,147} that ¹¹B signals at lowest frequencies belong to B(4,6) in 98, to B(1) in 99, and to B(1) in 100, namely to the B atoms which are opposite to the “extra” hydrogens in both 98 and 99 compounds and to the high electron density in the place of a missing vertex in the compound 100.

This study has strongly supported the hypothesis that it is “not the presence of the extra hydrogen but rather it is an electron cloud in the opposite position” that is responsible for the shift of the observed B* atom to the low frequency.¹⁴⁷

The hypothesis discussed explains the fact that in B compounds of the same geometrical arrangement 101 the B atom between two H bridges resonates either at high (compounds I) or at low (compounds II) frequencies (Table 11). An analysis of the distribution of bonds within these molecules has indicated that within the first group, the center of electron gravity is in front of the opposite edges (102) while with the second group it is behind the edges of two fused triangles with the B* atom in the common vertex (103). This has indicated that not only bonding electrons appertaining to

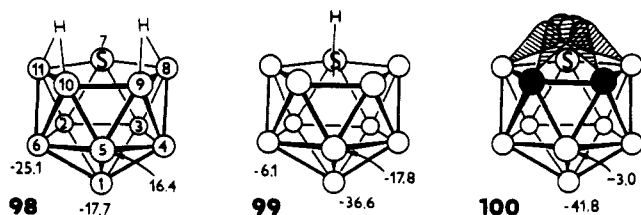


Figure 20. B atoms resonating at the lowest frequency of the given ^{11}B spectrum with eleven-vertex species 7-SB $_{10}\text{H}_{12}$ (98), 7-SB $_{10}\text{H}_{11}^-$ (99), and 7,8,10-C $_2$ SB $_8\text{H}_{10}$ (100).

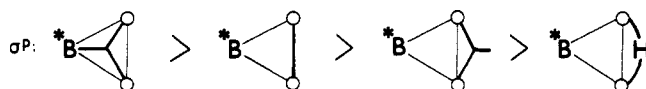


Figure 21. The relationship between the measure of paramagnetic deshielding σ^p of the atom *B (i.e. the position of its signal in the ^{11}B spectrum) and the location of the center of the bond connecting two neighboring atoms.

the observed B* atom but also bonding electrons *on* or *behind the neighbor skeletal atoms* influence its chemical shift.

By a combination of the “ μH rule” with this “edge rule” an order of bonding arrangements showing increasing shielding (or more correctly, a decreasing deshielding) of the B atom was presented²⁷ (Figure 21). This observation reveals a new factor, a long-range effect of bonding electrons around the observed nucleus. This is quite different from the long-range shielding known with organic compounds, and it has no precedent among known principles, governing the chemical shifts of nuclei in noncluster compounds.

The “ μH ” and “edge” rules indicate that chemical shifts of cluster-vertex atoms (1) are strongly influenced by the gradient of the density of bonding electrons not only in the first (in the front of neighboring skeletal atoms) but also in the second sphere (between and behind these atoms); (2) reflect both the location of μH bridges and also as subtle matter as the statistically important distribution of classical (2c2e) and three-center (3c2e) bonds within the cluster molecule. As shown in Table 11, the position of individual B signals within the spectrum allows one in some favorable cases to predict a particular arrangement of bonds, as do quantum chemical calculations³⁷ in a similar fashion.

3. NMR Isospectrality

A significant relationship between the chemical shift of individual B atoms and the character of chemical bonds and their distribution in front of and behind the adjacent skeletal atoms led to the statement that not isostructural but *isobonding groups or skeletons are NMR isospectral*.¹⁵¹ This means that isobonding moieties exhibit similar features of the relevant signals or of the whole spectrum modified only by perturbation brought about by heteroatom vertices or by substituents.

A group of compounds that demonstrates this effect is represented by the compounds 104–106. Their ^{11}B NMR spectra¹⁵¹ (Figure 22) have very similar features, reflecting (a) similar distribution of bonds in the group 104–106, and consequently, the presence of two free-electron pairs on the sulfur atom; and (b) sufficient stabilization of the endo free electron pair on sulfur by a delocalization within the inner sphere.¹⁵² This is the first support for the idea that the free endo electron

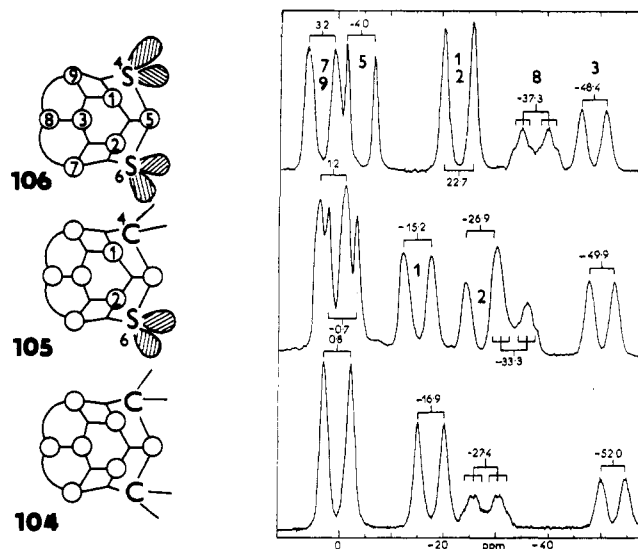


Figure 22. ^{11}B NMR spectra of the isobonding heteroboranes 4,6-S $_2$ B $_7\text{H}_9$ (106), 4,6-CSB $_7\text{H}_{11}$ (105), and 4,6-C $_2$ B $_7\text{H}_{13}$ (104).

pairs on heteroatoms are present and are not dissipated among the electron deficient skeletal atoms.¹⁵¹

NMR isospectrality is valid for the series of compounds in which the BH $_2$ group was changed to BHL, CH $_2$, NH, $\bar{\text{S}}$ and similar vertices (see Tables 25–27).

The discussed rule helps also to clarify the changes in ^{11}B NMR spectra brought by ligands of different electron attracting or donating power (cf. section IV. D.1.a,b).

4. Calculations of ^{11}B Chemical Shifts

Very recently, great progress was made in computing the ^{11}B chemical shifts. By using the IGLO method (individual gauge for localized orbitals), NMR chemical shifts were successfully calculated for lower boranes and their anions,^{115,153–156} *closo*-carboranes^{156,157} and *closo*-heteroboranes.^{157,158} The maximum deviation was less than 2.5 ppm and mostly only about 1 ppm (see Tables 8 and 9, ref 115). A necessary condition is that the precise coordinates of all the atoms in an isolated, noninfluenced molecule be known. These coordinates can be obtained either by high quality ab initio calculations or by diffraction methods. The precise coordinates are then used as input data for the IGLO calculations which directly yield the ^{11}B and ^1H chemical shifts of the individual atoms.

The IGLO method provides us not only with the chemical shifts but also with the principal values of the chemical shielding tensor components σ_{\parallel} and σ_{\perp} (one parallel and two perpendicular to the molecular axis). The differences between these two values provide information on the anisotropy of the electromagnetic field around the ^{11}B nucleus in question. The greater the anisotropy, the greater can be the P_u variable in eq 5 (section IV) and, consequently, the deshielding of the given ^{11}B nucleus.

The μH Rule indicates that the greatest difference in the anisotropy of the electromagnetic field can be expected for the B atoms in the 57 and 58 arrangements. To check this idea, the B $_{10}\text{H}_{14}$ and B $_{10}\text{H}_{14}^{2-}$ couple was selected, for which the signal of B(1,3) resonates at the highest and that of B(2,4) at the lowest frequency in B $_{10}\text{H}_{14}$, whereas the reverse order was

TABLE 8. ¹¹B NMR Data for *nido*-Boranes

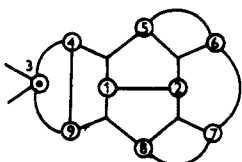
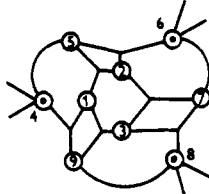
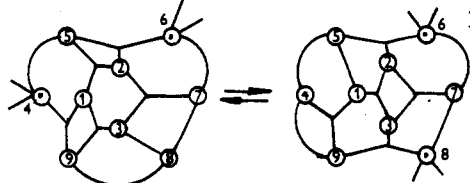
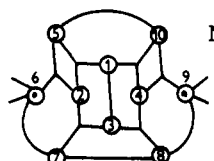
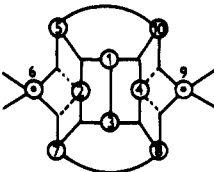
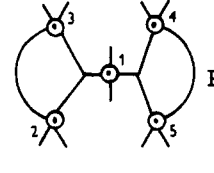
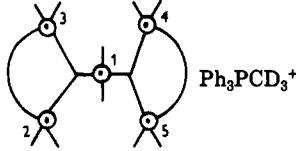
formulae		T, °C	vertex	δ ^{solv b}	J _{BH-μH}	ref ^c
empirical	topological ^a					
B ₂ H ₆ 2002 59			1, 2	18.6 ⁿ 17.5 15.6	137, 48	<u>109</u> <u>110</u> <u>115</u>
			2-5 1	-13.6° -53.1	164 175	<u>111</u> <u>112</u> <u>113</u> <u>115</u>
			2-5 1	-11.5 -55.2		
		2-5 1	-17.0° -52.8	129 158	<u>114</u>	
B ₆ H ₈ ⁻ 3130 61			2-5 1	-17.0° -52.8	129 158	<u>114</u>
			2-6 1	20.9 ^k -48.7	179 173	<u>96</u>
B ₈ H ₁₀ 4220 52		-80	3, 6 4, 5	18.6° 18.6 -6.5 -51.8		<u>36</u>
		>-70	2-6 1 3, 6 4, 5 2 1	16.5 -50.9 18.8 19.9 -7.4 -51.5	155	<u>96</u> <u>115</u>
			2-6 1	10.1° -49.3	137	<u>96</u> <u>114</u> <u>116</u>
			3, 5 } 6, 8 }	7.5	168	<u>117</u>
			4, 7	-19.4	170	
			1, 2	-22.0	175	
			7 2, 3 5, 9 4 6, 8 1	-10.47 -10.47 -14.74 -16.24 -35.00 -52.74	137 175.49 148 153	<u>27</u> <u>118</u>
B ₁₀ H ₁₂ 4420 62			1, 3 6, 9 5, 7	11.22 9.36	145 160	<u>32</u> <u>14</u> <u>23</u> <u>24</u> <u>32</u> <u>119</u>
			8, 10 } 2, 4	-0.35 -36.87	160 158	<u>32</u> <u>119</u>
			6, 9 3 1 5, 7, 8, 10 }	6.8 ⁱ 2.5 -5.0	140 135 135	<u>120</u> <u>121</u>
			2, 4	-35.20	150	
			int.	1 2 5 1 1	-1.44 -6.65 -25.9 -31.3 -36.2 -40.6	162 132 134 132
B ₁₀ H ₁₂ ⁻ 2640 66			1 2-6 7-11	-12.5 ^g -14.1 -14.9	156 138	<u>123</u> <u>124</u>
B ₁₁ H ₁₄ ⁻ 2821 67						
B ₁₁ H ₁₆ 4720	unknown structure			-14.8 -17.4	≈200 145	124

^a ○ = B; □ = BH. ^b For solvent abbreviations see Table 4. ^c δ from the first one is presented; for calculated δ, see ref 115.

TABLE 9. ^{11}B NMR Data for *aracho*- and *hypho*-Boranes and Their Anions

formulae		$T, ^\circ\text{C}$	vertex	$\delta^{\text{solv } b}$	$J_{\text{BH}-\mu\text{H}}$	i	ref ^c	
empirical	topological ^a							
B_3H_6^- 110(4) 68a			1 2, 3	-50.6 -7.5			<u>115</u>	
			1, 2, 3	-29.8			233	
2013 68b			1 2, 3	-9.3 -43.5			<u>115</u>	
			2, 4 1, 3 2, 4 1, 3	-5.2 ⁿ -41.8 -6.1 -42.7	132.30 160.23		<u>125</u> <u>126</u> <u>115</u>	
B_4H_9^- 2113 70		-90	3 2, 4 1 3	0.8 ^p -10.2 -54.5 0.9	113 99 101		127 <u>115</u>	
		calcd	2, 4 1 3	-9.9 -54.9 -10.4			<u>127</u>	
		20	2, 4 1, 3	-10.4 -27.0	99		<u>127</u>	
			3, 4 2, 5 1	0.5 ^o 7.4 -55.2	160.36 132 152		<u>126</u> 14	
B_5H_{11} 4112 71			3, 4 2, 5 1	0.5 ^o 7.4 -55.2	160.36 132 152		<u>126</u> 14	
		$\text{B}_5\text{H}_9^{2-}$ 2132 73	$\text{K}^+(\text{crown})$ -70	2-5 1	-16.1 ^f -51.7	132 157		128
B_6H_{12} 4212 74			3, 6 1, 4 2, 5	22.6 ⁿ 7.9 -22.6	156.40 133 158		<u>126</u> 14 125	
		$\text{B}_6\text{H}_{11}^-$ 3222 4131 75	-25	2, 5 6 3, 4 1	14.0 1.6 -0.9 -34.6	117 overlap 125 117		<u>127</u>
			-76		15.2 1.0 -21.7			
$\text{B}_7\text{H}_{12}^-$ 322(2) 76				-17.9 -22.4 -44.4		1 3 2	<u>129</u>	
		B_8H_{14} 4412 77	-45	4, 7 3, 5 1, 2	24.9 ^a -20.7 -38.2	160 155 160		

TABLE 9 (Continued)

formulae		T, °C	vertex	δ ^{solv b}	J _{BH-μH}	i	ref ^c
empirical	topological ^a						
n-B ₉ H ₁₅ 5421 78			1	17.2 ^a	155		17
					7.1	170	18
			3	3.5	125		
			4, 9	3.3	150		
			2	-32.0	155		
				-47.5	165		
i-B ₉ H ₁₆ 3603 79			5, 7, 9	4.39 ^c	150		129
			1, 2, 3	-32.9	155	130	
			4, 6, 8	-44.8	155, 60		
B ₉ H ₁₄ ⁻ 3522 80			5, 7, 9	-6.8 ^{id}	137		132
			4, 6, 8	-19.2	136	99	
			1, 2, 3	-22.4	138	130	
						131	
						133	
B ₉ H ₁₃ ²⁻ 3441 81			5, 7, 9	-4.55	122		134
			4, 6, 8	-24.9	125		
			1, 2, 3	-29.0	104		
B ₁₀ H ₁₅ ⁻ 3622 82			5, 7, 8, 10	-14.2 ^e			135
			1, 3, 2, 4	-19.8			
			6, 9	-21.8			
B ₁₀ H ₁₄ ²⁻ 2632 83			2, 4	-8.09 ^{hd}	124		32
			5, 7, 8, 10	-23.10	130	24	
			6, 9	-36.62	103	136	
			1, 3	-42.26	129		
hypho-B ₆ H ₁₂ ⁻ 84			-25 to -100 0 change	2-5	-15.9 ^c -57.6		127

^{a-c} For footnotes, see Table 8.

found for the B₁₀H₁₄²⁻ anion (see Figure 18).

An inspection of Table 12 indicates that the B atoms resonating at the lowest frequency, i.e. B(2,4) in B₁₀H₁₄ and B(1,3) in B₁₀H₁₄²⁻, exhibit the smallest chemical shift anisotropy, whereas those resonating at the highest frequency, i.e. B(1,3) in B₁₀H₁₄ and B(2,4) in B₁₀H₁₄²⁻, exhibit the highest chemical shift anisotropy. This finding is in agreement with the expectation that the μH Rule and the edge Rule reflect the distribution of the bonding electrons not only in the first but also in the second sphere.

The result of studies presented in sections IV.A-C indicate that the ¹¹B NMR shifts of individual atoms in basic boranes are controlled by three main factors: (1) strains arising from a compression of the bonding orbitals which predominate over the electron density in the case of a greater deviation of the mutual angles of the sp³ bonding orbitals from 109°; (2) the degree of "imbalance" of the distribution of the bonding electrons

in both the first and second spheres, which is reflected by the chemical shift anisotropy of the individual B atoms (this principle is practically absent for organic molecules, which is probably the reason for the low success in the transfer of NMR experience from organic to borane molecules); (3) electron density on individual B atoms.

Of the above factors, the former two are more significant. The character of individual skeletons determines which of them plays a leading role.

D. Effect of Substituent X on the ¹¹B NMR Chemical Shifts of Individual B Vertices in Borane Clusters

In borane and heteroborane skeletons, the terminal hydrogen (considered for H⁻) can be replaced either by another X⁻ (halogen⁻, R⁻, SH⁻, NH₂⁻, CN⁻, etc.) with the retention of the original charge (eqs 6 and 7) or by a neutral ligand (Lewis base) with the conversion of the

TABLE 10. ^{11}B NMR Data for *conjuncto*-Boranes

formulae		$T, ^\circ\text{C}$	vertex	$\delta^{\text{solv } b}$	$J_{\text{BH}-\mu\text{H}}$	i	ref ^c
empirical	topological ^a						
B_7H_{13} 5222 85			1', 2' 3, 5 2 4 1	-1.5 -10.9 -11 -12.0 -50.5	128.26 ^e 161.18 161.19 193		<u>106</u>
B_8H_{18} 1,1'-(B_4H_9) ₂ 86			2, 4 } 2', 4' } 1, 1' 3, 3'	-5.7 ^j -38.1 -39.5	131 ^t - 174		<u>15</u>
$2,2'(\text{B}_4\text{H}_9)_2$ 87			2, 2' 4, 4' 1, 3 } 1', 3' }	-1.2 ^j -5.9 -39.8	- 120 145		<u>15</u> <u>117</u>
$\text{B}_{10}\text{H}_{16}$ 852(-2) 88		1,1'-(B_5H_9) ₂	2-5 } 2'-5' }	-13.2 ^{GD} -55.4 -3.6 ^a	- - -		<u>137</u> <u>138</u>
89		1,2'-(B_5H_9) ₂	2-5 } 3', 5' }	-12.6 -13.4 -50.7 -56.2 -11.0 ^{bD}	overlap - -		<u>137</u> <u>139</u>
90		2,2'-(B_5H_9) ₂	4, 4' 3, 5 } 3', 5' }	-11.6 -12.6 -51.2	- -		<u>137</u> <u>139</u>
$\text{B}_{12}\text{H}_{16}$ 6640 91			1 ^{2D} 10, 12 11 3, 5, 6, 8 4,7 9 2	15.35 13.41 11.39 4.53 -18.37 -40.78 -43.10	193 ^a 203 213 overlap 150 156 159		<u>141</u>
$\text{B}_{13}\text{H}_{19}$ 764(-1) 92			1 ^{BG} 9 5/8 3 2 10 6 ^{BG} 13 3 1 9 7, 8	13.9 11.3 2.5 -4.0 -7.2 -9.3 -12.2 -20.4 -32.4 -43.2 -49.6 23.9 19.9 14.1 9.0 7.1	150 156 162 - 130 160 140 160 140 150 160	2 2	<u>142</u>
$\text{B}_{14}\text{H}_{18}$ 93			10 5 7, 8, 10 12 14 2 4 11	-49.6 4.4 3.1 2.1 ^a 0.4 -8.4 -18.8 -36.7 -39.8 -46.4	160		<u>143</u>
$\text{B}_{14}\text{H}_{20}$ 6830 94		-78 °C	2, 3 ^{2D} 5, 6, 8, 9 10, 11, 13, 14 7, 12 1, 4	34.6 ^K 8.8 6.0 -10.6 -36.1	150 160 160 150 160		<u>144</u>

TABLE 10 (Continued)

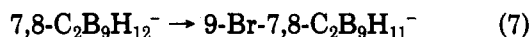
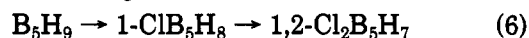
empirical		formulae		T, °C	vertex	δ ^{solv} ^b	J _{BH-μH}	i	ref ^c
		topological ^a							
B ₁₅ H ₂₃ 6922 95		canonical formulae	7 ^{BG}	21.0	150	35			
			11	14.2	140				
			13, 14	11.8	146				
			1	4.7	128				
			12, 15	4.1	160.50				
			5, 9	-3.5	139.5				
			6, 8	-24.5	113.5				
			2, 3	-36.8	115				
			10	-51.0	155				
			4	-52.2	101				
			3	15.1	151				
			10	9.4	161		145		
anti-B ₁₈ H ₂₂ 96		canonical formulae	6	5.4	146				
			5	5.4					
			9	4.9					
			1	1.2					
			8	-3.9					
			7	-11.4					
			2	-31.4					
			4	-39.3					
			3	15.1		151			
			10	9.4		161			
syn-B ₁₈ H ₂₂ 97		canonical formulae	6	11.3	145				
			8	10.2					
			9	3.4					
			3	3.0					
			10	-0.7					
			7	-2.8					
			5	-14.7					
			2	-26.7					
			4	-38.5					
			3	15.1		151			
10	9.4	161							

^{a-c} For footnotes, see Table 8.

TABLE 11. A Dependence of δ(¹¹B) of the B* Vertex on the Bonding Arrangement 102 and 103 in the Structural Fragment 101

102			103		
compound	δ	ref	compound	δ	ref
B ₄ H ₉ ⁻	0.8	Table 9	B ₅ H ₁₂	-16.2	Table 8
B ₆ H ₁₂	22.6	Table 9	B ₁₄ H ₁₈	-18.8	Table 10
B ₁₀ H ₁₄	9.4	Table 8	1,2-C ₂ B ₃ H ₇	-23.7	149
B ₁₄ H ₁₈	7.1	Table 10	4-CB ₅ H ₁₄	-34.0	Table 25
anti-B ₁₈ H ₂₂	4.9	Table 10	4-NB ₈ H ₁₃	-47.7	Table 25
syn-B ₁₈ H ₂₂	3.4	Table 10	4-SB ₈ H ₁₂	-41.8	Table 25
6-CB ₉ H ₁₂ ⁻	-2.6	39	4,6-C ₂ B ₇ H ₁₃	-27.8	Table 27
6-NB ₉ H ₁₂	14.0	39	4,6-CSEB ₇ H ₁₁	-33.1	Table 27
6-SB ₉ H ₁₁	17.7	39	4,6-S ₂ B ₇ H ₉	-38.5	Table 27
5,6-C ₂ B ₈ H ₁₂	-3.7	53	hypho-7,8-C ₂ B ₆ H ₁₃	-23.0	150
2,3-C ₂ B ₄ H ₈	-0.6	148	7,8-Me ₂ -7,8-S ₂ B ₆ H ₈	-54.2	108

original anion to an uncharged compound of a zwitterion character (eq 8).



Substituent X has a distinct and specific influence on the chemical shifts of the individual B atoms in the molecule, similarly as it has a substituent in an aromatic compound. A revelation of regularities determining changes in the chemical shifts in the individual positions and of their dependence on the character of substituent X and on the substituted molecule is very im-

TABLE 12. Correlation of ¹¹B Chemical Shifts δ(B) of Individual Atoms in nido-B₁₀H₁₄ (64) and arachno-B₁₀H₁₄²⁻ (83) with Individual Mutual Perpendicular Tensor Components and σ₁₁, σ₂₂, and σ₃₃ and Values Calculated Using IGLO Method (Basis DZ//3-21G) (The Resulting Chemical Shift Anisotropy σ = σ₁₁ - 1/2 (σ₂₂ + σ₃₃)^{175b})

	B 1,3	B 2,4	B 5,7,8,10	B 6,9
B ₁₀ H ₁₄				
σ ₁₁	158	178	168	165
σ ₂₂	129	176	116	101
σ ₃₃	55	158	101	94
σ	66	11	60	68
δ _{IGLO}	17.11	-39.1	3.4	11.7
δ _{exp.}	11.2	-36.9	-0.3	9.4
B ₁₀ H ₁₄ ²⁻				
δ ₁₁	185	159	170	177
σ ₂₂	171	148	154	174
σ ₃₃	166	94	134	147
σ	17	38	26	17
δ _{IGLO}	-42.4	-2.1	-21.2	-34.6
δ _{exp.}	-41.6	-7.4	-22.4	-36.0

portant both for determining the given structure, and for understanding transmissions of electrons within perturbed borane clusters and for predicting the positions of further substitution.

The number of substituted borane clusters is still very low. The directly available ones are mostly halogen, mercapto (electrophilic substitution), and alkyl derivatives (E⁺ substitution, alkylation of higher hydrido-borate salts), while -NO₂ and -NO derivatives are practically inaccessible; other examples such as NH₂, OH, COOH, SO₃H, CN, etc., derivatives must be prepared using special procedures. Substitutions of individual skeletons in all the possible positions by a single type of substituent are also exceptional.

Consequently, complete series of substituted basic skeletons are not available at the present time, and a true picture of perturbations by substituents X has to

TABLE 13. ^{11}B Chemical Shifts for the Substituted $\text{B}_6\text{H}_6^{2-}$ Anions^{159,160} Δ Increments α , β , and γ ($\Delta = \delta_{\text{subst}} - \delta_{\text{parent}}$) for Individual Positions

compound	B(1)	B(2-5)	B(6)	α	β	γ
$\text{B}_6\text{H}_6^{2-}$	-13.0	-13.0	-13.0			
1-Cl $\text{B}_6\text{H}_5^{2-}$	-1.0	-14.5	-30.4	12.0	-1.5	-17.4
1-Br $\text{B}_6\text{H}_5^{2-}$	-7.6	-14.0	-27.3	5.4	-1.0	-14.3
1-IB $\text{B}_6\text{H}_5^{2-}$	-23.2	-13.1	-21.6	-10.2	-0.1	-8.6

TABLE 14. (A) ^{11}B NMR Chemical Shifts of Individual B Atoms for Series $\text{XB}_{12}\text{H}_{11}(\text{NBu}_4)_2$ in Acetone- d_6 and (B) Δ Increments α , β , γ , and δ ($\Delta = \delta_{\text{subst}} - \delta_{\text{parent}}$) for Individual Positions

(A)					
subst	B(1)	B(2-6)	B(7-11)	B(12)	ref
H	-15.32	-15.32	-15.32	-15.32	161, 3
F	10.2	-16.7	-18.5	-24.0	161
Cl	-2.8	-14.8	-16.6	-20.2	161, 162
Br	-8.2	-14.3	-15.9	-18.9	161, 162
I	-21.3	-13.7	-15.2	-16.9	161, 162
OH	4.3	-16.5	-19.0	-25.1	161
OH	4.0	-16.0	-18.0	-24.3	161
SH	-10.0	-14.3	-16.4	-19.8	161, 163
S-S	-6.3	-15.0	-16.8	-19.2	161, 163
SCN	-10.2	-15.2	-16.0	-18.2	161
HgSCN	-2.80	-14.75	-15.32	-13.48	161
(B)					
subst	α	β	γ	δ	
F	25.1	-1.4	-3.2	-8.7	
Cl	12.5	0.5	-1.3	-4.9	
Br	7.1	1.0	-0.6	-3.6	
I	-6.0	1.6	0.1	-1.6	
OH	19.9	-1.2	-3.7	-9.8	
OH	20.4	0.4	-1.6	-7.7	
SH	6.4	2.1	0.0	-3.4	
S-S	10.1	1.4	-0.4	-2.8	
SCN	5.1	0.1	-0.7	-2.8	
HgSCN	12.5	0.6	0.0	1.9	

be composed of small fragments, i.e. of the results obtained for a number of derivatives of various *closo*, *nido*, and *arachno* compounds.

A further complication arises from the fact that many of these compounds were prepared at a time when the NMR technique was very simple; signals were often insufficiently separated due both to the low magnetic field used and, especially, to the use of spectrometers without ^1H broad-band decoupling. Many of these borane derivatives must therefore be newly prepared and their ^{11}B and ^1H signals assigned using modern techniques.

We have found¹¹ that the effects of substituents X on the chemical shifts of the individual atoms in substituted B clusters differ significantly for (a) rigid molecules with a static arrangement of the skeletal and H atoms in the NMR time scale and (b) fluxional molecules exhibiting H tautomerism or skeleton fluxionality.

While, for the first group of compounds, only electron transfers can be suggested, in the second one, substituent X can slow down or suppress the H tautomerism to such a degree that one of the possible tautomers can prevail in the given compound. As the ^{11}B NMR spectra of pure tautomers are very different from the averaged spectra, the substituent effects can be evaluated in three steps. First, the spectrum of the parent static H tautomer must be estimated, in the next step the degree of tautomerism suppression (i.e. the probable ratio of the tautomers present) has to be evaluated, and only then can the intrinsic influence of substituent X on the individual atoms be studied or assessed. Since the evaluation of the ^{11}B NMR spectra of these two

TABLE 15. ^{11}B NMR Chemical Shifts of Individual Vertices for 2-X-1,6- $\text{C}_2\text{B}_4\text{H}_6$ and Increments Δ for α , β , and γ Positions

subst	B(2)	α	B(3,5)	β	B(4)	γ	ref
H	-18.7		-18.7		-18.7		164
Cl	-8.8	9.9	-16.4	2.3	-26.0	-9.3	165
Br	-17.7	1.0	-16.3	2.4	-18.2	0.5	166
I	-32.7	-14.0	-15.9	2.8	-20.1	-1.4	167
CH_3	-5.9	12.8	-15.1	3.6	-19.3	-0.6	168

TABLE 16. ^{11}B (64.184 MHz) of Substituted 1-X- and 9-X-*o*-carboranes¹¹ (A) $\delta(^{11}\text{B})$ of Individual Signals (ppm relative to $\text{BF}_3 \cdot \text{OEt}_2$, CDCl_3) and (B) Differences ($\Delta = \delta_{\text{subst}} - \delta_{\text{parent}}$) for Individual X and Positions

(A) 1-X- <i>o</i> -carborane						
$\delta(^{11}\text{B})$						
subst	B9	B12	B8,10	B4,5	B7,11	B3,6
1-Cl	-2.98	-8.46	-10.94	-10.94	-13.98	-10.94
1-Br	-2.65	-7.39	-10.0	-10.0	-13.59	-10.70
1-I	-1.97	-5.26	-9.06	-9.06	-12.78	-10.05
1-Me	-2.73	-7.71	-10.10	-11.59	-13.06	-12.21
1-BH ₃	-3.01	-7.80	-9.15	-9.15	-10.31	-12.68
1-SH	-1.68	-6.79	-9.72	-9.72	-13.05	-11.66
1-CH ₂ S	-2.77	-6.11	-9.71	-10.91	-13.59	-13.59
1-EtO	-5.52	-12.86	-13.34	-13.34	-14.42	-15.97
1-OH	-5.05	-13.22	-13.16	-13.16	-15.61	-13.16
1-CH ₂ COOH	-3.23	-6.03	-10.27	-11.34	-13.84	-12.95
(B) 1-X- <i>o</i> -carborane						
Δ						
	γ	δ	γ	β	γ	β
1-Cl	0.43	-5.05	-0.69	3.73	0.69	4.86
1-Br	0.77	-3.97	-0.41	4.01	1.06	5.12
1-I	1.62	-1.85	1.19	1.19	1.89	5.75
1-Me	0.68	-4.30	0.15	3.08	1.01	3.58
1-BH ₃	0.16	-4.63	0.52	4.52	0.81	4.09
1-SH	1.73	-3.38	0.50	4.95	1.62	4.14
1-MeS	0.64	-2.70	0.54	3.76	1.08	2.21
1-EtO	-2.11	-9.44	-3.09	1.33	-0.17	0.25
1-OH	-1.64	-9.91	-2.91	1.51	-0.94	2.64
1-CH ₂ COOH	0.18	-2.62	-0.02	3.34	0.83	2.95
(A) 9X- <i>o</i> -carborane						
$\delta(^{11}\text{B})$						
subst	B(9)	B(12)	B(8,10)	B(4,5)	B(7,11)	B(3,6)
9-Cl	6.31	-2.99	-9.68	-14.77	-16.08	-17.25
9-Br	-0.86	-2.52	-9.36	-14.47	-15.44	-16.65
9-I	-17.56	-1.90	-8.44	-13.75	-14.20	-15.67
9-Me	6.29	-2.68	-9.45	-14.39	-15.41	-16.48
9-OH	13.71	-4.72	-11.16	-16.19	-17.42	-18.74
9-SH	3.87	-2.29	-8.91	-14.21	-15.25	-16.41
9-MeS	6.78	-3.38	-9.68	-14.81	-15.35	-16.47
(B) 9X- <i>o</i> -carborane						
Δ						
	α	β	β	β	γ	γ
9-Cl	9.72	0.33	0.49	-0.19	-1.50	-1.51
9-Br	2.55	0.89	0.89	0.20	-0.77	-0.85
9-I	-14.15	1.51	1.81	0.92	0.47	0.13
9-Me	9.70	0.72	0.80	0.28	-0.74	-0.68
9-OH	17.12	-1.31	-0.91	-1.52	-3.05	-2.94
9-SH	7.28	1.12	1.34	0.46	-0.58	-0.61
9-MeS	10.19	0.03	0.57	-0.14	-0.67	-0.67

groups requires different approaches, they will be treated separately.

1. Rigid Compounds

Typical representatives of this type of molecules are substituted six- and twelve-vertex *closo*-boranes 11, 17 (Tables 13 and 14) and *closo*-heteroboranes (Tables 15-17) for which effects of various substituents X on the substituted skeletal atom (α) as well as on neighboring (β) and remote (γ , δ) atoms can be unambiguously determined.

TABLE 17. ¹¹B (64.184 MHz) of Substituted 1-X- and 9-X-*m*-Carboranes¹¹ (A) $\delta(^{11}\text{B})$ of Individual Signals (ppm Relative to $\text{BF}_3 \cdot \text{OEt}_2$, CDCl_3) and (B) Differences ($\Delta = \delta_{\text{subst}} - \delta_{\text{parent}}$) for Individual X and Positions

(A) 1X- <i>m</i> -carborane						
subst	$\delta(^{11}\text{B})$					
	B(5)	B(12)	B(9,10)	B(4,6)	B(8,11)	B(2,3)
1-H	-7.72	-7.72	-11.55	-14.29	-14.29	-18.08
1-Br	-3.45	-11.45	-11.45	-10.14	-14.80	-14.80
1-I	-2.61	-9.12	-10.18	-13.87	-13.87	-18.17
1-Et	-5.10	-11.20	-11.64	-12.29	-14.77	-16.48
1-SH	-2.93	-11.21	-11.21	-9.70	-14.04	-14.71
1-MeS	-4.60	-11.33	-11.33	-14.32	-14.32	-15.62

(B) 1X- <i>m</i> -carborane						
X	Δ					
	β	δ	γ	β	γ	β
1-Br	4.15	-3.85	-0.01	4.11	0.55	3.12
1-I	4.99	-1.52	1.26	0.38	0.38	-0.25
1-Et	2.50	-3.60	-0.20	1.95	-0.52	1.44
1-HS	4.67	-3.61	0.23	4.55	0.21	3.21
1-MeS	3.00	-3.61	0.11	0.07	0.07	2.30

(A) 9X- <i>m</i> -carborane							
subst	$\delta(^{11}\text{B})$						
	B(5,12)	B(9)	B(10)	B(4,8)	B(6,11)	B(3)	B(2)
9-Cl	-7.31	0.15	-10.66	-14.06	-15.72	-19.52	-23.46
9-Br	-7.16	-7.16	-10.16	-13.62	-14.99	-18.80	-22.20
9-I	-6.45	-9.29	-12.90	-14.02	-17.79	-19.90	-24.42
9-Et	-6.44	2.15	-10.18	-13.53	-13.53	-17.53	-20.47
9-SH	-5.80	-6.70	-11.20	-14.10	-14.80	-18.30	-18.30
9-CH ₃ S	-7.53	-0.20	-10.84	-14.10	-14.99	-18.60	-21.57

(B) 9X- <i>m</i> -carborane							
X	Δ						
	β	α	β	β	γ	γ	δ
9-Cl	0.29	11.59	0.78	0.19	-1.47	-1.50	-5.54
9-Br	0.67	4.21	1.31	0.65	-0.72	-0.86	-4.26
9-I	1.20	-12.96	2.18	1.37	0.25	0.15	-1.96
9-Et	1.16	13.59	1.25	0.72	0.72	0.39	-2.55
9-SH	0.87	8.17	1.61	0.76	-0.55	-0.67	-3.00
9-CH ₃ S	0.07	11.24	0.60	0.15	-0.74	-0.68	-3.65

TABLE 18. ¹¹B NMR Chemical Shifts of 1-XB₅H₉ and Δ Increments for α and β Positions

X	B(1)	α	B(2-5)	β	ref
H	-53.1		-13.4		170
1-Cl	-28.5	24.6	-11.1	2.3	170, 171
1-Br	-36.3	16.8	-10.5	2.9	170, 171
1-I	-54.5	-1.4	-9.6	3.8	171
1-CH ₃	-45.3	7.8	-13.3	0.1	170

While all the ¹¹B signals in the spectra of 1- and 2-substituted pentaboranes(9) (skeleton 18) were reliably determined, due to the symmetry of the molecules (Tables 18 and 19), the assignment of the signals in the ¹¹B spectra of all the possible isomers of XB₁₀H₁₃ (X = Cl, Br, I) (Table 20) was feasible only by using the ¹¹B-¹¹B double resonance technique, which was available at that time only with experimental spectrometers.^{176,177}

In the arachno class, only ten-vertex compounds show no H tautomerism. Of these, the 5-X-6,9-C₂B₉H₁₃ series (107, Figure 23)^{11,178,187} has the greatest number of derivatives.

In addition to the presented data, a great many additional ¹¹B NMR substitution studies have been performed on various skeletons such as SB₉H₉,^{19,180} CB₁₁H₁₂,¹⁷⁹ SB₁₁H₁₁,¹⁸⁰ 5,6-C₂B₈H₁₂,⁵³ 4,6-C₂B₇H₁₃,¹⁸¹ C₂H₁₀H₁₂,¹⁸²⁻¹⁸⁴ C₂B₉H₁₁CoC₅H₅,¹⁸⁵ 8,8'- μ -X-(C₂B₉H₁₁)₂Co,¹⁸⁶ etc. In many of these compounds, unambiguous assignment of the ¹¹B NMR signals was made on the basis of the ¹¹B-¹¹B double resonance technique,^{176,177,184} ¹¹B-¹¹B 2D spectroscopy,^{181,187} se-

TABLE 19. ¹¹B Chemical Shifts of 2-XB₅H₉ (A) and Increments Δ for α , β , and γ (trans) Positions (B)

(A)					
X	B(1)	B(2)	B(3,5)	B(4)	ref
H	-53.1	-13.4	-13.4	-13.4	170, 111
2-F	-56.5	8.1	-18.2	-34.2	172
2-Cl	-52.2	-1.1	-13.7	-23.4	173
2-Br	-50.8	-8.7	-12.5	-19.6	170, 172, 173
2-I	-47.7	-27.9	-11.3	-14.4	172, 174
2-OCH ₃	-55.0	14.1	-16.8	-31.5	175
2-CH ₃	-51.5	1.6	-13.5	-19.1	170, 172
2-SiH ₃	-50.0	-15.0	-11.2	-7.1	192
2-SiMe ₃	-50.9	-9.8	-11.1	-8.2	192

(B)				
X	β	α	β	γ
2-F	-3.4	21.5	-4.8	-20.8
2-Cl	0.9	12.3	-0.30	-10.0
2-Br	2.3	4.7	0.9	-6.2
2-I	5.1	-14.5	2.1	-1.1
2-OCH ₃	-1.9	27.5	-3.4	-18.1
2-CH ₃	1.6	15.0	-0.1	-5.7
2-SiH ₃	3.1	-1.6	2.2	6.3
2-SiMe ₃	2.2	3.6	2.3	5.2

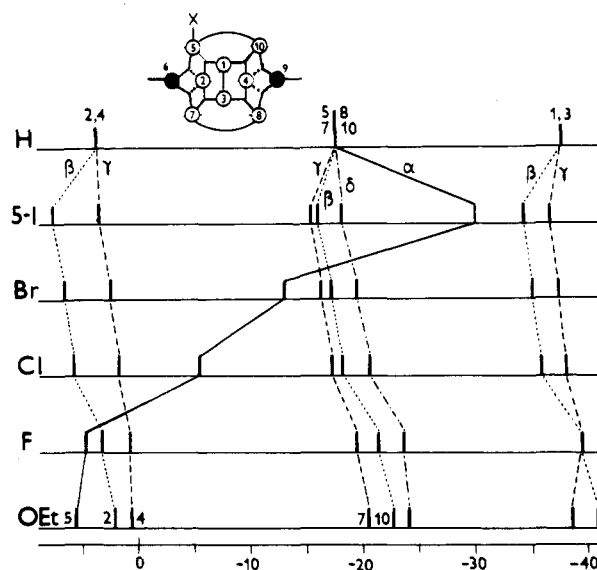


Figure 23. The dependence of α , β , γ , and δ ¹¹B chemical shifts on the substituent X at 5-X-6,9-C₂B₉H₁₃ (107).

lective deuteration,⁵³ or simplicity of the spectra.¹⁷⁰⁻¹⁷⁵

This extensive data base indicates that the changes in $\delta(^{11}\text{B})$ evoked by substituents X result from the combination of several effects, namely (1) the character of substituent X (inductive I, resonance R, conjugative, diamagnetic susceptibility, and anisotropy effects); (2) the character of the substituted vertex (electron density, a measure of the p- π interaction, and number and types of symmetry elements related to this vertex); and (3) conjugative pathways in the observed molecule.

The main effects evoked by substituent X in a rigid skeleton can be demonstrated by comparing the ¹¹B NMR spectra of a series of 5-X-6,9-C₂B₉H₁₃ (107) arachno carboranes (Figure 23). The following conclusions on the effects which can operate in cluster/substituent interactions can be drawn from the series of substituted skeletons described above.

a. I Effect. All substituents X in B clusters exhibit inductive effects +I or -I, which are analogous to those in organic chemistry¹⁸⁸ and show an increasing electron donation (+I effect) in the order H < Me < Et < iPr < tBu < SiMe₃, and an increasing acceptance (-I effect) in the order NMe₃ < RSO₂ < CN < RSO < F < Cl <

TABLE 20. ^{11}B Chemical Shifts for Halogen-Substituted $\text{X-B}_{10}\text{H}_{13}$ in CH_2Cl_2 ¹⁷⁶ (A) and Values of Individual Δ Increments ($\Delta = \delta_{\text{subst}} - \delta_{\text{parent}}$) (B)

	(A)									
	B(1)	B(2)	B(3)	B(4)	B(5)	B(6)	B(7)	B(8)	B(9)	B(10)
$\text{B}_{10}\text{H}_{14}$	11.9	-36.1	11.9	-36.1	0.4	10.3	0.4	0.4	10.3	0.4
1-Cl	22.9	-34.8	13.5	-34.8	-0.5	7.8	2.3	2.3	7.8	-0.5
2-Cl	12.8	-20.2	12.8	-36.5	1.0	9.6	1.0	-0.5	6.2	-0.5
5-Cl	12.0	-34.7	12.8	-36.6	11.0	7.9	-4.3	-1.1	11.1	4.0
6-Cl	8.3	-33.1	8.3	-39.9	-3.3	17.8	-3.3	1.3	9.3	1.3
1-Br	16.1	-34.1	13.5	-34.1	-0.3	8.7	2.5	2.5	8.7	0.2
2-Br	13.3	-27.5	13.3	-35.7	1.3	10.2	1.3	0.2	7.7	0.2
5-Br	13.0	-34.3	13.0	-36.3	3.1	9.5	-2.9	-0.7	10.8	3.8
6-Br	9.6	-33.2	9.6	-38.7	-1.2	10.4	-1.2	9.6	9.6	1.0
1-I	0.3	-33.6	12.8	-33.6	-0.5	9.4	1.8	1.8	9.4	-0.5
2-I	13.9	-45.9	13.9	-35.0	1.4	10.5	1.4	0.6	9.2	0.6
5-I	14.7	-33.4	13.4	-35.5	-13.8	11.2	-0.2	0.5	10.8	4.5
6-I	11.2	-33.3	11.2	-37.0	2.0	-6.0	2.0	0.3	11.1	0.3
	(B)									
	B(1)	B(2)	B(3)	B(4)	B(5)	B(6)	B(7)	B(8)	B(9)	B(10)
$\text{B}_{10}\text{H}_{14}$										
1-Cl	11.0	1.3	1.6	1.3	-0.9	-2.5	1.9	1.9	-2.5	-0.9
2-Cl	0.9	15.9	0.9	-0.4	0.6	-0.7	0.6	-0.9	-4.1	-0.9
5-Cl	0.1	1.4	0.9	-0.5	10.6	-2.4	-4.7	-1.5	0.8	3.6
6-Cl	-3.6	3.0	-3.6	-3.8	-3.7	7.5	-3.7	0.9	-1.0	0.9
1-Br	4.2	2.1	1.6	2.0	-0.7	-1.6	2.1	2.1	-1.6	-0.7
2-Br	1.4	8.6	1.4	0.4	0.9	-0.1	0.9	-0.2	-2.6	-0.2
5-Br	1.1	1.8	1.1	-0.2	2.7	-0.8	-3.3	-1.1	0.5	3.4
6-Br	-2.3	2.9	-2.3	-2.6	-1.6	0.1	-1.6	0.6	-0.7	0.6
1-I	-11.6	2.5	0.9	2.5	-0.9	-0.9	1.4	1.4	-0.9	-0.9
2-I	2.0	-9.8	2.0	1.1	1.0	0.2	1.0	0.2	-1.1	0.2
5-I	2.8	2.7	1.5	0.6	-14.2	0.9	-0.6	0.1	0.5	4.1
6-I	-0.7	2.8	-0.7	-0.9	1.6	-16.3	1.6	-0.1	0.8	-0.1

$\text{Br} < \text{I} < \text{COOR} < \text{OR} < \text{SH} < \text{NR}_2$.¹¹ These I effects are symmetry independent¹⁸⁹ and decrease rapidly with distance. The -I effect generally causes β vertices to resonate at higher frequencies (vicinal,¹⁸² ortho,¹⁹⁰ neighbor effect⁹¹) than γ vertices. The reverse $\gamma > \beta$ sequence can be observed only rarely, either with strong π donors (OR, F) and/or skeletal atoms that are especially sensitive to electron acceptance.

b. R Effect. Differences in shifts arising from the resonance effect +R of substituent X exhibit additional shielding (i.e. an increase in the electron density) at all vertices in the order $\text{I} < \text{Br} < \text{HS} < \text{Cl} < \text{NR} = \text{OR} = \text{F}$, which corresponds to the degree of electron donation by these substituents, and indicates the transfer of part of the p electrons from substituent X to the skeleton as a whole (cf. a gradual shift of the whole spectrum from higher frequencies at 5-iodo to lower ones at 5-ethoxy derivatives in Figure 23). The relatively lower electron donation of the NR_2 group was inferred from several known examples, as well as from the $\text{B}(\text{NR}_2)_3/\text{B}(\text{NR}_2)_4^-$ couple (section IV.A.1) and probably indicates a qualitative difference in the C-N and B-N interactions.

c. Trans and Antipodal Effects. The trans (T) and antipodal (A) effects are a special type of long-range substituent effects. The former was discovered in 1969 by Onak et al.^{170,191} for 2- XB_5H_9 (108), in which the 2-X substituent causes an increasing shift of the signal of the trans B(4) vertex to lower frequencies in the order $\text{I} < \text{Me} = \text{Br} < \text{Cl} < \text{OMe} < \text{F}$, compared to B_5H_9 (see Table 19).

The SiH_3 and SiMe_3 substituents have a special character and exhibit a decrease in shielding at the β and, especially, at the γ (trans) positions.¹⁹² The trans effect indicates that both the SiX_3 substituents exhibit " π "-type interactions but with the reverse character to those exhibited by substituents X bearing a free electron pair. This idea is in agreement with the electron diffraction results and EHMO calculations¹⁹³ which

document the 2p and 3d-" π " interactions. The opposite signs of the ^{11}B chemical shift increments (i.e. $+\Delta$) compared to strong X donors ($-\Delta$) indicate that these substituents draw electrons from the skeleton and, especially, from the α vertex which significantly interacts with the trans (γ) vertex.

In 1974, Heřmánek et al. reported on the *antipodal effect* of substituents^{182,185} which shifted the signal of the opposite (antipodal) atom in an icosahedral skeleton to lower frequencies. The A-shift increments showed a linear correlation with Sanderson's electronegativities and increased in the order $\text{I} < \text{Br} < \text{Cl} < \text{F}$.¹⁹⁴ Shortly thereafter, this effect was confirmed by two other groups.^{183,195}

The A effect was later extended to fragments of the icosahedron, in which the antipodally related atoms were located in a plane of symmetry.¹⁹⁶ This was documented for $\text{B}_{10}\text{H}_{14}$ (109) in which the couples B(2)-B(9) and B(4)-B(6) are antipodally related. In agreement with a hypothesis, comparable A shifts of the B(9) and B(4) signals produced by 2-X and 6-X substituents, respectively, were observed for 2-X and 6- $\text{XB}_{10}\text{H}_{13}$,¹⁹⁶ but only a weak A effect was found for 5- $\text{XB}_{10}\text{H}_{13}$ (cf. Table 20). A linear correlation between the A shifts in four different series (2- $\text{XB}_{10}\text{H}_{13}$; 6- $\text{XB}_{10}\text{H}_{13}$; 1-X-1,2- $\text{C}_2\text{B}_{10}\text{H}_{11}$; 8-X-1,2- $\text{C}_2\text{B}_9\text{H}_{11}$ -3-Co- C_5H_5) and the ^{13}C para shift of the XC_6H_5 derivatives indicated the quasi-mesomeric character of the A effect which was valid only for substituents X bearing a free electron pair, i.e. exhibiting a +R effect.¹⁹⁶ These results implied that the A effect is not produced by a ring current but involves the " π " orbitals in the skeleton.¹⁹⁶ The present view on the origin of the A and T effects is presented in the section IV.F.

d. Neighbor Anisotropy Effect. The B-X bond which has cylindrical symmetry can be situated in the magnetic field H_0 in two main orientations: parallel || (110) and perpendicular \perp (111) to the applied field H_0 ¹⁹⁷ (Figure 24).

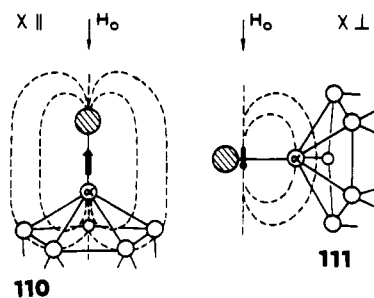
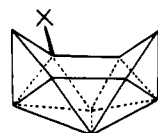


Figure 24. Substituent-induced secondary magnetic fields in the substituted part of $IB_{12}H_{11}^{2-}$: (a) increased B_{α} shielding in 110; (b) decreased magnetic shielding in 111.



112

nido (24 skel. el.)	arachno (26 skel. el.)																								
<table border="0"> <tr><td>○</td><td>BH</td></tr> <tr><td>●</td><td>CH</td></tr> </table>	○	BH	●	CH	<table border="0"> <tr><td>○</td><td>BH</td></tr> <tr><td>●</td><td>CH</td></tr> </table>	○	BH	●	CH																
○	BH																								
●	CH																								
○	BH																								
●	CH																								
<table border="0"> <tr><td>1</td><td>0.2</td><td>0.5</td></tr> <tr><td>Br</td><td>-2.9</td><td>-0.7</td></tr> <tr><td>Cl</td><td>-4.3</td><td>-1.1</td></tr> </table>	1	0.2	0.5	Br	-2.9	-0.7	Cl	-4.3	-1.1	<table border="0"> <tr><td>1</td><td>2.0</td><td>-0.5</td></tr> <tr><td>Br</td><td>1.2</td><td>-2.0</td></tr> <tr><td>Cl</td><td>0.4</td><td>-3.0</td></tr> <tr><td>F</td><td>-1.9</td><td>-6.1</td></tr> <tr><td>OEt</td><td>-3.1</td><td>-6.6</td></tr> </table>	1	2.0	-0.5	Br	1.2	-2.0	Cl	0.4	-3.0	F	-1.9	-6.1	OEt	-3.1	-6.6
1	0.2	0.5																							
Br	-2.9	-0.7																							
Cl	-4.3	-1.1																							
1	2.0	-0.5																							
Br	1.2	-2.0																							
Cl	0.4	-3.0																							
F	-1.9	-6.1																							
OEt	-3.1	-6.6																							
113	107																								

Figure 25. Increments Δ in parts per million evoked by the substituent X for trans and antipodal positions in 5-XB₁₀H₁₃ (113) and 5-X-6,9-C₂B₈H₁₃ (107).

In the orientation 110, free diamagnetic circulation of electrons occurs and generates a secondary magnetic field which is opposite to the applied field H_0 . The B atom is increasingly shielded with increasing orbital radius of atom X (e.g. $F < Cl < Br \ll I$).

In the orientation 111, free diamagnetic circulation is highly hindered; the resulting local field is small and decreases with increasing B-X distance. Averaging over all the orientations results in net neighbor anisotropy shielding. This principle is active together with those discussed in the previous sections, and is especially pertinent for heavy substituents X, e.g. I.

In skeletons with the same geometry (e.g. 112) but a different number of skeletal electrons, the long-distance transmissions of π electrons can follow diverse pathways. This is true of *nido*-5-XB₁₀H₁₃ (113) and *arachno*-5-X-6,9-C₂B₈H₁₃ (107) species which have 24 and 26 skeletal electrons, respectively, and, consequently, differ in their distribution within the molecule. While in the former species, a significant T effect and a weak A effect can be observed, in the latter series, strong T and A effects were found¹¹ (Figure 25). In addition, both types exhibited a general increase in shielding (i.e. an increase in electron density) of the skeletal atoms from the I to EtO (F) derivatives.

e. Effect of Distance: α , β , γ , and δ Substituent Effects. From a practical point of view, the substituent effects are usually classified according to increasing distance from the substituent, namely as α , β , γ , and δ effects. Each of these effects is, in reality, a result of a superposition of several of the effects discussed above.

i. α Substituent Effect. The factors determining the α shift were analyzed earlier by Sprecher et al.,²³ who

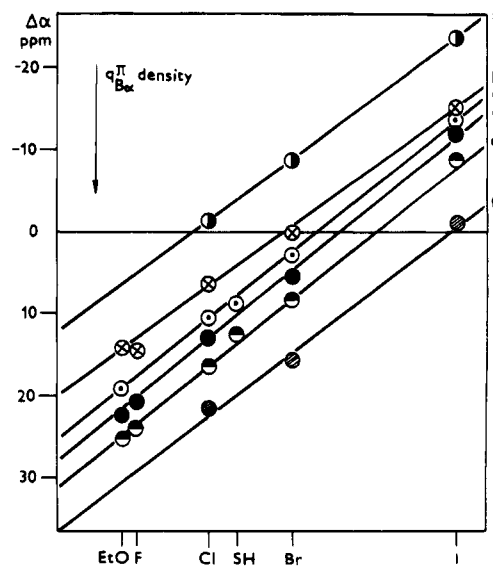


Figure 26. A relationship between the magnitude of the $\Delta\alpha$ increment and the π electron density on the substituted B(α) atoms: (a) 10-X-1-SB₉H₉; (b) 6-X-B₁₀H₁₃; (c) 9-X-1,2-C₂B₁₀H₁₁; (d) 5-X-6,9-C₂B₈H₁₃; (e) 2-XB₁₀H₁₃; (f) 1-XB₅H₉.

considered anisotropic susceptibility and, consequently, induced paramagnetic shielding of the α boron, polarity parameters, changes in the dimension of the 2p orbitals, and the electronegativity of substituent X. Of these, the last two factors were in agreement with the observed shielding trend $F < Cl < Br \ll I$.

In the present review, conclusions drawn from a statistically significant amount of data are presented.

When comparing α shifts caused by X in a number of fundamental types of boron compounds and in different positions (cf. e.g. Figure 23), it can be seen that the α shielding in the given position almost generally increases in the order $RO \leq F \leq NR_2 \leq Cl < Br \leq SH \ll I$. While the absolute values of differences in parts per million for individual substituents X can differ very substantially (e.g. 24.6 to -1.1 for Cl in Table 21), the differences in parts per million between two neighbors, e.g. Cl/Br are nearly the same, irrespective of the framework and of the substituted vertex. The averaging of these differences made it possible to create a universal scale for the compounds that were compared (Figure 26).

From the correlation in Figure 26¹¹ and the data presented in Table 21, the following conclusions can be drawn: (1) similar line slopes can be observed for substituted closo, nido, and arachno compounds; (2) increments Δ increase in the positive sense with growing electron density on the α vertex; (3) provided we know increment Δ for one substituent X in a given molecule and position, we can estimate the probable shift values of the other α signals in analogously substituted derivatives.

ii. β Substituent Effect. Earlier NMR data indicated that halogens, mercapto, and alkyl groups shift the signals of β vertices to higher frequencies. With a growing number of compounds and, especially, of fluoro and alkoxy derivatives, the β effect has been found to be more complicated. At present, it is possible to consider the β shift as being produced by the inductive attraction of electrons (i.e. deshielding) and by " π " donation (i.e. shielding). While the inductive attraction of electrons ($-I$ effect) decreases rapidly from the α to the δ vertex and is significant at the β position, the " π "

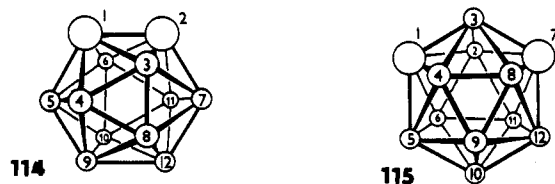
TABLE 21. Changes $\Delta\alpha$ in ^{11}B Chemical Shifts $\delta(^{11}\text{B})$ Caused by Substituent X in Different Positions of Various Skeletons

compound		B-X							ref ^b
vertex	skeleton	I	Br	Cl	F ^a	OR	CH ₃		
1	nido-B ₅ H ₉	-1.4	16.8	24.6				T-18	
2	nido-B ₇ H ₉	-14.5	4.7	12.3	21.5	27.5 ^{OMe}	15.0	T-19	
1	closo-B ₈ H ₆ ²⁻	-10.2	5.4	12.0				T-13	
2	nido-B ₈ H ₁₀	-5.6		18.2			15.3		
2	nido-B ₁₀ H ₁₄	-9.8	8.6	15.9				T-20	
1	nido-B ₁₀ H ₁₄	-11.6	4.2	11.0				T-20	
5	nido-B ₁₀ H ₁₄	-14.2	2.7	10.6		21.4 ^{OEt}		T-20	
6	nido-B ₁₀ H ₁₄	-16.3	-0.1	7.5		15.6 ^{OEt}	12.2	T-20	
1	closo-B ₁₂ H ₁₂ ²⁻	-6.0	7.1	12.5	(25.1)	19.9 ^{OH}		T-14	
6	SB ₉ H ₉	-6.5	7.6	13.4				R-19	
10	SB ₉ H ₉	-24.4	-8.9	-1.1				R-19	
3	nido-5,6-C ₂ B ₈ H ₁₂		5.8	12.5				R-198	
4	nido-5,6-C ₂ B ₈ H ₁₂	-8.2	9.7	17.3				R-53	
8	nido-5,6-C ₂ B ₈ H ₁₂		-0.6	8.1				R-53	
10	nido-5,6-C ₂ B ₈ H ₁₂			-0.9				R-53	
7	nido-5,6-C ₂ B ₈ H ₁₂	-11.3	2.8	8.8				R-53	
5	arachno-6,9-C ₂ B ₈ H ₁₄	-12.8	4.2	11.7	21.8	20.5	12.3	R-187	
1	arachno-6,9-C ₂ B ₈ H ₁₄	-5.8	11.7	19.1				R-199	
3	4,6-C ₂ B ₇ H ₁₃	-4.8	13.0	20.2				R-181	
5	4,6-C ₂ B ₇ H ₁₃	-14.8	0.0					R-181	
1	2,4-C ₂ B ₆ H ₇				12.1				
3	2,4-C ₂ B ₆ H ₇				13.2				
5	2,3-C ₂ B ₅ H ₇				14.2		7.3		
3	closo-1,2-C ₂ B ₁₀ H ₁₂				15.0 ^a		10.0	R-182-184	
4	closo-1,2-C ₂ B ₁₀ H ₁₂	-14.2					9.7		
9	closo-1,2-C ₂ B ₁₀ H ₁₂	-14.2	2.6	9.7	14	17.1 ^{OH}	9.7		
2	closo-1,12-C ₂ B ₁₀ H ₁₂	-13.2	2.7	10.3					
9	closo-1,7-C ₂ B ₁₀ H ₁₂	-13.0	4.2	11.0		25.2	13.6		
2	closo-1,7-C ₂ B ₁₀ H ₁₂			10.8	16.2				

^aFor solvent abbreviations see Table 4. ^bT = table; R = reference.

donation seems to enrich all the positions with electrons. The transfer of an electron pair into the "ortho" position, as in benzene derivatives, is not operative here.

In contrast to benzene derivatives, most borane and heteroborane skeletons exhibit a distinct specificity, namely great differences in electron densities on the individual types of vertices. It was therefore expected that the $\Delta\beta$ increments will increase with (i) decreasing electron density on the α vertex, and (ii) increasing ed on the β vertex. This idea was confirmed for 1- and 9-mercapto-substituted *o*-carboranes (114) and *m*-carboranes (115) HSC₂B₁₀H₁₁ (Figure 27)^{11,200} for which the HS group is joined either to the most positive center on carbon vertices (1-HS) or to the most negative centers on the remote boron atoms (9-HS). Figure 27 shows that the effect of the α -vertex charge is predominant, while the sign and the value of the charge on the β vertex only modifies this basic value. The above



conclusions are valid for icosahedral systems. The situation for other skeletons is more complicated, and the inductive effect is significantly overlapped by the " π " effect. The degree of transmission pathways of " π " electrons into single β positions is, however, still unclear and should be studied.

iii. γ Substituent Effect. In the γ positions of closo and open skeletons, the -I effect of substituent X is already very weak, and the γ shift can thus indicate the degree of " π " electron donation from X to the whole

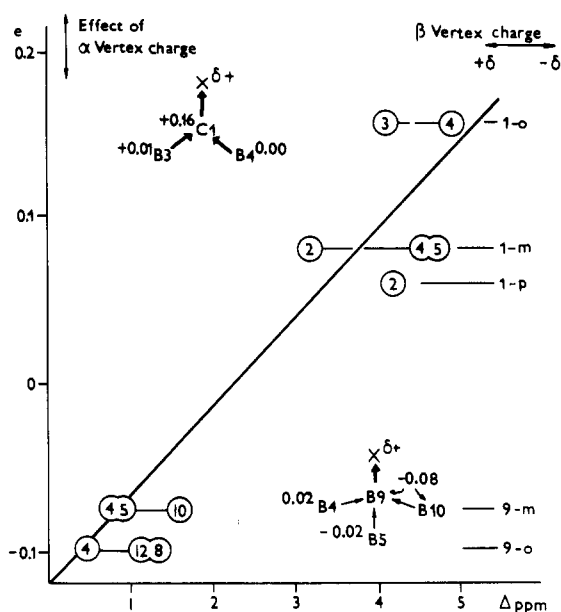


Figure 27. The effect of the α -vertex and the β -vertex charges (in e) on the β -shift increments Δ (ppm) caused by the HS group in XC₂B₁₀H₁₃.¹¹

molecule (cf. Figure 23).

A special case of the γ effect, the trans effect (rediscovered recently as the rhomboidal effect⁹¹) was discussed in section IV.D.1.

iv. δ Substituent Effect. At δ vertices which do not fulfill the conditions for the antipodal effect (see sections IV.D.1 and IV.F), practically no -I effect operates, and only " π " electron donation from substituent X to the whole cluster is operative and, consequently, a small shift to lower frequencies (i.e. the $-\Delta$ change) can be expected.

TABLE 22. ¹¹B Chemical Shift Additivities at Bu₄N⁺ Salts of 1,7-X₂B₁₂H₁₀²⁻ and 1,2-X₂B₁₂H₁₀²⁻ Derivatives in CD₃COCD₃ (X = Halogen): (A) δ(¹¹B) Found and (B) Calculated from Shifts of B₁₂H₁₂²⁻ (-15.3 ppm) and Increments Δ for Individual Positions α, β, γ, and δ (Table 14) (δ_{calc} = δ_{parent} + Δ)

(A) 1,7-X ₂ B ₁₂ H ₁₀ ²⁻					
vertex	1,7	2,3	4,6,8,11	9,10	5,12
F	7.0	-18.1	-19.9	-21.7	-25.4
Cl	-4.1	-14.3	-16.1	-17.9	-19.7
Br	-8.8	-13.3	-14.9	-16.5	-17.9
I	-21.2	-12.1	-13.6	-15.1	-15.3

(B) 1,7-X ₂ B ₁₂ H ₁₀ ²⁻					
vertex	α + γ	β + β	β + γ	γ + γ	β + δ
F	6.6	-18.1	-19.5	-21.7	-25.4
Cl	-3.7	-13.8	-15.4	-17.5	-19.2
Br	-9.0	-13.4	-14.6	-16.2	-17.9
I	-21.8	-12.0	-13.3	-15.0	-15.0

(A) 1,2-X ₂ B ₁₂ H ₁₀ ²⁻					
vertex	1,2	3,6	4,5,7,11	8,10	9,12
Cl	-2.3	-14.3	-16.1	-17.9	-21.5
Br	-7.2	-13.3	-14.9	-16.5	-19.5
I	-19.7	-12.1	-13.6	-15.1	-16.8

(B) 1,2-X ₂ B ₁₂ H ₁₀ ²⁻					
vertex	α + β	β + β	β + γ	γ + γ	γ + δ
Cl	-3.7	-13.8	-15.3	-18.1	-20.1
Br	-8.9	-13.3	-14.7	-16.9	-18.7
I	-20.8	-11.9	-13.6	-15.0	-16.3

f. *Additivity of Substituent Effects in B Skeletons.* The additivity of ¹¹B NMR shift changes evoked by two substituents (9) was studied for disubstituted pentaboranes (9) (skeleton 9),¹⁷⁰ decaboranes (14),¹⁷⁶ hexahydro-*closo*-hexaborates (2-),¹⁶⁰ dodecahydro-*closo*-dodecaborates (2-),¹⁶¹ (Table 22), *o*-carboranes (114),^{11,184} *m*-carboranes (115)^{11,184} (Table 23), and polymethyl-2,4-dicarba-*closo*-hexaboranes.²⁰¹

Most of the calculated ¹¹B-shift values were in good agreement with the values found, and the deviation was usually close to ±0.5 ppm. Thus, most of the effects discussed above do not cross in individual positions.

Exceptions have, however, been observed for vicinally and antipodally substituted skeletons. In the former case, the calculated δ ¹¹B values of substituted atoms [B(1,2) in B₁₂H₁₂²⁻ skeleton, Table 22; B(9,12) in *o*-carborane (114), Table 23] show systematic and distinct shifts to lower frequencies, and those of antipodally unsubstituted atoms [B(9,12) in B₁₂H₁₂²⁻ skeleton, Table 22 and in 1-Me-2-HS-*o*-carborane, Table 23] show a systematic shift to higher frequencies. In principle, an analogous ¹¹B-shift anomaly can also be observed at antipodally disubstituted vertices (e.g. 1,12-XY-*o*-carboranes, Table 23) the signals of which are shifted more to lower frequencies, i.e. are more shielded, than would be expected from the δ ¹¹B calculated values. These observations indicate that in the discussed compounds, mutual "π" interactions which are not involved in increments Δ must be present.

Analogous additivity regularities are also to be expected with other groups of boron compounds.

2. B Skeletons with H Tautomerism

As mentioned in section IV.C.1 which deals with the μH rules, the B skeletons exhibiting H tautomerism exhibit ¹¹B NMR spectra in which two or several signals are averaged and are, therefore, located in the central

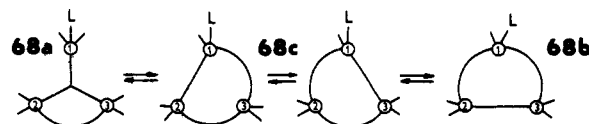
TABLE 23. ¹¹B (64.184 MHz) of Substituted *o*-Carboranes¹¹ (A) δ(¹¹B) of Individual Signals (ppm Relative to BF₃·OEt₂, CDCl₃) (B) Differences (Δ = δ_{calc} - δ_{obs}); δ_{calc} = δ_{parent} + Increments for Individual X and Positions

substituents	9	12	8,10	4,5	7,11	3,6
(A)						
1-HS-9-Cl	7.87	-6.47	-9.46	-9.46	-14.71	-13.77
1-HS-9-Br	0.39	-6.15	-8.93	-9.63	-12.58	-13.97
1-HS-9-I	-16.32	-5.43	-8.15	-9.19	-12.98	-11.76
1-HS-12-Cl	-1.20	4.96	-8.98	-10.96	-12.94	-12.94
1-HS-12-Br	-0.90	-2.40	-8.62	-10.31	-12.50	-12.50
1-HS-12-I	-0.10	-19.19	-7.88	-9.29	-11.68	-11.68
9-Cl-12-HS	6.19	3.99	-8.20	-15.54	-15.54	-18.62
9-Br-12-HS	-0.52	4.10	-7.78	-15.23	-15.23	-17.54
9-I-12-HS	-15.20	4.37	-6.95	-14.75	-14.35	-16.38
1-Me-2-HS	-5.33	-5.33	-10.39	-10.39	-8.85	-8.85
1-Me-9-HS	4.50	-6.49	-8.83	-11.17	-14.29	-12.94
1-Me-12-HS	-1.51	0.51	-8.79	-12.16	-13.00	-12.16
1-HS-9,12-Cl ₂	7.05	3.99	-8.64	-11.30	-14.86	-14.86
(B)						
1-HS-9-Cl	0.17	0.01	0.20	-0.45	0.15	0.65
1-HS-9-Br	0.49	0.25	0.08	0.11	0.15	0.07
1-HS-9-I	0.49	-0.47	0.21	0.39	0.53	0.06
1-HS-12-Cl	0.06	2.03	-0.20	-0.17	-0.16	-0.17
1-HS-12-Br	0.11	1.84	-0.24	-0.15	-0.30	-0.01
1-HS-12-I	0.07	1.75	-0.45	0.04	-0.04	0.06
9-Cl-12-HS	1.24	0.30	-0.14	0.19	-0.08	0.38
9-Br-12-HS	0.78	0.66	-0.24	0.18	0.25	0.28
9-I-12-HS	-1.24	1.01	-0.15	0.42	0.61	0.10
1-Me-2-HS	-0.85	-0.74	0.71	0.38	0.05	0.75
1-Me-9-HS	-0.02	-0.19	-0.01	-0.05	-0.04	1.31
1-Me-12-HS	-0.18	-1.03	0.05	-0.10	-0.29	-0.69
1-HS-9,12-Cl ₂	1.41	-0.64	0.03	0.07	0.35	0.30

part of their original positions. The introduction of substituent X into the open face can usually slow or suppress the H tautomerism to such a degree that one of the possible tautomers can predominate in the "static" spectrum which, consequently, is significantly enlarged.

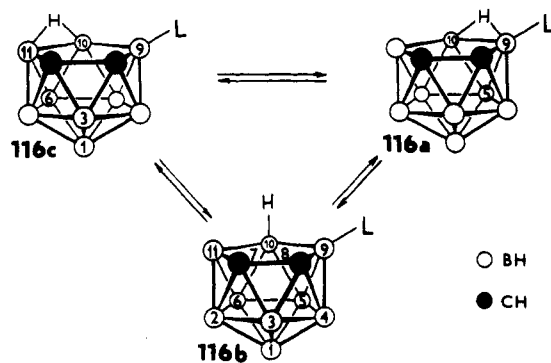
Interpretation of the ¹¹B spectra of the title compounds requires basic information on (1) the probable ¹¹B spectra of the individual static H tautomers of the parent skeleton taking part in the equilibrium, (2) the degree of slowing of the H tautomerism by the introduction of a given substituent (ligand) X, and (3) the effect of substituent X on the consequent distribution of endo hydrogen atoms and of chemical bonds in the molecule.

The estimation of ¹¹B spectra of static H tautomers can be carried out by (i) measurements at low temperature [e.g. B₄H₉⁻, Table 9 (70)] or in solid phase; (ii) extrapolation from the spectra of related compounds in which substituent X stops the H tautomerism but shows a similar influence on the individual vertices as H⁻ does (e.g. CN⁻, SCN⁻);³² (iii) IGLO calculations of the ¹¹B chemical shifts of the individual H tautomers, as was carried out for B₃H₈⁻ (Table 8, structures 68a and 68b), B₄H₉⁻ (Table 9, 70), and B₆H₁₀ (Table 8, 52).¹¹⁵



The effect of substituent X on the H_{endo} tautomerization rate was revealed for 9-substituted derivatives of the *nido*-C₂B₉H₁₂ carborane anion (116) in which the surplus H atom rapidly oscillates between two bridge positions B(9)-B(10) (116a) and B(10)-B(11) (116c),

passing through symmetrical intermediate state 116b with an extra H bound only to the B(10) atom.



In the 116a tautomer, the μH is opposite to vertex B(5) which should therefore resonate—according to the μH rules—at the low(est) frequency, while the vertex B(6) at the high(est) frequency (see section IV.C.1). Rapid H tautomerism between these two arrangements should lead to the mixing of both extreme shifts to yield an averaged ^{11}B shift, which is in the agreement with the observed results.

A preliminary study²⁰² of several 5,6- D_2 -9-X-7,8- $\text{C}_2\text{B}_9\text{H}_{11}$ carborane anions (116) has shown that, in the parent anion (X = H) the signals of the B(5) and B(6) atoms are identical and located at the middle frequencies, which confirms the fast H tautomerism discussed above. The relatively high additional splitting (ca. 55 Hz) of the HB(10) doublet, produced by the surplus endo hydrogen also documents significant participation of the quasi-BH₂ group (116b) in the μH -BH₂ equilibrium.

The introduction of substituent X (X = Me₂S, Py, Br⁻, I⁻) into the 9-position caused a distinct but different separation of the B(5) and B(6) signals, which was interpreted as being a result of the preferred location of the bridge hydrogen in one of two possible μH positions. The extent of the separation of these signals was considered to be a measure of the H-tautomerism rate.²⁰²

Recently, large series of 9-X-7,8- $\text{C}_2\text{B}_9\text{H}_{11}$ carboranes (116), differing in the character of substituent X was prepared and the ^{11}B spectra of all the members were analyzed by the 2D method (cf. section III).²⁰³ It follows, from the comparison of individual spectra in Figure 28, that

(1) Electron-attracting substituents repulse the H bridge to the remote position 116c. The repulsion power can be estimated from the difference $D = \delta_{\text{B}(5)} - \delta_{\text{B}(6)}$ and decreases in the order $\text{Me}_2\text{S} = \text{CN}^- \geq \text{Py} \geq \text{UR} \geq \text{I}^- > \text{Me}_2\text{SCH}_2 > \text{MeS}^- > \text{HS}^- > \text{Br}^- > \text{CH}_3\text{COO}^-$.

(2) Electron-donating substituents attract the μH bridge (116a): $\text{HO}^- \geq \text{CH}_3^-$ (probably also F^- , NR_2^-). Because of the simultaneous +R donation and -I attraction of electrons for the majority of substituents X, the resulting donation is relatively low, and the formation of a positional isomer exhibiting a statistical maximum μH on the BX vertex is exceptional.

The information presented in this section permits us to estimate the preferred location of H bridges and the corresponding distribution of bonds within the given molecule and, consequently, the chemical shifts of the individual B atoms involved (cf. section IV.C.). The

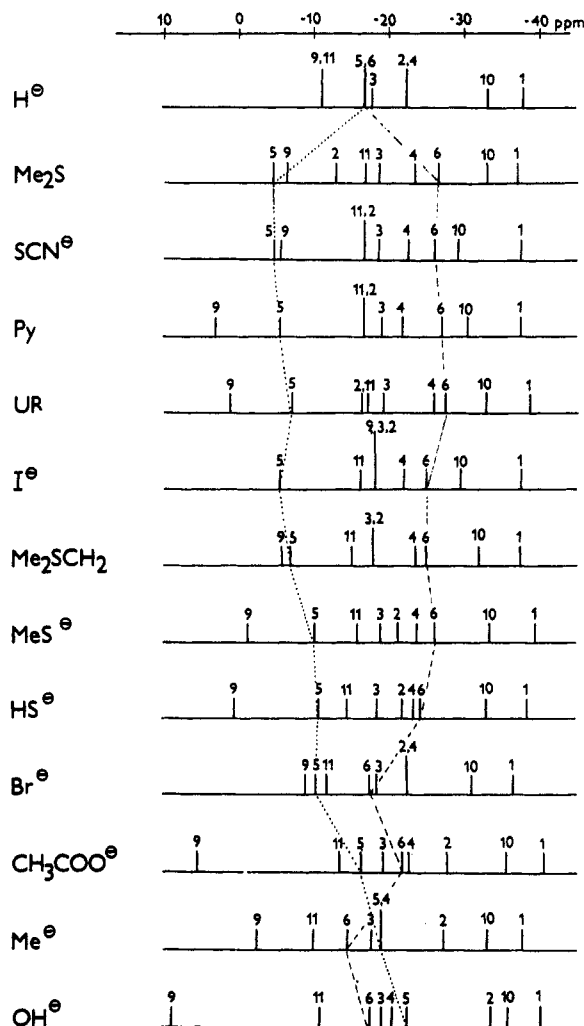
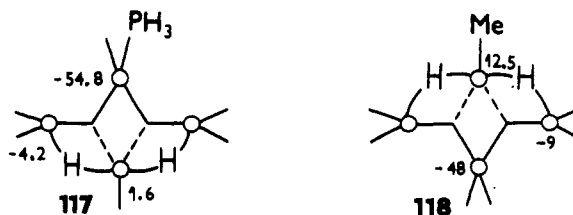


Figure 28. Stick diagrams of the ^{11}B chemical shifts for the 9-L-7,8- $\text{C}_2\text{B}_9\text{H}_{11}$ derivatives. The separation of B(5) and B(6) signals indicates a suppressed H tautomerism; the signal resonating at lower frequency corresponds to the B atom which is opposite to the μH bridge (i.e. B(6) for L = Me₂S, structure 116c, and B(5) for L = OH⁻, structure 116a).

whole complex subject will be demonstrated on several examples.

a. ^{11}B Spectra and Structures of 1-XB₄H₉⁻ (for X = PH₃ (117) and Me⁻ (118)). In both cases, the H tautomerism is suppressed and the ^{11}B spectra can be compared with that of the static form of B₄H₉⁻ obtained at a low temperature (cf. Table 9, 70). The ^{11}B chem-



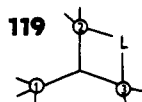
ical shifts of B(1) and B(3) atoms of both derivatives confirm the validity of the above conclusions. Structure 117 is general for all the compounds bearing uncharged ligands such as are substituted phosphines,^{205,206-211} amines,²¹² urotropine,²¹³ dialkyl sulfides,^{214,215} and carbon monoxide.²¹⁶ Structure 118 is still unique in this series but can be expected for OR⁻ and NR₂⁻ derivatives, when these are prepared.

b. ¹¹B Spectra and Probable Structures of LB₃H₇. At present, more than 30 compounds of this group are known,²¹⁷⁻²³⁷ and all of them exhibit two signals with the relative ratio 2:1. This ratio corresponds to any of the three isomers, 68a, 68b, and 119, as well as to equilibrium 68c. The ¹¹B spectra of the two main tautomers derived from the parent anion B₃H₈⁻ (68, L = H⁻), although inaccessible by direct measurement, have recently been computed by the IGLO method,¹¹⁵ which also allows us to calculate an averaged spectrum for equilibrium 68c. The totals of average chemical shifts for the individual tautomers are -21.9, -20.7, and -32.1 ppm for 68a, 68c, and 68b, respectively, of which the latter is closest to the experimental value of -29.8 ppm^{228,231,233} and represents the probable structure of B₃H₈⁻ in solution.¹¹⁵ Similar conclusions were drawn from the SCF-CI and STO-4-31G results.²³⁸

It can be expected that the strong electron-attracting substituents in LB₃H₇ will adopt arrangement 68a, that the donating-attracting substituents will prefer equilibrium 68c, and that the strong donating substituents will be located between two bridges in arrangement 68b.

The ¹H NMR spectra of various LB₃H₇ derivatives exhibit only one signal for all the hydrogen atoms bound to the skeleton,²³⁹ which indicates the presence of a fast H tautomerism in all of them. The ¹¹B spectra of LB₃H₇ compounds are therefore very likely a result of an equilibrium involving the individual tautomers, 68a ⇌ 68c ⇌ 68b, in which one tautomer predominates. On the basis of the μH rules, confirmed here by the IGLO results, we can expect that the substituted α vertex will resonate at low frequencies with 68a and at high frequencies with 68b tautomers, and the reverse effect should be observed at the β vertex. Providing that the ligand does not dramatically influence the vicinal β vertex, we can consider the β shift to be an indicator of the center of gravity in the discussed equilibrium. The calculated ¹¹B chemical shifts for the β vertices in the parent (L = H⁻) species are -7.5, -26.4, and -43.5 ppm, respectively (Figure 29a). Inspection of the set of schematic spectra in Figure 29b indicates that a successive decrease in the electron attraction and an increase in the donation caused by ligand X shifts the signals of the β vertices to lower frequencies and the signal of the α vertex (influenced, in addition, by a strong α effect) to higher frequencies. This observation is in agreement with the conclusions drawn for the 9-X-7,8-C₂B₉H₁₁ series and indicates that substituents X shift the equilibrium 68a ⇌ 68c ⇌ 68b successively to the right in the order CO ≥ PH₃ > CN⁻ > Br⁻ > NCS⁻ > Cl⁻ > OCN⁻ > F⁻ >> OH⁻.

Surprisingly, the group of methyl amines is analogous to the above series (Figure 29c). It is still not known whether the same or a different mechanism is active here. A special group of LB₃H₇ derivatives have ether as a ligand (Figure 29c) and the possibility of intermediate structure 119 was considered in the ligand migration.²³⁸



The ¹¹B NMR spectra of LB₃H₇ derivatives and their analysis complement and modify the results of the

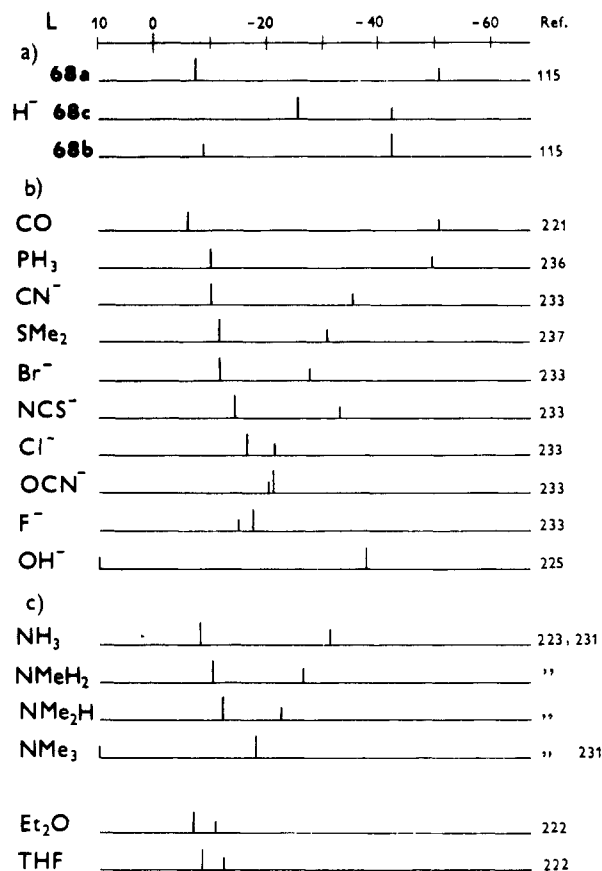


Figure 29. Stick diagrams of the ¹¹B chemical shifts of α (B1) and β (B2,3) vertices in the 1-LB₃H₇ adducts: (a) for individual H tautomers 68a, 68b, and equilibrium 68c (from IGLO calculations) for the parent B₃H₈⁻ anion and for the observed (fully averaged) parent B₃H₈⁻ anion (L = H⁻); (b) the dependence of chemical shifts of α and β vertices on the decreasing electron attraction and increasing electron donation of the Lewis base, i.e. a successive shift of the center of equilibrium 68a ⇌ 68c ⇌ 68b to the right; (c) the dependence of α and β shifts on the increasing bulk and -I,+R character for L = amine or ether.

TABLE 24. ¹¹B Chemical Shifts of Substituted 2-XB₆H₉^{120,121}

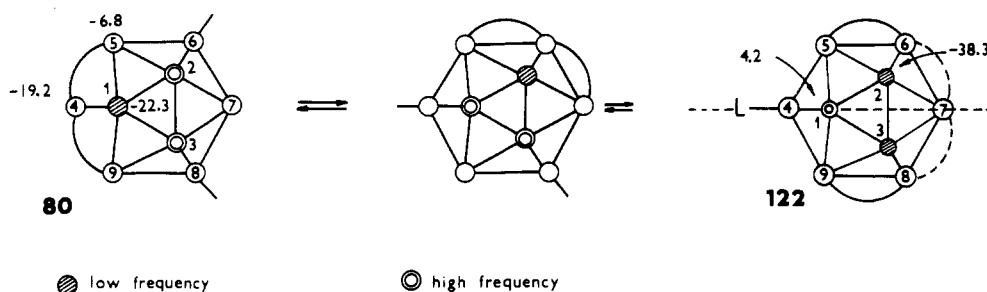
X	B(2)	B(3,6)	B(4,5)	B(1)	ref
H	14.1	14.1	14.1	-51.8	36, 96
Cl	32.3	15.9 (160)	5.6	-48.8 (160)	240
Br		18.1	6.2	-48.3	36
I	8.5	20.2 (153)	7.1 (161)	-48.3 (159)	240
CH ₃	29.36	5.77	17.26	-50.53	241

quantum chemical calculations of the local energy minima (PRDDO, STO-3G, STO-4-31G methods) which always preferred the isomers 68a, irrespective of substituent X (NH₃, H₂O, CO, Me₂O, F⁻).²³⁸

These results demonstrate that, in spite of a considerable effort of several teams, the effect of substituents on H-tautomerizing B skeletons has not yet been completely elucidated.

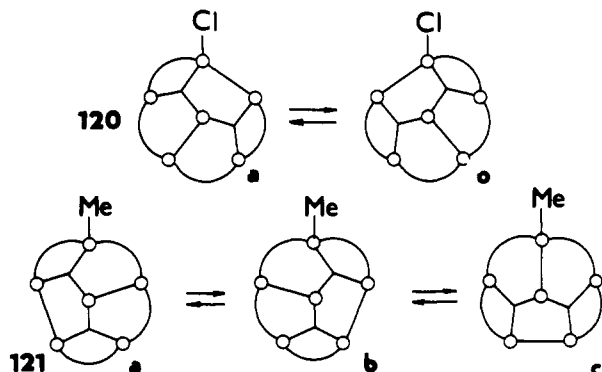
c. ¹¹B Spectra and Preferred H Tautomers at 2-XB₆H₉ Derivatives. Table 24 shows that the β and γ shifts for 2-halogenohexaboranes(10) (120) are distinctly different from that for 2-MeB₆H₉ (121). This difference diversity can be explained on the basis of the fact that halogens repulse, whereas methyl attracts μH bridges. In the former compounds, we can expect a preference for only one bridge on the halogen-substituted α vertex and, consequently, only two H tautomers 120. The chemical shifts of individual B atoms in the

CHART 1

TABLE 25. ^{11}B Chemical Shifts of 4- EB_8H_{12}

E	no.	B(7)	B(1)	B(5,9)	B(6,8)	B(2,3)	ref
BH_2^-	80	-6.8	-24.0	-6.8	-19.2	-24.0	132
CH_2	123	17.21	-4.17	-7.06	-34.02	-42.28	102, 243
NH	124	7.76	-25.41	-7.11	-47.69	-45.97	102
S	125	13.40	-13.53	-4.62	-41.77	-42.80	102, 244
4-BHNCS	122	14.8	4.2	-16.4	-18.0	-38.3	132

static 120 structure of the parent B_6H_{10} (Table 8, 51) can be exploited to calculate a resultant shift of 18.6 ppm (found 15.9 to 20.2 ppm), for the β vertex derived from the averaged shifts of B(3) and B(4) in B_6H_{10} , i.e. 18.6 and 18.6 ppm. Similarly, a resultant shift of 6.1 ppm (found 5.6 to 7.1 ppm), derived from averaged shifts of B(2) and B(3) in B_6H_{10} , i.e. -6.5 and 18.6 ppm, respectively, can be calculated for the γ vertex.



The preferred H-tautomeric equilibrium at 2-Me B_6H_9 (121) exhibits three structures with methyl between two μH bridges. Similarly as above, a β shift of 10.2 ppm (found 5.8 ppm), obtained by averaging ^{11}B shifts of three vertices, namely B(2,3,4), i.e. -6.5, 18.6, and 18.6 ppm, has been observed. Analogously, the γ shift of 18.6 ppm (found 17.3 ppm) results from the averaging of the B(3,4,4) signals showing shifts of 18.6, 18.6, and 18.6 ppm in the parent B_6H_{10} .

All these calculations were performed assuming a low β and γ substituent effect of X, which was confirmed

TABLE 26. ^{11}B Chemical Shifts for 6-L-4- CB_8H_{12} (127-129)

L	5	9	7	2	1	6	8	3	ref
SMe_2	-1.0	0.2	-5.6	-10.1	-21.0	-32.5	-23.9	-53.2	169
UR	-1.7	-0.2	-6.0	-13.8	-22.2	-25.0	-25.0	-53.5	169
NMe_3	0.4	0.5	-4.8	-12.2	-22.1	-18.9	-25.9	-52.7	241
Py	1.2	0.1	-2.8	-8.7	-20.7	-22.8	-24.0	-51.9	278

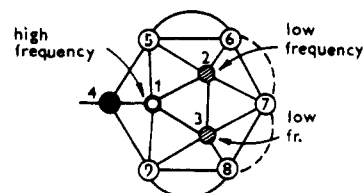
TABLE 27. ^{11}B Chemical Shifts of 4,6- EGB_7H_9

no.	4-E	6-G	B(5)	B(7)	B(9)	B(1)	B(2)	B(8)	B(3)	ref
104	CH_2	CH_2	0.16	0.87	0.87	-17.36	-52.58	-27.84	-52.58	39, 84
130	CH_2	NH	-6.78	-1.22	-7.59	-19.17	-39.56	-40.89	-50.37	39
105	CH_2	S	-0.55	1.41	1.41	-14.71	-27.17	-33.09	-50.07	102, 241
106	S	S	-5.18	2.08	2.08	-23.33	-49.62	-38.45	-49.62	102
131	S	Se	-1.0	5.8	4.6	-16.2	-21.7	-34.3	-48.9	245

by the good agreement of the found and calculated values.

d. ^{11}B NMR Spectra and H Tautomerism with Nine-Vertex B Skeletons. The basic compound in this series is the anion $\text{B}_9\text{H}_{14}^-$ (80) which exhibits fast tautomerism and has a restricted spectrum with three doublets of the geometrically equivalent vertices resonating at -6.8 (5,7,9), -19.2 (4,6,8), and -22.4 ppm (1,2,3) (Chart 1).¹³² Measurements at temperatures up to -90 °C as well in the solid state at ambient temperature did not indicate a suppressed H tautomerism.²⁴² To estimate one of the possible $\text{B}_9\text{H}_{14}^-$ tautomers, the ^{11}B NMR spectrum of the 4- $\text{SCNB}_9\text{H}_{13}^-$ anion (122)¹³² was considered, because we have found that $-\text{NCS}^-$ and several other ligands such as CN^- or PH_3 suppress the tautomerism but influence other vertices similar to H-. This was also confirmed for the 4- $\text{SCNB}_9\text{H}_{13}^-/\text{B}_9\text{H}_{14}^-$ couple while the chemical shifts of the averaged signals of the B(5,7,9), B(4,6,8), and B(1,2,3) vertices for the former anion have the values -6.0, -19.3, and -24.0 ppm, respectively, which are very similar to those for $\text{B}_9\text{H}_{14}^-$. This indicates that the structure of the static molecule of $\text{B}_9\text{H}_{14}^-$ will very likely have structure 122 with $\text{BH}_2-\mu\text{H}$ migration between the B(6)-B(7)-B(8) atoms.

The same character, as far as the H tautomerism, can be predicted for the 4- EB_8H_{12} molecules, in which E = CH_2 (123), NH (124), or S (125). All these compounds



123 4- CH_2
124 4-NH
125 4-S

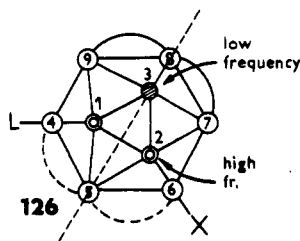
have, in agreement with the μH rules (section IV.D.1), similar ^{11}B NMR spectra and main features, i.e. one

TABLE 28. ¹¹B Chemical Shifts and Increments Δ (Δ = δ_{subst} - δ_{BH₄⁻) for LBH₃ (132)^a}

L	δ(¹¹ B) ^a	Δ
H ⁻	-42.2 ^e	-
CO	-52.0 ^a	-9.8
PF ₃	-48.3 ^f	-6.1
PH ₃	-43.0 ^e	-0.8
PMe ₃	-38.2 ^e	4.0
PPh ₃	-37.5 ^f	4.7
NH ₃	-23.8 ^l	18.4
NH ₂ Me	-19.1 ^g	23.1
NHMe ₂	-13.5 ^h	28.7
NMe ₃	-8.3 ^h	33.9
OMe ₂	2.5 ^a	39.7
THF	-0.7 ^f	42.9
SMe ₂	-20.1 ^c	22.1
CN ⁻	-43.9 ^f	-1.7
PH ₂ ⁻	-37.3 ^f	4.9
CO ₂ ⁻	-37.1 ^f	10.5
NC ⁻	-27.2 ^f	15.0
SH ⁻	-25.0 ^f	17.2
NMe ₂ ⁻	-14.7 ^h	27.5
OH ⁻	-13.9 ^e	28.3

^aFor abbreviations of solvents see Table 4.

signal of intensity 2 at low frequency, belonging to B(2,3), and another one of intensity 1 at high frequency, belonging to B(1) (Table 25). On the basis of the μH rules and information on the effect of substituent X on the final distribution of the endo hydrogens (μH, BH₂), we can predict that the introduction of an additional substituent X or of a heteroatom G into the 6-position will change the structure of the heteroborane 122 into 126 and those of 4-EB₃H₁₂ (123–125) to 4-E-6-LB₈H₁₁



(127–129) (Table 26), or to 4,6-EGB₇H₉ (e.g. 130 and 131, Table 27). This substitution is associated with a change in the character of the ¹¹B spectra, in which the B(2) signal in arrangement 58 appears at the lowest frequency (cf. section IV.C.1) together with the B(8) signal in the arrangement 103 (cf. section IV.C.2), while the signals of B(1,3) are shifted to higher frequencies.

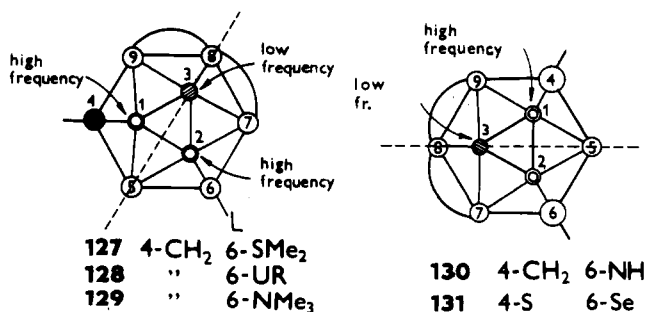
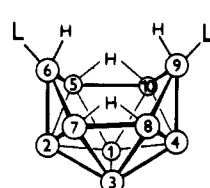


TABLE 29. ¹¹B Chemical Shifts for Selected 6-L-B₁₀H₁₃ (133)

L	B(4)	B(2)	B(5,7)	B(8,10)	B(9)	B(1,3)	B(6)	ref
H ⁻	-8.09	-8.09	-23.10	-23.10	-36.62	-42.26	-36.62	39
CN ⁻	-3.40	-2.49	-18.52	-20.36	-32.68	-38.22	-39.18	39
Py	-4.2	-5.9	-18.0	-20.2	-30.2	-39.3	-17.2	246
NEt ₃	-6.5	-8.6	-19.6	-20.7	-31.6	-40.6	-15.0	246
PPh ₃	-1.6	-5.4	-17.1	-19.6	-27.1	-38.0	-38.0	246

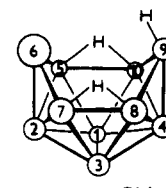
3. Effect of Uncharged Ligands on Chemical Shifts in B Skeletons

The Lewis base–borane adducts represent the most common derivatives of borane anions B_nH_n^{x-} in which a neutral ligand was substituted for hydridic atom H⁻. The changes evoked by single substituents can be evaluated by comparing ¹¹B spectra of individual derivatives with those of the parent anion. This can be done, however, either with nontautomerizing anions, the structure of which is not influenced by the ligand introduced, or with anions for which we know the ¹¹B spectra of individual H tautomer(s) from measurements at low temperature or from IGLO calculations. The former group is represented by LBH₃ (132, Table 28), 6-LB₁₀H₁₃⁻ (133, Table 29), 6,9-L₂B₁₀H₁₂ (134, Table 30), and 9-L-6-EB₉H₁₂ [E = CH₂ (135), NH (136), S (137); Table 31], the latter one by 1-LB₄H₈ (117, Table 32).



133 L' = H

134 L' = L



135 6-CH₂

136 6-NH

137 6-S

From the δ(¹¹B) of individual vertices gathered in Tables 28–32 and from other series, it is possible to infer that the neat effect of ligand L on ¹¹B chemical shifts of individual atoms evokes: (i) a relatively small shift of signals of β and γ vertices to higher frequencies (1–8 ppm); (ii) an imperceptible influence on δ vertices (including those of antipodal character); (iii) a very different influence on α vertex, the ¹¹B shift of which is similar to H⁻ with PH₃, many PX₃ derivatives, and CN⁻ (which allows one to assume a similar ¹¹B spectrum for a H tautomer of the pertinent hydroborate) and drops by 20–35 ppm with amines, dialkyl sulfides, and ether adducts. These values should, however, be treated carefully, as further influences can be active in some heteroskeletons, changing the α vertex–ligand interactions (cf. Table 31).

E. Effect of Heteroatom Vertex on Chemical Shifts

A substitution of a B vertex by a heteroatom E has quite a different impact on (a) rigid *closo*-boranes, (b) fluxional *closo*-boranes, (c) open-face boranes with no H tautomerism, and (d) open-face boranes with H tautomerism.

In the next paragraphs, the changes that such a substitution brings will be discussed in some detail.

1. Rigid *closo*-Heteroboranes Derived from *closo*-Boranes B_nH_n²⁻ for n = 5, 6, 7, 10, 12

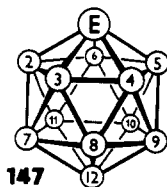
Structures of the parent rigid hydroborates 10–12, 15, and 17 are shown in Figure 6. A formal exchange of a

TABLE 30. ^{11}B Chemical Shifts for *arachno*-6,9- $\text{L}_2\text{B}_{10}\text{H}_{12}$ (134)

L	2,4	5,7,8,10	9,6	1,3	ref
H	-8.1	-23.1	-36.6	-42.3	39
Me_2S	-3.8	-20.3	-24.4	-40.4	39
MeCN	-5.7	-20.4	-31.2	-42.8	247
EtNC	-1.3	-18.3	-39.9	-44.7	247

heteroatom E or of an E-X unit for a BH vertex evokes only small changes in the original geometry of these skeletons, namely in bonding distances between E and its neighbors. In the case of an electron-satisfied heteroatom E (C, N, P, S, etc.), the more electrons the element E bears (δ^+ , $\text{C} < \text{N} < \text{S}$) and the easier it releases them (δ^+ , $\text{N} < \text{P} < \text{As}$; $\text{S} < \text{Se} \leq \text{Te}$) the more positive the heteroborane is, in comparison with the original formal BH^- or $:\text{BH}:^{2-}$ vertices. A positively charged vertex E evokes a successive decrease of electron density on β (vicinal, neighbor), γ (meta), and δ (antipodal, opposite, para) vertex (see Figure 16b).

It was expected that the decrease in electron density caused by the introduction of a negative heteroatom into the B skeleton will result in decreasing shielding of β vertices and in shifting their signals to higher frequency. In reality, this expectation has been met only in a few cases of rigid *closo*-heteroboranes (cf. Tables 33 and 5) and quite failed with $\text{EB}_{11}\text{H}_{11}$ compounds (147, Table 34), for which a reverse trend in shielding was observed. The most significant high-frequency shift is shown by the B atom antipodal to S.^{265,266} This Vertex Antipodal effect (VA effect), reported by us in 1974, was assigned to the strong δ^+ character of the heteroatom E: "the ^{11}B chemical shift of a skeletal boron atom does not depend on its electron density but is mainly influenced by the electron density on the atom located on the opposite side of the molecule; the δ^+ charged atom shifts the signal of an antipodal atom to higher frequency, while the δ^- charged atom shifts it to lower frequency (compared with the nonperturbed atom)".²⁶⁵



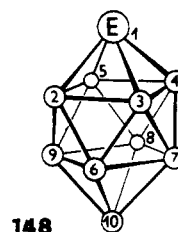
A comparison of $\delta(^{11}\text{B})$ of the B(2-6) and B(7-11) atoms in $\text{SB}_{11}\text{H}_{11}$ (cf. 147) with expected electron densities suggests that also in this case the relative chemical shift is ruled by ed on the antipodal atom (Table 35). The lower the ed is the greater deshielding of the antipodal atom (^{11}B , ^{13}C).

TABLE 31. ^{11}B Chemical Shifts for *arachno*-9-L-6- EB_9H_{12} (135-137)

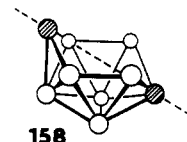
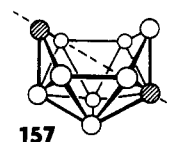
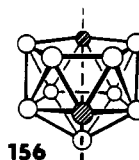
E	L	B(4)	B(2)	B(5,7)	B(9)	B(8,10)	B(1,3)	ref
CH_2	H	-1.25	-10.23	-12.80	-22.56	-28.41	-39.52	248
CH_2	CH_3CN	0.7	-8.4	-13.5	-26.1	-26.1	-40.6	249, 250
CH_2	Me_2S	-0.27	-6.0	-11.9	-20.2	-26.0	-38.6	249, 250
CH_2	PPh_3	1.6	-3.9	-11.8	-30.6	-24.6	-38.0	249, 250
NH	H	-1.20	-21.05	-12.46	-21.05	-41.00	-41.30	251
NH	Py	2.4	-11.4	-11.4	-19.5	-38.1	-40.8	251
NH	tBuNC	4.6	-12.7	-12.7	-38	-36.1	-40.5	251
NH	MeNC	5.26	-12.04	-12.04	-38.52	-35.6	-39.9	262
S	H	-3.6	-1.9	-8.4	-14.9	-33.8	-37.1	251, 252
S	THF	2.3	-7.8	-7.8	-13.1	-33.4	-38.6	253
S	CH_3CN	8.7	-3.1	-8.6	-34.6	-29.4	-35.5	253
S	CN^-	8.3	-7.9	-6.9	-19.5	-30.7	-34.5	252

This idea was then extended to the B-B antipodal vertices to explain the order of $\delta(^{11}\text{B})$ in *o*- and *m*-carborane (Table 35)¹⁸² and, in turn, to estimate vertex charges from the ^{11}B shifts in metallaboranes.²⁷⁰

The above cited prediction has been recently confirmed on $\text{MeAlB}_{11}\text{H}_{11}$ (147, $\text{E} = \text{AlMe}$)²⁶⁹ in which the Al heteroatom is presumably of higher electron density than the boron vertex in the isostructural $\text{B}_{12}\text{H}_{12}^{2-}$ parent; the antipodal B(12) atom being then significantly shifted to lower frequency. For real values of the ^{11}B chemical shifts in two-heteroatom icosahedral skeletons of the 1,2- $\text{EBG}_{10}\text{H}_{10}$ type (148; E,G = CH, P, As, Sb) see Table 36.



A different situation is with the compounds EB_9H_9 (148, Table 37), in which both antipodal and trans effects of individual vertices can operate simultaneously.



The former effect is active along the main axis intersecting the 1,10 vertices and is approximately twice as high as the A effect in icosahedral molecules.²⁶⁵ The latter operates across the base of the present tetrahedral pyramid in the same sense as does the A effect. Both effects are nicely documented by the ^{11}B spectrum of the carborane 1,6- $\text{C}_2\text{B}_8\text{H}_{10}$ (145, Table 33), in which the signals of both the antipodal (B10) and trans vertex (B8) are significantly shifted to the low field.

Our experience has shown that the δ^+ charged heterovertices exhibit stronger but reverse A and T effects than do electron-donating substituents in the same positions (Figure 30). This has indicated the possibility of a common mechanism for the electron transfer caused by the exo and endo substituents (see section IV.F).

In 1986, Teixidor et al.⁹¹ described a qualitative procedure for the estimation of a distribution of ^{11}B signals in the NMR spectrum of *closo* heteroboranes by utilizing Williams' coordination rule and five parameters termed antipodal, rhomboidal, butterfly, neighbor,

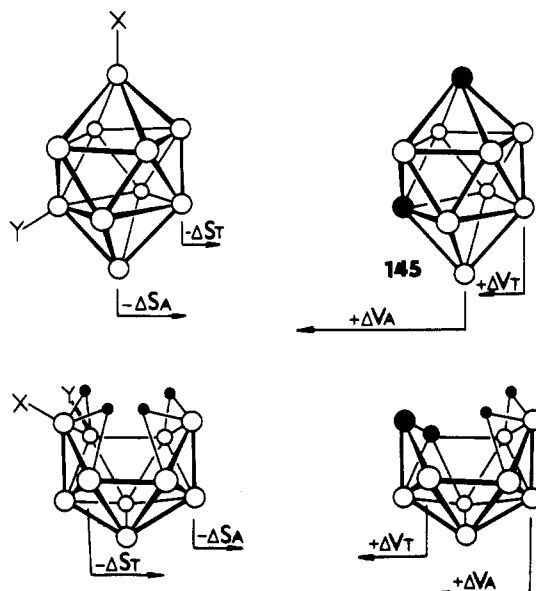


Figure 30. Reverse signs of changes Δ in the +M substituent antipodal (S_A) and substituent trans (S_T) shifts in comparison with the $\delta+$ vertex antipodal (V_A) and vertex trans (V_T) shifts.

TABLE 32. ¹¹B Chemical Shifts for LB_4H_8 (117)

L	3	2,4	1	ref
H ⁻ (-90 °C)	0.8	-10.2	-54.4	127
CO				216
PF ₃	1.9	-2.7	-57.5	204, 207
PH _{3(exo)}	1.6	-4.2	-54.8	208, 209
PH _{3(endo)}	5.1	-3.5	-57.0	208, 209
PMe ₃	-1.8	-7.0	-51.5	210
NMe ₃	1.1	-8.5	-22.5	212
UR	-1.1	-9.3	-28.5	213
SMe ₂	1.3	-6.9	-34.2	215, 214
SEt ₂	1.3	-7.0	-36.8	215

and symmetrical neighbor effects. This procedure is, however, applicable only to rigid and symmetrical molecules, although it fails in some cases. The four main effects, the coordination number, antipodal, trans (= rhomboidal), and neighbor effects have been known for a long time and their principles are discussed in this review. Our studies, based partially on calculations, are also at variance with the conclusions drawn in the paper.⁹¹ In spite of these objections, a correct distribution of signals was obtained for mono- and dicarba derivatives of *closo*-B₇, B₁₀ and B₁₂ boranes.

2. Fluxional *closo*-Heteroboranes Derived from B_nH_n²⁻ for n = 8, 9, 11

The main representatives of the fluxional *closo*-boranes are B₈H₈²⁻ (13), B₉H₉²⁻ (14), and B₁₁H₁₁²⁻ (16). The fluxionality itself can be described by several models.^{279,280} The most popular is the Lipscomb's di-

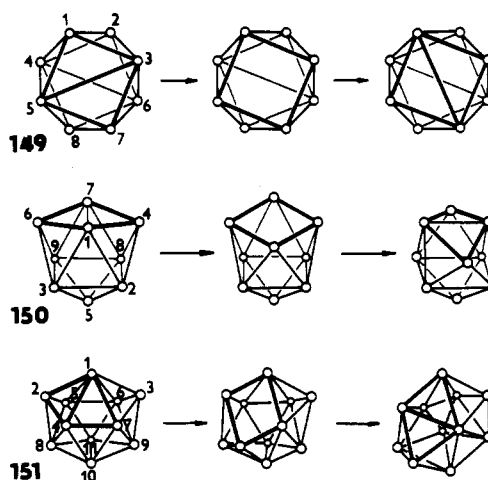


Figure 31. Diamond-square-diamond model of averaging ¹¹B signals of some or all B atoms in eight- (149), nine- (150), and eleven-vertex (151) boranes. In any of these skeletons, the introduced $\delta+$ charged heteroatom (C, N, S, etc.) occupies and keeps the position of the lowest connectivity (i.e. 1- in 149, 4- in 150, and 2- in 151; Williams' rule) while other B atoms can continue in the process of reorganization.

amond-square-diamond (DSD) concept,²⁸¹ consisting in the elimination of a common edge between two fused triangles under the formation of a square, and of subsequent combination of originally nonconnected vertices to a new deltahedral isotopomer. In this way, a reorganization of eight-vertex (149), nine-vertex (150), and eleven-vertex (151) skeletons can be described (Figure 31).

Inspection of structures of individual species a,b,c, etc. participating in the isomerization of 149-151 shows that each vertex changes its connectivity during the process of reorganization. This is also connected with a change in the chemical shielding of each vertex, the resulting frequency of which is an average of all possible connectivities and their contributions to the final state.

Substitution of a heteroatom for a boron vertex brings distinct changes in the charge on the heterovertex (in comparison with the original borane), which forces the heteroatom (C, N, S, etc.) to occupy the position of a lowest connectivity (Williams' rule)⁴ and keep this position and the connectivity constant. In the remaining part of the molecule, the fluxionality can be either suppressed or it can continue, averaging some signals.

For illustration, the anion 1-CB₇H₈⁻ (for geometric structure see 149) can be considered as a tetragonal pyramid joined by the base (2,3,4,5) to the triangle (6,7,8) which can change the connectivities from five (C5) to four (C4) and back by the DSD mechanism. The proportional population of C5:C4 connectivities is

TABLE 33. ¹¹B Chemical Shifts for Individual Atoms in Rigid *closo*-Heteroboranes Derived from Basic Five-, Six-, Seven-, and Ten-Vertex Skeletons (for $\delta(^{11}B)$ See Table 5)

compound	compd no.	parent no. (B _n H _n ²⁻)	δ (B vertices)	ref
1,5-C ₂ B ₃ H ₅	138	10	1.1 (2-4); $\delta(^{13}C)$ 102.4	168, 255
1-CB ₅ H ₆ ⁻	139	11	2.2 (6); -15.5 (2-5)	256
1,2-C ₂ B ₄ H ₆	140	11	-1.6 (4, 6); -15.3 (3, 5)	257
1,6-C ₂ B ₄ H ₆	141	11	-18.7 (2-5)	164, 168
2,3-C ₂ B ₅ H ₇	142	12	15.0 (4, 6); -2 (5); -25 (1, 7)	100
2,4-C ₂ B ₅ H ₇	143	12	5.0 (3); 2.0 (5, 6); -23.5 (1, 7)	258
1,2-C ₂ B ₆ H ₁₀	144	15	34.8 (10); -10.0 (4); -21.0 (3, 5); -26.8 (6, 9); -27.3 (7, 8)	39
1,6-C ₂ B ₆ H ₁₀	145	15	22.3 (10); -18.9 (8); -20.4 (2, 3); -22.5 (4, 5); -27.5 (7, 9)	39
1,10-C ₂ B ₈ H ₁₀	146	15	-13.7 (2-9)	39

TABLE 34. ^{11}B Chemical Shifts for $\text{EB}_{11}\text{H}_{11}$ (147)

E	B(12)	B(7-11)	B(2-6)	ref
BH^{2-}	-15.3	-15.3	-15.3	39
CH^-	-7.0	-13.1	-16.0	259
NH	2.7	11.9	-9.8	260
N^-	-1.0	-10.3	-10.3	260
PPh	-3.0	-8.4	-15.0	261
PMe	-1.1	-6.7	-14.4	262
As^-	8.0	-7.6	-8.6	263
Sb^-	9.4	-6.9	-9.3	264
S	18.7	-3.7	-5.7	39, 265, 266
Se	22.9	-3.5	-4.4	267
Te	24.1	-2.6	-3.5	268
Te	22.3	-4.3	-4.3	267
AlEt^{2-}	-25.5	-17.8	-18.8	269

2:2 for the (2,3,4,5) square, and 1:2 for the (6,7,8) triangle. Due to the fact that the vertex of lower connectivity resonates at higher frequency, we can expect that signal of the B(6,7,8) atoms with prevailing number of C4 will resonate at higher frequency (cf. Table 38).

The same procedure can be used in predicting the order of signals in the ^{11}B spectra of other fluxional heteroboranes.

3. Open-Face Boranes without and with H Tautomerism

With these compounds, the majority of conclusions, drawn in previous sections (IV.E.1,2) is valid. When treating the heteroboranes with H tautomerism, the probable chemical shifts for a static molecule must be derived first, and this spectrum can be used to estimate the influence of heteroatom(s).

Also in this group of compounds, the heteroatom antipodal and trans effects can operate, as observed for a number of open frameworks. It was found that following conclusions are necessary for causing A and T effects:

Trans coupled are those three contiguous skeletal atoms which are—inclusive of their exo orbitals—intersected by a molecular plane of symmetry to which the conjugated π orbitals are perpendicular. This ar-

angement is common to the 1-2-4 vertices in a tetragonal pyramid 18 wherever these conditions are met in a boron framework. It is also encountered with the three equatorial atoms 2,3,4, as well with 1,2,5 atoms in a trigonal bipyramid 10 where the T effect should also be expected. Surprisingly, strong T effects are also exhibited both by the 5-substituents and 5-C-heteroatom in the nido ten-vertex skeletons 5- $\text{XB}_{10}\text{H}_{13}$ (113, see Figure 25) and 5,6- $\text{C}_2\text{B}_8\text{H}_{12}$ (38),⁵³ respectively.

In contrast, *antipodally coupled* are two atoms lying—inclusive of their exo orbitals—on a straight line which is a part of a cage symmetry plane, to which the involved orbitals are perpendicular, e.g. 156-158.

F. Probable Origin of Antipodal and Trans Effects of Substituents and Heteroatoms

The title effects are very important for understanding both the ^{11}B and ^{13}C NMR spectra and the chemistry of the skeletons exhibiting these effects. A plausible explanation of them was therefore very desirable.

Since the discovery of the A effect in 1974, several hypotheses on its origin have been discussed or mentioned. The heteroatom-induced increase in the deshielding of the A vertex can be considered to be the result of (a) a decrease in ed on the leading α vertex caused by a heteroatom²⁶⁵ and the increase in ed brought by a +M substituent,¹⁹⁶ (b) an increase in ed on the α vertex caused by a heteroatom,⁹¹ (c) change in paramagnetic ring currents,²⁸⁴ which can be rejected on the basis of our finding that in the 2-chlorodecaborane(14) the chlorine positioned on the top of a regular pentagonal pyramid evokes the same A shift as does the 6-Cl atom located on the top of an incomplete pyramid,¹⁹⁶ and (d) decrease in the average excitation energy ΔE (cf. section IV).²⁸⁵

The most plausible hypothesis seemed to be our earlier idea, wherein the A effect was considered to be similar to the +M effect; explicitly, an increase in electron density was expected in the A position to a vertex bearing a +M substituent. A reverse effect was

TABLE 35. Relationships between ^{11}B Chemical Shifts and Electron Densities on Antipodal Atoms^a

		$\text{SB}_{11}\text{H}_{11}$										
		E	S		B(2-6)		B(7-11)		B(12)			
		A	B(12)	B(12)	B(7-11)	B(7-11)	B(2-6)	B(2-6)	S			
		S	B(12)	B(12)	B(7-11)	B(7-11)	B(2-6)	B(2-6)	-			
		$1,2\text{-C}_2\text{B}_{10}\text{H}_{12}$										
E	C(1)	C(2)	B(3)	B(6)	B(4)	B(5)	B(7)	B(11)	B(8)	B(10)	B(9)	B(12)
A	B(9)	B(12)	B(8)	B(10)	B(4)	B(5)	B(7)	B(11)	B(3)	B(6)	C(1)	C(2)
S	B(9)	B(12)	B(8)	B(10)	B(4)	B(5)	B(7)	B(11)	B(3)	B(6)	-	-
		$1,7\text{-C}_2\text{B}_{10}\text{H}_{12}$										
E	C(1)	C(7)	B(2)	B(3)	B(4)	B(6)	B(8)	B(11)	B(5)	B(12)	B(9)	B(10)
A	B(5)	B(12)	B(9)	B(10)	B(4)	B(6)	B(8)	B(11)	C(1)	C(7)	B(2)	B(3)
S	B(5)	B(12)	B(9)	B(10)	B(4)	B(6)	B(8)	B(11)	-	-	B(2)	B(3)

^aE: vertices ordered according to increasing electron densities. A: vertices antipodal to those in the above line. S: B vertices ordered according to increasing shielding.

TABLE 36. ^{11}B Chemical Shifts and 1,2-EGB $_{10}\text{H}_{10}$ (114)

E	G	B(12)	B(9)	B(8,10)	B(5,4)	B(7,11)	B(3,6)	ref
BH^-	BH^-	-15.3	-15.3	-15.3	-15.3	-15.3	-15.3	32
CH	BH^-	-6.9	-13.3	-13.3	-16.3	-13.3	-16.3	259
CH	CH	-3.4	-3.4	-10.2	-14.5	-14.5	-15.7	183, 271
P	CH	9.1	2.0	-1.6	-7.8	-8.8	-12.7	195, 272
As	CH	10.2	-0.3	-2.7	-5.0	-8.9	-9.6	273, 274
Sb	CH	6.2	-1.4	-5.8	-5.8	-10.2	-11.1	273, 274
P	P	17.7	17.7	4.6	0.8	-0.8	-1.2	195
As	As	15.5	15.5	3.8	0.9	0.9	-0.8	263
As	Sb	14.2	12.3	3.0	-0.1	-2.0	-3.5	264
Sb	Sb	13.9	13.9	3.9	-1.7	-1.7	-4.6	264

TABLE 37. ¹¹B Chemical Shifts for 1-EB_nH_n Compounds (148)

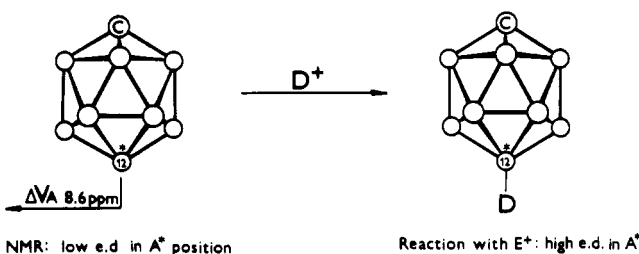
E	B(10)	B(2-5)	B(6-9)	ref
BH ²⁻	-2.0	-28.0	-28.0	275
	-6.8 ^a	-26.9 ^a	-26.9 ^a	95
AlH ²⁻	-26.4 ^a	-37.2 ^a	-31.4 ^a	95
CH ⁻	28.4	-20.0	-24.1	276
	32.2 ^a	-14.7 ^a	-21.2 ^a	95
SiH ⁻	12.4 ^a	-27.9 ^a	-24.3 ^a	95
N ⁻	50.0	-8.3	-18.3	251
	45.8 ^a	-5.3 ^a	-14.7 ^a	95
P	40.7 ^a	-9.6 ^a	-18.6 ^a	95
NH	61.0	-6.1	-21.5	251
	65.6 ^a	2.5 ^a	-16.1 ^a	95
PH	49.8 ^a	-22.6 ^a	-22.6 ^a	95
O	78.6 ^a	15.8 ^a	-11.7 ^a	95
S	74.5	-4.8	-17.6	277
	80.4 ^a	9.6 ^a	-12.7 ^a	95

^a Values calculated by IGLO method.⁹⁵

expected with 1-EB₉H₉ and 1-EB₁₁H₁₁ heteroboranes (E = C, N, P, S, etc.) the A atom of which is significantly deshielded (compared with the parent B_nH_n²⁻) and, consequently, a decreased ed on the A vertex was expected.

The results of the electrophilic substitution were, however, in sharp contrast to the predictions: an increase in electron density in position 12 was observed in the deuteration of the anion CB₁₁H₁₁⁻, proceeding preferentially in the antipodal position⁸⁵ (Scheme 1),

SCHEME 1



while a decrease in the 12-position was found in the halogenation of the anions XB₁₂H₁₁²⁻ (X = Cl, Br, I), affording largely 1,7- and no 1,12-dihalogen-substituted isomers¹⁶¹ (Scheme 2). Analogous results followed from

SCHEME 2

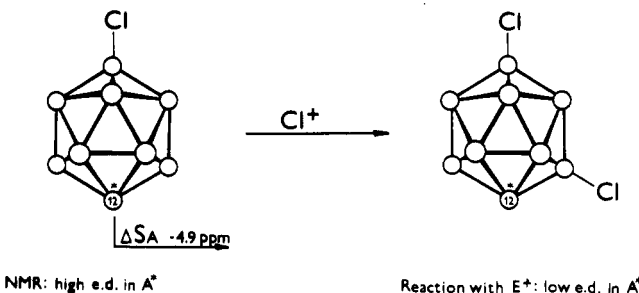


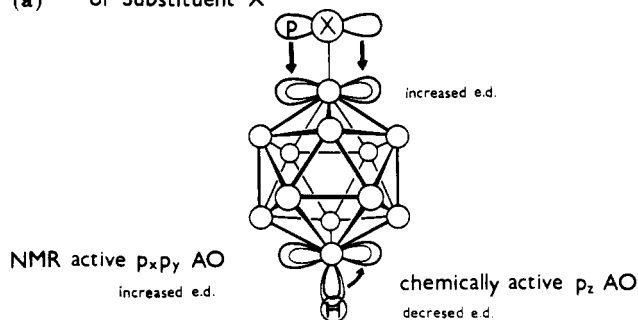
TABLE 38. ¹¹B Chemical Shifts of Individual Atoms in Fluxional *closo*-Heteroboranes Derived from Basic Eight, Nine, and Eleven Vertex Skeletons (for δ(¹¹B) See Table 5)

compd	compd no.	no. of parent (B _n H _n ²⁻)	δ (B vertices)	ref
1-CB ₇ H ₈ ⁻	152	13	3.14 (6, 7, 8); -4.35 (2, 3, 4, 5)	241
1,7-C ₂ B ₈ H ₈ ^a	153	13	7.18 (2, 8); -4.26 (3, 4, 5, 6)	282
2-CB ₁₀ H ₁₁ ⁻	154	16	-4.3 (9); -12.0 (3, 6, 7, 10, 11)	259
			-16.2 (1, 4, 5, 8)	
2,3-C ₂ B ₉ H ₁₁	155	16	-1.2 (4-7); -7.3 (8, 9)	283
			-10.5 (10, 11); -17.3 (1)	

^a C,C-Dimethyl derivative.

Antipodal Effect

(a) of Substituent X



(b) of Vertex E

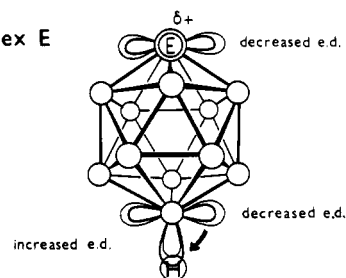


Figure 32. Probable mechanism of the antipodal effect of the substituent X and of the vertex E.

the pK_a values of 1-halogen-12-SH-1,2-C₂B₁₀H₁₀.²⁸⁶

To explain these discrepancies, two types of atom orbitals were considered: (i) the tangential p_x and p_y i.e. "π" orbitals which are NMR active; and (ii) radial p_z orbitals which are chemically active.¹¹ In addition, a possibility of a transmission of electrons between these orbitals reflecting the situation on the antipodal leading vertex was accepted.

As Figure 32a indicates, a substituent of +M character increases the ed in the "π" orbital, which is reflected on the A atom by an increase in "π" ed on the account of electrons in the radial orbital. This explains an enhanced shielding of this skeletal atom and the shift of its signal to lower frequencies.

A reverse situation holds for EB₉H₉ and EB₁₁H₁₁ heteroboranes (Figure 32b, E = C,N,S) with small p_xp_y orbitals on E representing the positive end of the skeleton. This is reflected by a contraction of the antipodal p_xp_y orbitals and a transfer of "surplus" electrons to the p_z orbital, i.e. to the B-H bond.

The latter hypothesis was confirmed with the EB₁₁-H₁₁ and 1-EB₉H₉ series, in which the CNDO/2 and Hückel type calculations have shown that with decreasing electron density on the vertex E: AlR²⁻ > BH²⁻ > CH⁻ > NH > S the electron density on the antipodal skeletal atom decreases proportionally in the tangential p_x and p_y (π) atomic orbitals (Figure 33a) and increases

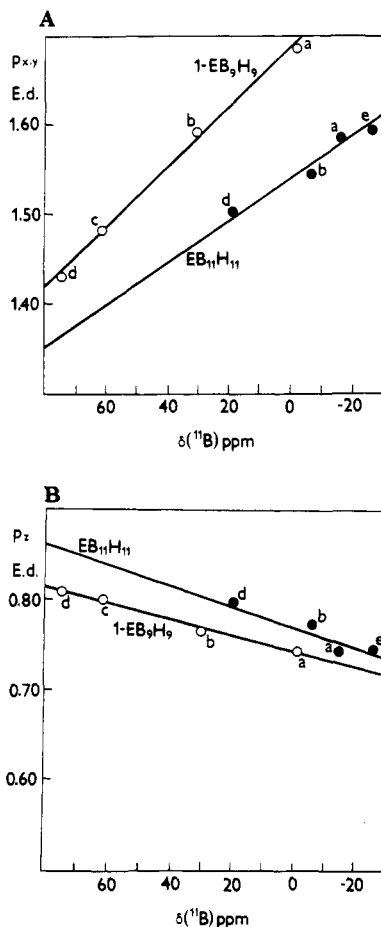


Figure 33. Correlation between $\delta(^{11}\text{B})$ and CNDO/2 electron densities (ed) with compounds $1\text{-EB}_9\text{H}_9$ and $\text{EB}_{11}\text{H}_{11}$ for E: (a) BH^{2-} , (b) CH^- , (c) NH , (d) S , (e) AlMe_2^- in (A) $p_x + p_y$ and (B) p_z atom orbitals.

in the radial p_z (Figure 33b) orbital through both series.⁹⁴

The changes caused by the +M substituent are markedly lower and were found by calculations only with strong donors (F , O^-). Also here, however, the predicted changes in ed were confirmed.⁹⁴

These results support significantly the idea that the changes in B chemical shift evoked by the antipodal substituent or heteroatom are dominated mainly by the electron density term $\langle r^{-3} \rangle_{2p}$ (see section IV, eq 5). A participation of the electron "imbalance" P_u cannot be excluded because of acting in the same direction.

Very recently, the ^{11}B chemical shifts of individual atoms of $1\text{-EB}_9\text{H}_9$ series have been computed using the IGLO method. The results have justified the term "NMR-active orbitals" introduced by the author of this review. In addition, tensor components σ_{\perp} and σ_{\parallel} were calculated. A difference between these values grows significantly from $\text{E} = \text{BH}^{2-}$ to S , which indicates the cooperation of the factor P_u in the A shift. The changes in ΔE were found less significant, as opposed to the results of Fehner et al.²⁸⁵ who described an application of the Fenske-Hall MO method to the calculation of ^{11}B NMR shifts and got good agreement of calculated and found ^{11}B shifts for compounds with B atoms surrounded by different metals.

The probable mechanism of the transmission of electrons between the atomic orbitals on a single vertex, inferred from ^{11}B NMR chemical shifts and supported

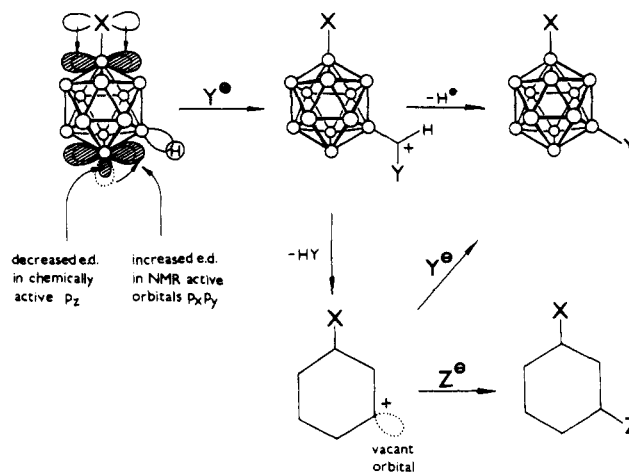


Figure 34. Possible explanation of the meta directive effect of halogen in an electrophilic substitution and "a nucleophilic reaction under electrophilic conditions".

by CNDO/2 and further methods allow now the explanation of the unusual directive effect of halogens in icosahedral clusters. According to our hypothesis, the electrophilic particle attacks the center of the B-H bond, forming a three-center bond arrangement



which can either eliminate the H^+ particle under the formation of a product of an electrophilic substitution or eliminate the HX molecule forming a species with a vacant orbital that can be filled by a free electron pair of any nucleophilic reagent present in the solution (Figure 34). This is a possible explanation of the nucleophilic substitution under strictly electrophilic conditions.

The highest electron density on the B-H bond and, consequently, the highest probability to be attacked can be expected in the meta position which is less affected by both the +I effect and A effect of the +M substituent X. An analogous approach can be also used in the explanation of the unexpected but predominant A substitution of the $\text{CB}_{11}\text{H}_{12}^-$ anion.

This information shows that an analysis of ^{11}B chemical shifts allows both the determination of the structure of the B-cluster compounds but also the obtention of some additional knowledge on the distribution of bonds within the molecule and, in a favorable case, the prediction of some chemical behavior.

V. Conclusions

^{11}B NMR spectroscopy is the most economical and reliable method for the determination of the structure of most of the boron skeleton compounds. In addition to this, we have found that ^{11}B chemical shifts reflect the distribution of electrons within the molecule. This review represents an attempt to reveal basic relationships between the ^{11}B NMR chemical shifts, structural features, fluxional behavior, and electronic structure of B skeleton compounds. The searching for regularities was based on the comparison of a great amount of ^{11}B NMR spectra of compounds differing in geometrical structure, number of skeletal electrons, in substituents, heteroatoms, etc. To get groups of maximum information value, series of compounds differing in one

variable were prepared, measured using FT NMR spectrometers with superconductive magnets, and the majority of signals was reliably assigned. Many of these results are published for the first time.

Chemical shifts of both the ¹¹B and ¹⁰B nuclei are dominated by the paramagnetic term σ_p showing the measure of a deshielding (correctly, of a paramagnetic shielding) which increases with: (a) decreasing π back-donation from the substituent to the B(sp²) atom: (H) < Br = SH < Cl < NR₂ < F < OR (+100 to 0 ppm), (b) increasing distortion of the "bonding angles" on a B(sp³): pentagonal < tetragonal < trigonal pyramid (-30 to 30 ppm), (c) an increasingly uneven distribution of bonding electrons around given B atoms within open-skeleton frameworks (-60 to 20 ppm), and (d) decreasing π electron density.

The effect of a substituent X upon individual skeletal atoms depends on the competition of its electron-attracting power (termed the -I and +I effects), its π back-donation power (the +M effect), and the electronic character of the substituted vertex (electron density, interest in π electrons).

In compounds, showing an H tautomerism, the presence of a substituent suppresses the μ H migration; in addition, the electron-attracting substituents (or ligands) repel the μ H bridge to a remote position, whereas the electron-donating substituents attract the μ H bridge to the α vertex.

The heteroatoms C, N, P, S, etc., present within the skeleton, influence the cage primarily by its positive charge, the effect of which drops sharply with distance.

Explanation of the two significant effects—the antipodal and trans shifts caused by substituents or heteroatoms—based on the separation of π (NMR active) and exo (chemically active) orbital electron density is presented.

The transmission of electrons from the NMR-active π orbital to the chemically active σ orbital is used for the explanation of a meta directive effect of halogens in electrophilic reactions of icosahedral skeletons and of the nucleophilic substitution under electrophilic conditions.

VI. Acknowledgements

I am grateful to Prof. J. Plešek, Drs. B. Štíbr, T. Jelínek, Z. Janoušek, and B. Grüner for preparing the great series of compounds necessary for systematic NMR studies, Dr. D. Hnyk for quantum chemical calculations, Dr. J. Fusek for measuring a portion of the NMR spectra, and Mrs. M. Procházková for technical help. Part of this research has been supported by the Grant Agency of the Czechoslovak Academy of Sciences, Grant NO. 43202.

VII. References

- (1) Dickinson, W. C. *Phys. Rev.* 1951, 81, 717.
- (2) Schaeffer, R. *Prog. Boron Chem.* 1964, 1, 417.
- (3) Eaton, G. R.; Lipscomb, W. N. *NMR Studies of Boron Hydrides and Related Compounds*; Benjamin: New York, 1969.
- (4) Williams, R. E. *Prog. Boron Chem.* 1970, 2, 90.
- (5) Nöth, H.; Wrackmeyer, B. *Nuclear Magnetic Resonance Spectroscopy of Boron Compounds, in NMR-Basic Principles and Progress*; Diehl, P., Fluck, E., Kosfeld, R., Eds.; Springer-Verlag: Berlin, 1978.
- (6) Todd, L. J.; Siedle, A. R. *Prog. NMR Spectrosc.* 1979, 13, 87-176.
- (7) Siedle, A. R. *Annu. Rep. NMR Spectrosc.* 1982, 12, 177-261.

- (8) Kidd, R. G. In *NMR of the Newly Accessible Nuclei*; Laszlo, P., Ed.; Academic: London, 1983; Vol. 2, Chapter 3, pp 49-77.
- (9) Wrackmeyer, B.; Köster, R. In *Houben-Weyl, Methoden der Organischen Chemie*; Köster, R., Ed.; Thieme: Stuttgart 1984; Vol. 13/c, pp 377-611.
- (10) Kennedy, J. D. In *Multinuclear NMR (NMR in Inorganic and Organometallic Chemistry)*; Mason, J., Ed.; Plenum Press: New York, 1987; Chapter 8, 221-258.
- (11) Heřmánek, S.; Jelínek, T.; Plešek, J.; Štíbr, B.; Fusek, J.; Mareš, F. In *Boron Chemistry*; Heřmánek, S., Ed.; World Scientific: Singapore, 1987; pp 26-73.
- (12) Wrackmeyer, B. *Annu. Rep. NMR Spectrosc.* 1988, 20, 61-203.
- (13) Siedle, A. R. *Annu. Rep. NMR Spectrosc.* 1988, 20, 205-314.
- (14) Clouse, A. O.; Moody, D. C.; Rietz, R. R.; Roseberry, T.; Schaeffer, R. *J. Am. Chem. Soc.* 1973, 95, 2496.
- (15) Corcoran, E. W.; Sneddon, L. G. *J. Am. Chem. Soc.* 1984, 106, 7793.
- (16) Weiss, R. N.; Grimes, R. N. *J. Am. Chem. Soc.* 1977, 99, 1036.
- (17) Weiss, R. N.; Grimes, R. N. *J. Am. Chem. Soc.* 1978, 100, 1401.
- (18) Wright, W. F.; Garber, A. R.; Todd, L. J. *J. Magn. Reson.* 1978, 30, 595.
- (19) Smith, W. L.; Menegheli, B. J.; McClure, N.; Rudolph, R. W. *J. Am. Chem. Soc.* 1976, 98, 624.
- (20) Gaines, D. F. In *Boron Chemistry*; Heřmánek, S., Ed.; World Scientific: Singapore, 1987; pp 118-145.
- (21) Gaines, D. F.; Coons, D. E.; Heppert, J. A. In *Advances in Boron and the Boranes*; Liebman, J. F., Greenberg, A., Williams, R. E., Eds.; VCH Publishers: New York, 1988; p 106.
- (22) Jelínek, T.; Plešek, J.; Mareš, F.; Heřmánek, S.; Štíbr, B. *Polyhedron* 1987, 6, 1981.
- (23) Sprecher, R. F.; Aufderheide, B. E.; Luther, G. W.; Carter, J. C. *J. Am. Chem. Soc.* 1974, 96, 4404.
- (24) Venable, T. L.; Hutton, W. C.; Grimes, R. N. *J. Am. Chem. Soc.* 1984, 106, 29.
- (25) Alcock, N. W.; Taylor, J. G.; Wallbridge, M. G. H. *J. Chem. Soc., Chem. Commun.* 1983, 1168.
- (26) Reed, D. J. *J. Chem. Res.* 1984, 198.
- (27) Heřmánek, S.; Fusek, J.; Štíbr, B.; Plešek, J.; Jelínek, T. *Polyhedron* 1986, 5, 1873.
- (28) Onak, T. *Inorg. Chem.* 1968, 7, 1043.
- (29) Tucker, P. M.; Onak, T. *J. Am. Chem. Soc.* 1969, 91, 6869.
- (30) Köster, R.; Seidel, G.; Wrackmeyer, B. *Angew. Chem.* 1984, 96, 520.
- (31) Fontaine, X. L. R.; Kennedy, J. D. *J. Chem. Soc., Chem. Commun.* 1986, 779.
- (32) Heřmánek, S. Personal observation.
- (33) Heřmánek, S.; Jelínek, T.; Plešek, J.; Štíbr, B.; Fusek, J. *J. Chem. Soc., Chem. Commun.* 1987, 927; *Collect. Czech. Chem. Commun.* 1988, 53, 2742. (a) Jelínek, T.; Štíbr, B.; Mareš, F.; Plešek, J.; Heřmánek, S. *Polyhedron* 1987, 6, 1737.
- (34) Allerhand, A.; Clouse, A. O.; Rietz, R. R.; Roseberry, T.; Schaeffer, R. *J. Am. Chem. Soc.* 1972, 94, 2445.
- (35) Rathke, J.; Schaeffer, R. *Inorg. Chem.* 1974, 13, 3008.
- (36) Brice, V. T.; Johnson, H. D., II; Shore, S. G. *J. Am. Chem. Soc.* 1973, 95, 6629.
- (37) Hall, J. J., Jr.; Dixon, D. A.; Kleier, D. A.; Halgren, T. A.; Brown, L. D.; Lipscomb, W. N. *J. Am. Chem. Soc.* 1975, 97, 4202.
- (38) Klanberg, F.; Eaton, D. R.; Guggenberger, L. J.; Muettterties, E. L. *Inorg. Chem.* 1967, 6, 1271.
- (39) Heřmánek, S. 2D measurements.
- (40) Dixon, D. A.; Kleier, D. A.; Halgren, T. A.; Hall, J. H.; Lipscomb, W. N. *J. Am. Chem. Soc.* 1977, 99, 6226.
- (41) Marynick, D.; Onak, T. *J. Chem. Soc. (A)* 1969, 1797.
- (42) Lipscomb, W. N. *Boron Hydrides*; Benjamin: New York, 1963.
- (43) Mingos, D. M. P.; Slee, T.; Zhenyang, L. *Chem. Rev.* 1990, 90, 383-402.
- (44) Wade, K. *Adv. Inorg. Chem. Radiochem.* 1976, 18, 1.
- (45) Williams, R. E. *Adv. Inorg. Chem. Radiochem.* 1976, 18, 67.
- (46) Rudolph, R. W. *Acc. Chem. Res.* 1976, 9, 446.
- (47) Heřmánek, S. "Seco" versus "Debor" Concept, 23.5.1985, The University Munich, BRD.
- (48) Štíbr, B.; Plešek, J.; Heřmánek, S. *Collect. Czech. Chem. Commun.* 1966, 34, 194.
- (49) Tolpin, E. I.; Lipscomb, W. N. *Inorg. Chem.* 1973, 12, 2257.
- (50) Freyberg, D. P.; Weiss, R.; Sinn, E.; Grimes, R. N. *Inorg. Chem.* 1977, 16, 1847.
- (51) Plešek, J.; Štíbr, B.; Heřmánek, S. *Chem. Ind. (London)* 1974, 662.
- (52) Rietz, R. R.; Schaeffer, R. *J. Am. Chem. Soc.* 1971, 93, 1263.
- (53) Štíbr, B.; Heřmánek, S.; Janoušek, Z.; Dolanský, J.; Plizák, Z.; Plešek, J. *Polyhedron* 1982, 1, 822.
- (54) Webb, G. A. In *NMR and Periodic Table*; Harris, R. K., Mann, B. E., Eds.; Academic Press: London, 1978. (a) Ramsey, N. F. *Phys. Rev.* 1950, 78, 689. (b) Pople, J. A. *Mol. Phys.* 1964, 7, 301.

- (55) *Multinuclear NMR*; Mason, J., Ed.; Plenum: New York, 1987.
- (56) Thompson, R. J.; Davis, J. C., Jr. *Inorg. Chem.* **1965**, *4*, 1464.
- (57) Vandeberg, J. T.; Moore, C. E.; Cassaretto, F. P. *Org. Magn. Reson.* **1973**, *5*, 57.
- (58) Hall, L. W.; Odom, J. D.; Ellis, P. D. *J. Am. Chem. Soc.* **1975**, *97*, 4527.
- (59) Lappert, M. F.; Litzow, M. R.; Pedley, J. B.; Tweedale, A. J. *Chem. Soc. (A)* **1971**, 2426.
- (60) Nöth, H.; Vahrenkamp, H. *Chem. Ber.* **1966**, *99*, 1049.
- (61) Good, C. D.; Ritter, D. M. *J. Am. Chem. Soc.* **1962**, *84*, 1162.
- (62) Mooney, E. F.; Anderson, M. G. *Ann. Rev. NMR-Spectrosc.* Academic Press: New York, 1969; Vol. 2, p 219.
- (63) Hartmann, J. S.; Schrobilgen, G. J. *Inorg. Chem.* **1972**, *11*, 940.
- (64) Nöth, H.; Pommering, H. *Chem. Ber.* **1981**, *114*, 3044.
- (65) Dill, J. D.; Schleyer, P. v. R.; Pople, J. A. *J. Am. Chem. Soc.* **1975**, *97*, 3402.
- (66) Gaines, D. F.; Iorns, T. V. *J. Am. Chem. Soc.* **1970**, *92*, 4571.
- (67) Gaines, D. F.; Ulman, J. *J. Organometal. Chem.* **1975**, *93*, 281.
- (68) Heřmánek, S.; Plešek, J. *Chem. Listy* **1968**, *62*, 794.
- (69) O'Neill, M. E.; Wade, K. *Polyhedron* **1984**, *3*, 199.
- (70) Vinitskii, D. M.; Rezvova, J. V.; Solntsev, K. A.; Kuznetsov, N. T. *Russ. J. Inorg. Chem.* **1980**, *33*, 450.
- (71) Muetterties, E. L.; Hoel, E. L.; Salentine, C. G.; Hawthorne, M. F. *Inorg. Chem.* **1975**, *14*, 950.
- (72) Muetterties, E. L.; Wiersema, R. J.; Hawthorne, M. F. *J. Am. Chem. Soc.* **1973**, *95*, 7520.
- (73) Muetterties, E. L. *Inorg. Chem.* **1967**, *6*, 1271.
- (74) Wilks, P. H., Ph.D. Thesis. University of Pittsburgh, 1966.
- (75) Klanberg, F.; Muetterties, E. L. *Inorg. Chem.* **1966**, *5*, 1955.
- (76) Pitochelli, A. R.; Ettinger, R.; DuPont, J. A.; Hawthorne, M. F. *J. Am. Chem. Soc.* **1962**, *84*, 1057.
- (77) Preetz, W.; Srebny, H.-G.; Marsmann, H. C. *Z. Naturforsch.* **1984**, *39b*, 6.
- (78) Tolpin, E. T.; Lipscomb, W. N. *J. Am. Chem. Soc.* **1973**, *95*, 2384.
- (79) Middaugh, R. L.; Wiersema, R. J. *Inorg. Chem.* **1971**, *10*, 423.
- (80) Greenwood, N. N.; Morris, J. M. *Proc. Chem. Soc. London* **1963**, 338.
- (81) Preetz, W.; Srebny, H. G.; Marsmann, H. C. *Z. Naturforsch.* **1984**, *39b*, 189.
- (82) Onak, T.; Lockman, B.; Haran, G. *J. Chem. Soc., Dalton Trans.* **1973**, 2115.
- (83) Wrackmeyer, B. *Z. Naturforsch.* **1982**, *37b*, 412.
- (84) Garrett, P. M.; Ditta, G. S.; Hawthorne, M. F. *J. Am. Chem. Soc.* **1971**, *93*, 1265.
- (85) Heřmánek, S.; Jelínek, T. Unpublished results.
- (86) Davan, T.; Morrison, J. A. *J. Chem. Soc., Chem. Commun.* **1981**, 250. Klusik, H.; Berndt, H. *J. Organometal. Chem.* **1982**, *234*, C17. Morrison, J. A. *Chem. Rev.* **1991**, *91*, 35.
- (87) Levy, G. C.; Nelson, G. L. *Carbon-13 NMR For Organic Chemists*; Wiley: New York, 1972.
- (88) Clouse, A. O. *J. Chem. Soc. (D)* **1969**, 729.
- (89) Williams, R. E. In *Progress in Boron Chemistry*; Brotherton, R. J.; Steinberg, H., Eds.; Pergamon Press: Oxford, 1970; Vol. 2, 37.
- (90) Todd, L. J. *Pure Appl. Chem.* **1972**, *30*, 587.
- (91) Teixidor, F.; Viñas, C.; Rudolph, R. W. *Inorg. Chem.* **1986**, *25*, 3339.
- (92) Hall, J. H., Jr.; Dixon, D. A.; Kleier, D. A.; Halgren, T. A.; Brown, L. D.; Lipscomb, W. N. *J. Am. Chem. Soc.* **1975**, *97*, 4202.
- (93) Kroner, J.; Wrackmeyer, B. *J. Chem. Soc., Farad. Trans. 2* **1976**, *72*, 2283.
- (94) Heřmánek, S.; Hnyk, D.; Havlas, Z. *J. Chem. Soc., Chem. Commun.* **1989**, 1859.
- (95) Bühl, M.; Schleyer, P. v. R.; Havlas, Z.; Hnyk, D.; Heřmánek, S. *Inorg. Chem.* **1991**, *30*, 3107.
- (96) Johnson, H. D., II; Brice, V. T.; Brubaker, G. L.; Shore, S. G. *J. Am. Chem. Soc.* **1972**, *94*, 6711.
- (97) Olah, G. A.; Mateescu, G. D. *J. Am. Chem. Soc.* **1970**, *92*, 1430.
- (98) Plešek, J.; Heřmánek, S. *Collect. Czech. Chem. Commun.* **1979**, *44*, 24.
- (99) Heřmánek, S.; Plešek, J. *Z. Anorg. Allg. Chem.* **1974**, *409*, 115.
- (100) Rietz, R. R.; Schaeffer, R. J. *Am. Chem. Soc.* **1973**, *95*, 6254.
- (101) Pretzer, R. W.; Rudolph, R. W. *J. Am. Chem. Soc.* **1976**, *98*, 1441.
- (102) Dolanský, J.; Heřmánek, S.; Zahradník, R. *Collect. Czech. Chem. Commun.* **1981**, *46*, 2479.
- (103) Štíbr, B.; Baše, K.; Heřmánek, S.; Plešek, J. *J. Chem. Soc., Chem. Commun.* **1976**, 150.
- (104) Knoth, W. H. *Inorg. Chem.* **1971**, *10*, 598.
- (105) Baše, K.; Heřmánek, S.; Štíbr, B. *Chem. Ind. (London)* **1977**, 951.
- (106) Corcoran, E. W., Jr.; Sneddon, L. G. *J. Am. Chem. Soc.* **1985**, *107*, 7446.
- (107) Jelínek, T.; Štíbr, B.; Heřmánek, S.; Plešek, J. *J. Chem. Soc., Chem. Commun.* **1989**, 804.
- (108) Kang, S. O.; Sneddon, L. G. *J. Am. Chem. Soc.* **1989**, *111*, 3281.
- (109) Phillips, W. D.; Miller, H. C.; Muetterties, E. L. *J. Am. Chem. Soc.* **1959**, *81*, 4496.
- (110) Gaines, D. F. *Inorg. Chem.* **1963**, *2*, 523.
- (111) Johnson, H. D., II; Geanangel, R. A.; Shore, S. G. *Inorg. Chem.* **1970**, *9*, 908.
- (112) Odom, J. D.; Ellis, P. D.; Walsh, H. C. *J. Am. Chem. Soc.* **1971**, *93*, 3529.
- (113) Onak, T. P.; Williams, R. E. *Inorg. Chem.* **1962**, *1*, 106.
- (114) Nelson, M. A.; Kodama, G. *Inorg. Chem.* **1981**, *20*, 3579.
- (115) Bühl, M.; Schleyer, P. v. R. In *Electron Deficient Boron and Carbon Clusters*; Wiley: New York, 1991.
- (116) Brice, V. T.; Johnson, H. D., II; Denton, D. L.; Shore, S. G. *Inorg. Chem.* **1972**, *11*, 1135.
- (117) Brice, R. R.; Schaeffer, R.; Sneddon, L. G. *Inorg. Chem.* **1972**, *11*, 1242.
- (118) Jacobsen, G. B.; Meina, D. G.; Morris, J. H.; Thomson, C.; Andrews, S. J.; Reed, D.; Welch, A. J.; Gaines, D. F. *J. Chem. Soc., Dalton Trans.* **1985**, 1645.
- (119) Greenwood, N. N.; Kennedy, J. D. *J. Chem. Soc., Chem. Commun.* **1979**, 1099.
- (120) Siedle, A. R.; Bodner, G. M.; Todd, L. J. *J. Inorg. Nucl. Chem.* **1971**, *33*, 3671.
- (121) Heřmánek, S.; Plotová, H.; Plešek, J. *Collect. Czech. Chem. Commun.* **1975**, *40*, 3593.
- (122) Greenwood, N. N.; Youll, B. *J. Chem. Soc., Dalton Trans.* **1975**, 158.
- (123) Hosmane, N. S.; Wermer, J. R.; Hong, Z.; Getman, T. D.; Shore, S. G. *Inorg. Chem.* **1987**, *26*, 3638.
- (124) Getman, T. D.; Krause, J. A.; Shore, S. G. *Inorg. Chem.* **1988**, *27*, 2398.
- (125) Leach, J. B.; Onak, T.; Spielman, J.; Rietz, R. R.; Schaeffer, R.; Sneddon, L. G. *Inorg. Chem.* **1970**, *9*, 2170.
- (126) Jaworivsky, I. S.; Long, J. R.; Barton, L.; Shore, S. G. *Inorg. Chem.* **1979**, *18*, 56.
- (127) Remmel, R. J.; Johnson, H. D., II; Jaworivsky, I. S.; Shore, S. G. *J. Am. Chem. Soc.* **1975**, *97*, 5395.
- (128) Wermer, J. R.; Shore, S. G. *Inorg. Chem.* **1987**, *26*, 1644.
- (129) Moody, D. C.; Schaeffer, R. *Inorg. Chem.* **1976**, *15*, 233.
- (130) Keller, P. C. *Inorg. Chem.* **1970**, *9*, 75.
- (131) Schaeffer, R.; Sneddon, L. G. *Inorg. Chem.* **1972**, *11*, 3102.
- (132) Jacobsen, G. B.; Morris, J. H.; Reed, D. *J. Chem. Soc., Dalton Trans.* **1984**, 415.
- (133) Meina, D. G.; Morris, J. H. *J. Chem. Soc., Dalton Trans.* **1985**, 1903.
- (134) Getman, T. D.; Krause, J. A.; Niedenzu, P. M.; Shore, S. G. *Inorg. Chem.* **1989**, *28*, 1507.
- (135) Rietz, R. R.; Siedle, A. R.; Schaeffer, R.; Todd, L. J. *Inorg. Chem.* **1973**, *12*, 2100.
- (136) Lipscomb, W. N.; Wiersema, R. J.; Hawthorne, M. F. *Inorg. Chem.* **1972**, *11*, 651.
- (137) Anderson, J. A.; Astheimer, R. J.; Odom, J. D.; Sneddon, L. G. *J. Am. Chem. Soc.* **1984**, *106*, 2275.
- (138) Grimes, R. N. Ph.D. Thesis. University of Minnesota, 1962.
- (139) Gaines, D. F.; Iorns, T. V.; Clevenger, E. N. *Inorg. Chem.* **1971**, *10*, 1096.
- (140) Rietz, R. R.; Schaeffer, R. *J. Am. Chem. Soc.* **1973**, *95*, 4580.
- (141) Brewer, C. T.; Swisher, R. G.; Sinn, E.; Grimes, R. N. *J. Am. Chem. Soc.* **1985**, *107*, 3558.
- (142) Rathke, J.; Moody, D. C.; Schaeffer, R. *Inorg. Chem.* **1974**, *13*, 3040.
- (143) Heřmánek, S.; Fetter, K.; Plešek, J.; Todd, L. J.; Garber, A. R. *Inorg. Chem.* **1975**, *14*, 2250.
- (144) Huffman, J. C.; Moody, D. C.; Schaeffer, R. *J. Am. Chem. Soc.* **1975**, *97*, 1621.
- (145) Todd, L. J.; Siedle, A. R. *Prog. NMR Spectrosc.* **1979**, *13*, 147.
- (146) Fontaine, X. L. R.; Greenwood, N. N.; Kennedy, J. D.; MacKinnon, P. *J. Chem. Soc., Dalton Trans.* **1988**, 1785.
- (147) Heřmánek, S.; Plešek, J.; Štíbr, B. 3rd International Meeting on Boron Chemistry, München, Ettal, 5-9 July, 1976; Abstr. no. 52.
- (148) Akitt, J. W.; Savory, C. G. *J. Magn. Reson.* **1975**, *17*, 122.
- (149) Franz, D. A.; Grimes, R. N. *J. Am. Chem. Soc.* **1970**, *92*, 1438.
- (150) Jelínek, T.; Plešek, J.; Heřmánek, S.; Štíbr, B. *Main Group Met. Chem.* **1987**, *10*, 401.
- (151) Plešek, J.; Heřmánek, S.; Janoušek, Z. *Collect. Czech. Chem. Commun.* **1977**, *42*, 785.
- (152) Lipscomb, W. N. *Inorg. Chem.* **1979**, *18*, 2328.
- (153) Schleyer, P. v. R.; Bühl, M.; Fleischer, U.; Koch, W. *Inorg. Chem.* **1990**, *29*, 153.
- (154) Schleyer, P. v. R.; Bühl, M. *Angew. Chem., Int. Ed. Engl.* **1990**, *29*, 304.
- (155) Williams, R. E. In *Electron Deficient Boron and Carbon Clusters*; Olah, G. A.; Wade, K.; Williams, R. E., Eds.; Wiley: New York, 1990; ref 83b.
- (156) Bühl, M.; Schleyer, P. v. R. *Inorg. Chem.* **1992**, in press.
- (157) Bühl, M.; Schleyer, P. v. R.; Havlas, Z.; Hnyk, D.; Heřmánek, S. *Inorg. Chem.* **1991**, *30*, 3107.

- (158) Hnyk, D.; Vajda, E.; Bühl, M.; Schleyer, P. v. R. *Inorg. Chem.*, in press.
- (159) Preetz, W.; Fritze, J. Z. *Naturforsch.* 1984, 39b, 1472.
- (160) Preetz, W.; Fritze, J. Z. *Naturforsch.* 1987, 42b, 287.
- (161) Heřmánek, S.; Grüner, B. Unpublished results.
- (162) Srebný, H.-G.; Preetz, W.; Marsmann, H. C. Z. *Naturforsch.* 1983, 39b, 189.
- (163) Tolpin, E. I.; Wellum, G. R.; Berley, S. A. *Inorg. Chem.* 1978, 17, 2867.
- (164) Onak, T.; Williams, R. E.; Weiss, H. G. *J. Am. Chem. Soc.* 1962, 84, 2830.
- (165) Spielman, J. R.; Warren, R. G.; Bergquist, D. A.; Allen, J. K.; Marynick, D.; Onak, T. *Synth. React. Inorg. Met.-Org. Chem.* 1975, 5, 347.
- (166) Olsen, R. R.; Grimes, R. N. *Inorg. Chem.* 1971, 10, 1103.
- (167) Reilly, T. J.; Burg, A. B. *Inorg. Chem.* 1973, 12, 1450.
- (168) Grimes, R. N. *J. Am. Chem. Soc.* 1966, 88, 1895.
- (169) Heřmánek, S.; Plešek, J. Unpublished results.
- (170) Tucker, P. M.; Onak, T.; Leach, J. B. *Inorg. Chem.* 1970, 9, 1430.
- (171) Lowman, D. W.; Ellis, P. D.; Odom, J. D. *Inorg. Chem.* 1973, 12, 681.
- (172) Burg, A. B. *J. Am. Chem. Soc.* 1968, 90, 1407.
- (173) Gaines, D. F.; Martens, J. A. *Inorg. Chem.* 1968, 7, 704.
- (174) Burg, A. B.; Sandhu, J. S. *J. Am. Chem. Soc.* 1965, 87, 3787.
- (175) Gaines, D. F. *J. Am. Chem. Soc.* 1969, 91, 1230.
- (176) Sprecher, R. F.; Aufderheide, B. E. *Inorg. Chem.* 1974, 13, 2287.
- (177) Sprecher, R. F.; Carter, J. C. *J. Am. Chem. Soc.* 1973, 95, 2369.
- (178) Heřmánek, S.; Fusek, J.; Mareš, F.; Štíbr, B.; Jelínek, T.; Janoušek, Z.; Plešek, J. 4th International Symposium on NMR, Tábor, Czechoslovakia, 16–20th June 1986.
- (179) Jelínek, T.; Plešek, J.; Heřmánek, S.; Štíbr, B. *Collect. Czech. Chem. Commun.* 1986, 51, 819.
- (180) Smith, W. L.; Meneghelli, B. J.; Thompson, D. A.; Klymko, P. A.; McClure, N.; Rudolph, R. W. *Inorg. Chem.* 1977, 16, 3008.
- (181) Jelínek, T.; Heřmánek, S.; Štíbr, B.; Plešek, J. *Polyhedron* 1986, 5, 1303.
- (182) Heřmánek, S.; Gregor, V.; Štíbr, B.; Plešek, J.; Janoušek, Z.; Antonovich, V. A. *Collect. Czech. Chem. Commun.* 1976, 41, 1492.
- (183) Stanko, V. I.; Babushkina, T. A.; Klimova, T. P.; Goltiapin, Yu. V.; Klimova, A. I.; Vasilev, A. M.; Alimov, A. M.; Khrapov, V. V. *Zh. Obsh. Khim.* 1976, 46, 1071.
- (184) Aufderheide, B. E.; Sprecher, R. F. *Inorg. Chem.* 1974, 13, 2286.
- (185) Heřmánek, S.; Plešek, J.; Štíbr, B. 2nd International Meeting on Boron Compounds, Leeds, 25–29th March, 1974; Abstr. no. 38.
- (186) Plešek, J.; Heřmánek, S.; Baše, K.; Todd, L. J.; Wright, W. F. *Collect. Czech. Chem. Commun.* 1976, 41, 3509.
- (187) Štíbr, B.; Janoušek, Z.; Plešek, J.; Jelínek, T.; Heřmánek, S. *Collect. Czech. Chem. Commun.* 1987, 52, 103.
- (188) Exner, O. In *Advances in Linear Free Energy Relationships*; Chapman, N. B., Shorter, J., Eds.; Plenum Press: London, 1972; p 1.
- (189) Ulman, J. A.; Fehlner, T. P. *J. Am. Chem. Soc.* 1976, 98, 1119.
- (190) Todd, L. J.; Siedle, A. R.; Bodner, G. M.; Kahl, S. B.; Hicke, J. P. *J. Magn. Reson.* 1976, 23, 301.
- (191) Tucker, P. M.; Onak, T. P. *J. Am. Chem. Soc.* 1969, 91, 6869.
- (192) Gaines, D. F.; Iorns, T. V. *J. Am. Chem. Soc.* 1968, 90, 6617.
- (193) Wieser, J. D.; Moody, D. C.; Huffman, J. C.; Hildebrandt, R. L.; Schaeffer, R. J. *Am. Chem. Soc.* 1975, 97, 1074.
- (194) Heřmánek, S.; Plešek, J.; Štíbr, B. NMR Symposium, Prague, Czechoslovakia, 18th–21st Nov, 1974; Abstr. no. 11.
- (195) Siedle, A. R.; Bodner, G. M.; Garber, A. R.; Beer, D. C.; Todd, L. J. *Inorg. Chem.* 1974, 10, 2321.
- (196) Heřmánek, S.; Plešek, J.; Gregor, V.; Štíbr, B. *J. Chem. Soc., Chem. Commun.* 1977, 561.
- (197) Spiesscke, H.; Schneider, W. G. *J. Chem. Phys.* 1961, 35, 722.
- (198) Heřmánek, S.; Drdáková, E. Unpublished results.
- (199) Janoušek, Z.; Plešek, J.; Heřmánek, S.; Štíbr, B. *Polyhedron* 1985, 4, 1797.
- (200) Heřmánek, S.; Plešek, J.; Mareš, F.; Dolanský, J. International Symposium on NMR Spectroscopy, Proceedings No. 15, Smolenice, Czechoslovakia, 29th Sept–3rd Oct, 1980.
- (201) Ditter, J. F.; Klusmann, E. G.; Williams, R. E.; Onak, T. *Inorg. Chem.* 1976, 15, 1063.
- (202) Heřmánek, S.; Plešek, J.; Štíbr, B.; Janoušek, Z.; Mareš, F. 3rd International Symposium on NMR Spectroscopy, Tábor, Czechoslovakia, 7–11th June, 1982.
- (203) Heřmánek, S.; Plešek, J.; Štíbr, B.; Jelínek, T.; Fusek, J. *Torun*, July 30–Aug 3, 1990; Abstr. CA-13.
- (204) Pain, R. T.; Parry, R. W. *Inorg. Chem.* 1972, 11, 1237.
- (205) Shore, S. G. Personal communication 1979. In *Williams, R. E., Prakash, G. K. S., Field, L. D., Olah, G. A. Advances in Boron and the Boranes*; Liebman, J., Greenberg, A., Williams, R. E., Eds.; VCH Publishers: New York, 1988; p 191.
- (206) La Prade, M. D.; Nordman, C. E. *Inorg. Chem.* 1969, 8, 1669.
- (207) Centofani, L. F.; Kodama, G.; Parry, R. W. *Inorg. Chem.* 1969, 8, 2072.
- (208) Jock, C. P.; Kodama, G. *Inorg. Chem.* 1988, 27, 3431.
- (209) Bishop, V. L.; Kodama, G. *Inorg. Chem.* 1981, 20, 2724.
- (210) Kameda, M.; Shimoi, M.; Kodama, G. *Inorg. Chem.* 1984, 23, 3705.
- (211) Odom, J. D.; Moore, T. F.; Dawson, W. H.; Garber, A. R.; Stampf, E. J. *Inorg. Chem.* 1979, 18, 2179.
- (212) Dodds, A. R.; Kodama, G. *Inorg. Chem.* 1979, 18, 1465.
- (213) Kondo, H.; Kodama, G. *Inorg. Chem.* 1979, 18, 1460.
- (214) Kodama, G.; Saturnino, D. J. *Inorg. Chem.* 1975, 14, 2243.
- (215) Ishii, M.; Kodama, G. *Inorg. Chem.* 1990, 29, 2986.
- (216) Stampf, E. J.; Garber, A. R.; Odom, J. D.; Ellis, P. D. *Inorg. Chem.* 1975, 14, 2446.
- (217) Phillips, W. D.; Müller, H. C.; Muetterties, E. L. *J. Am. Chem. Soc.* 1959, 81, 4496.
- (218) Marynick, D.; Onak, T. *J. Chem. Soc. A* 1970, 1160.
- (219) Lorry, E. R.; Ritter, D. M. *Inorg. Chem.* 1971, 10, 939.
- (220) Paine, R. T.; Parry, R. W. *Inorg. Chem.* 1972, 11, 268.
- (221) Glore, J. D.; Rathke, J. W.; Schaeffer, R. *Inorg. Chem.* 1973, 12, 2175.
- (222) Kodama, G. *Inorg. Chem.* 1975, 14, 452.
- (223) Dodds, A. R.; Kodama, G. *Inorg. Chem.* 1976, 15, 741.
- (224) Dolan, P. J.; Kindsvater, J. H.; Peters, D. G. *Inorg. Chem.* 1976, 15, 2170.
- (225) Jolly, W. L.; Reed, J. W.; Wang, F. T. *Inorg. Chem.* 1979, 18, 377.
- (226) Kondo, H.; Kodama, G. *Inorg. Chem.* 1979, 18, 1460.
- (227) Kodama, G.; Kameda, M. *Inorg. Chem.* 1979, 18, 3302.
- (228) Nelson, M. A.; Kodama, G. *Inorg. Chem.* 1979, 18, 3276.
- (229) Bishop, V. L.; Kodama, G. *Inorg. Chem.* 1981, 20, 2724.
- (230) Jacobsen, G. B.; Morris, J. H. *Inorg. Chim. Acta* 1982, 59, 207.
- (231) Jacobsen, G. B.; Morris, J. H.; Reed, D. J. *Chem. Res. (S)* 1983, 42.
- (232) Chung Choi, P.; Morris, J. H. *J. Chem. Soc., Dalton Trans.* 1984, 2119.
- (233) Arunchaiya, M.; Morris, J. M.; Andrews, S. J.; Welch, D. A.; Welch, A. J. *J. Chem. Soc., Dalton Trans.* 1984, 2525.
- (234) Meina, D. G.; Morris, J. H. *J. Chem. Soc., Dalton Trans.* 1986, 2645.
- (235) Meina, D. G.; Morris, J. H.; Reed, D. *Polyhedron* 1986, 5, 1639.
- (236) de Poy, R. E.; Kodama, G. *Inorg. Chem.* 1988, 27, 4077.
- (237) Ishii, M.; Kodama, G. *Inorg. Chem.* 1990, 29, 817.
- (238) Brown, L. D.; Lipscomb, W. N. *Inorg. Chem.* 1977, 16, 1.
- (239) Arunchaiya, M.; Morris, J. H. *Inorg. Chim. Acta* 1985, 103, 31.
- (240) Dolan, P. J. Ph.D. Dissertation, Indiana University, Bloomington, IN, 1974.
- (241) Plešek, J.; Jelínek, T.; Štíbr, B.; Heřmánek, S. *J. Chem. Soc., Chem. Commun.* 1988, 348.
- (242) Heřmánek, S.; Fusek, J.; Jelínek, T. Preliminary results.
- (243) Howarth, O. W.; Jasztal, M. J.; Taylor, J. G.; Wallbridge, M. G. H. *Polyhedron* 1985, 4, 1461.
- (244) Baše, K.; Wallbridge, M. G. H.; Fontaine, X. L. R.; Greenwood, N. N.; Jones, J. M.; Kennedy, J. D.; Štíbr, B. *Polyhedron* 1989, 8, 2089.
- (245) Friesen, G. D.; Barriola, A.; Daluga, P.; Ragatz, P.; Huffman, J. C.; Todd, L. J. *Inorg. Chem.* 1980, 19, 458.
- (246) Arunchaiya, M.; Chung Choi, P.; Morris, J. H. *J. Chem. Res. (S)* 1985, 216.
- (247) Hyatt, D. E.; Scholer, F. R.; Todd, L. J. *Inorg. Chem.* 1967, 6, 630.
- (248) Štíbr, B.; Jelínek, T.; Plešek, J.; Heřmánek, S. *J. Chem. Soc., Chem. Commun.* 1987, 963.
- (249) Baše, K.; Heřmánek, S.; Štíbr, B. *Chem. Ind. (London)* 1976, 1068.
- (250) Baše, K.; Štíbr, B.; Dolanský, J.; Duben, J. *Collect. Czech. Chem. Commun.* 1981, 46, 2345.
- (251) Arafat, A.; Baer, J.; Huffman, J. C.; Todd, L. J. *Inorg. Chem.* 1986, 25, 3757.
- (252) Štíbr, B.; Fontaine, X. L. R.; Kennedy, J. D. 2D results.
- (253) Bown, M.; Fontaine, X. L. R.; Kennedy, J. D. *J. Chem. Soc., Dalton Trans.* 1988, 1467.
- (254) Siedle, A. R.; Bodner, G. M.; Garber, A. R.; Todd, L. J. *Inorg. Chem.* 1974, 13, 1756.
- (255) Onak, T.; Wan, E. *J. Chem. Soc., Dalton Trans.* 1974, 665.
- (256) Prince, S. R.; Schaeffer, R. *J. Chem. Soc., Chem. Commun.* 1968, 451.
- (257) Onak, T.; Drake, R. P.; Dunks, G. B. *Inorg. Chem.* 1964, 3, 1686.
- (258) Warren, R.; Paquin, D.; Onak, T.; Dunks, G. B.; Spielman, J. R. *Inorg. Chem.* 1970, 9, 2285.
- (259) Wiersema, R. J.; Hawthorne, M. F. *Inorg. Chem.* 1973, 12, 785.
- (260) Müller, J.; Runsink, J.; Paetzold, P. *Angew. Chem., Int. Ed. Engl.* 1991, 30, 175.

- (261) Little, J. L.; Moran, J. T.; Todd, L. J. *J. Am. Chem. Soc.* **1967**, *89*, 5495.
- (262) Getman, T. D.; Deng, M.-B.; Hsu, L.-Y.; Shore, S. G. *Inorg. Chem.* **1989**, *28*, 3612.
- (263) Little, J. L.; Pao, S. S.; Sugathan, K. K. *Inorg. Chem.* **1974**, *13*, 1752.
- (264) Little, J. L. *Inorg. Chem.* **1979**, *18*, 1598.
- (265) Plešek, J.; Heřmánek, S. *J. Chem. Soc., Chem. Commun.* **1975**, 127.
- (266) Hilty, T. K.; Thompson, D. A.; Butler, W. M.; Rudolph, R. W. *Inorg. Chem.* **1979**, *18*, 2642.
- (267) Friesen, G. D.; Todd, L. J. *J. Chem. Soc., Chem. Commun.* **1978**, 349.
- (268) Ferguson, G.; Parvez, M.; MacCurtain, J. A.; Dhubhgail, O. N.; Spalding, T. R. *J. Chem. Soc., Dalton Trans.* **1987**, 699.
- (269) Getman, T. D.; Shore, S. G. *Inorg. Chem.* **1988**, *27*, 3439.
- (270) Heřmánek, S.; Plešek, J.; Štibr, B.; Janoušek, Z. XIX. International Conference on Coordination Chemistry, Prague, Czechoslovakia, Sept 4-8, 1978; Abstr. no. 35.
- (271) Garber, A. R.; Bodner, G. M.; Todd, L. J.; Siedle, A. R. *J. Magn. Reson.* **1977**, *28*, 383.
- (272) Wong, H. S.; Lipscomb, W. N. *Inorg. Chem.* **1975**, *14*, 1350.
- (273) Todd, L. J.; Burke, A. R.; Garber, A. R.; Silverstein, H. T.; Storhoff, B. N. *Inorg. Chem.* **1970**, *9*, 2175.
- (274) Todd, L. J. In *Metal Interactions with Boron Clusters*; Grimes, R. N., Ed.; Plenum Press: New York, 1982; p 158.
- (275) Hawthorne, M. F.; Pilling, R. L.; Stokely, P. F. *J. Am. Chem. Soc.* **1965**, *87*, 1893.
- (276) Knoth, W. J. *J. Am. Chem. Soc.* **1967**, *89*, 1274.
- (277) Rudolph, R. W.; Pretzer, W. R. *J. Am. Chem. Soc.* **1973**, *95*, 931.
- (278) Plešek, J.; Štibr, B.; Fontaine, X. L. R.; Jelínek, T.; Heřmánek, S.; Kennedy, J. D. Manuscript in preparation.
- (279) Muetterties, E. L.; Knoth, W. H. *Polyhedral Boranes*; M. Dekker: New York, 1968.
- (280) Gimarc, B. M.; Ott, J. J. *J. Math. Chem.* **1990**, *5*, 359.
- (281) Lipscomb, W. N. *Boron Hydrides*; Benjamin: New York, 1963.
- (282) Tebbe, F. N.; Garrett, P. M.; Hawthorne, M. F. *J. Am. Chem. Soc.* **1968**, *90*, 869.
- (283) Schooler, F. R.; Brown, R. D.; Gladkowski, D.; Wright, W. F.; Todd, L. J. *Inorg. Chem.* **1979**, *18*, 921.
- (284) Leyden, R. N.; Sullivan, B. P.; Baker, R. T.; Hawthorne, M. F. *J. Am. Chem. Soc.* **1978**, *100*, 3758.
- (285) Fehlner, T. P.; Czech, P. T.; Fenske, R. F. *Inorg. Chem.* **1990**, *29*, 3103.
- (286) Plešek, J.; Heřmánek, S. *Collect. Czech. Chem. Commun.* **1981**, *46*, 687.